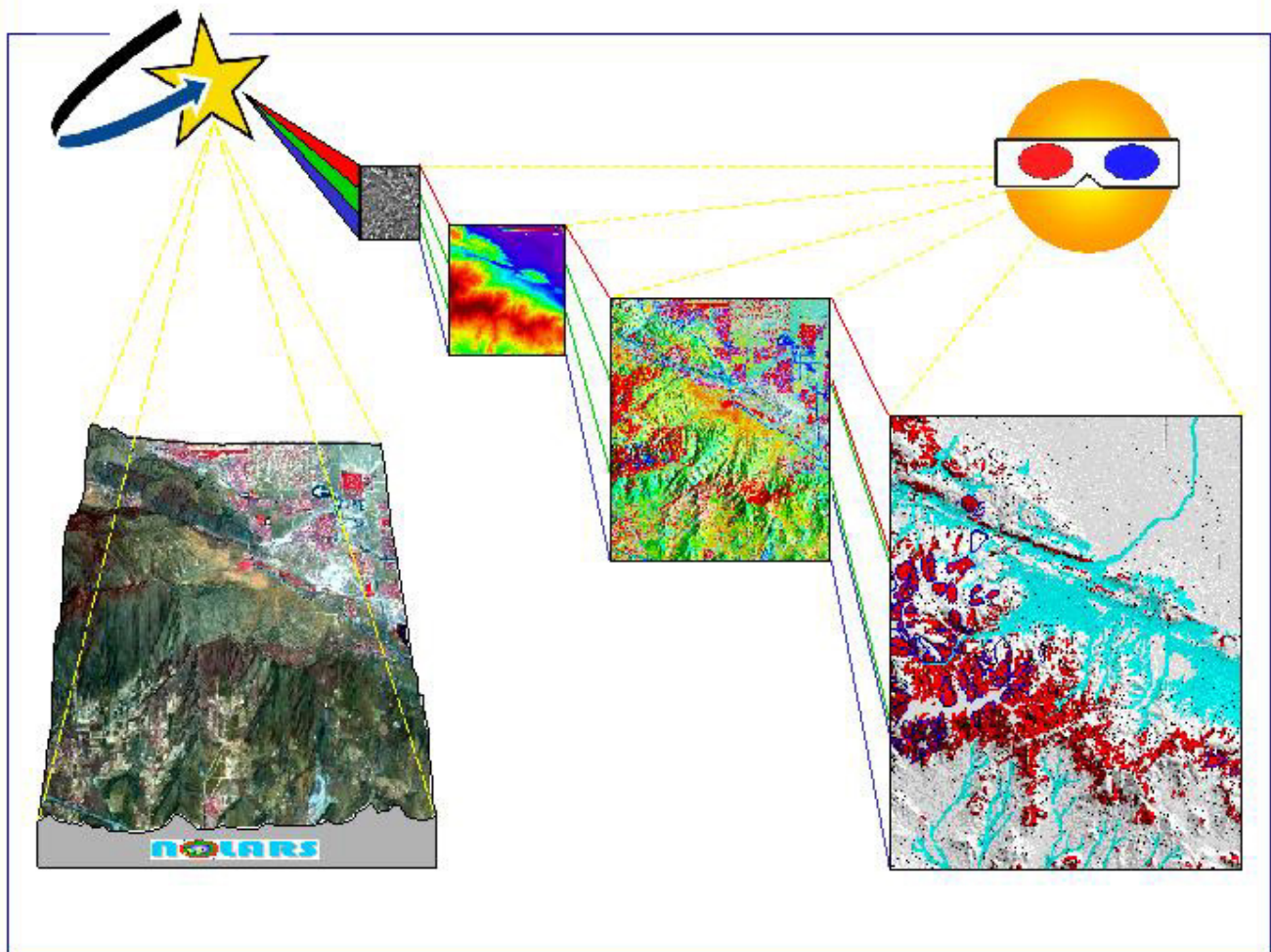


**EVALUATION OF USE OF REMOTE-SENSING IMAGERY  
IN REFINEMENT OF GEOLOGIC MAPPING FOR  
SEISMIC HAZARD ZONING IN NORTHERN  
LOS ANGELES COUNTY, CALIFORNIA**



**DEPARTMENT OF CONSERVATION  
CALIFORNIA GEOLOGICAL SURVEY  
SEISMIC HAZARDS MAPPING PROGRAM**

# **EVALUATION OF USE OF REMOTE-SENSING IMAGERY IN REFINEMENT OF GEOLOGIC MAPPING FOR SEISMIC-HAZARD ZONING IN NORTHERN LOS ANGELES COUNTY, CALIFORNIA**

**By**

**Chris T. Higgins and Florante G. Perez , Geologists**

**California Geological Survey**

**2003**

## **BACKGROUND OF PROJECT**

The Northern Los Angeles County Remote Sensing (NOLARS) project was begun in spring of 2002 at the request of Charles Real, Supervising Geologist of the Seismic Hazards Mapping Program (SHMP), which is part of the California Geological Survey (CGS). This request was to determine if remote-sensing products could enhance available geologic information that is used for mapping and zoning of both liquefaction and landslides potentially induced by earthquakes. The quality and availability of detailed geologic mapping will vary in future study areas; consequently, management is searching for ways to enhance geologic mapping when necessary.

The study area was chosen for this evaluation for two main reasons: 1) its range of exposed rock materials and geologic features, many of which are potentially amenable to evaluation by remote sensing, and 2) three Landsat 7 ETM satellite scenes that cover the entire study area were provided to CGS at no charge. Two CGS staff geologists, Ante Perez and Chris Higgins, were assigned part-time to complete this evaluation under the supervision of Al Barrows, Senior Geologist in SHMP.

This report summarizes the results of this evaluation and contains conclusions and recommendations regarding use of remote-sensing imagery in future SHMP projects. Some of the more obscure terms used in remote-sensing are defined in Appendix A. Readers are also advised that the display of imagery in the figures is generally superior in the digital version of this report compared to the hardcopy version.

## **SCOPE AND SETTING OF PROJECT**

The study area is in northern Los Angeles County and includes all or parts of nineteen 7.5-minute quadrangles (Figure 1). Its northeastern part is within the arid Antelope Valley, while the southwestern part is along the northern flank of

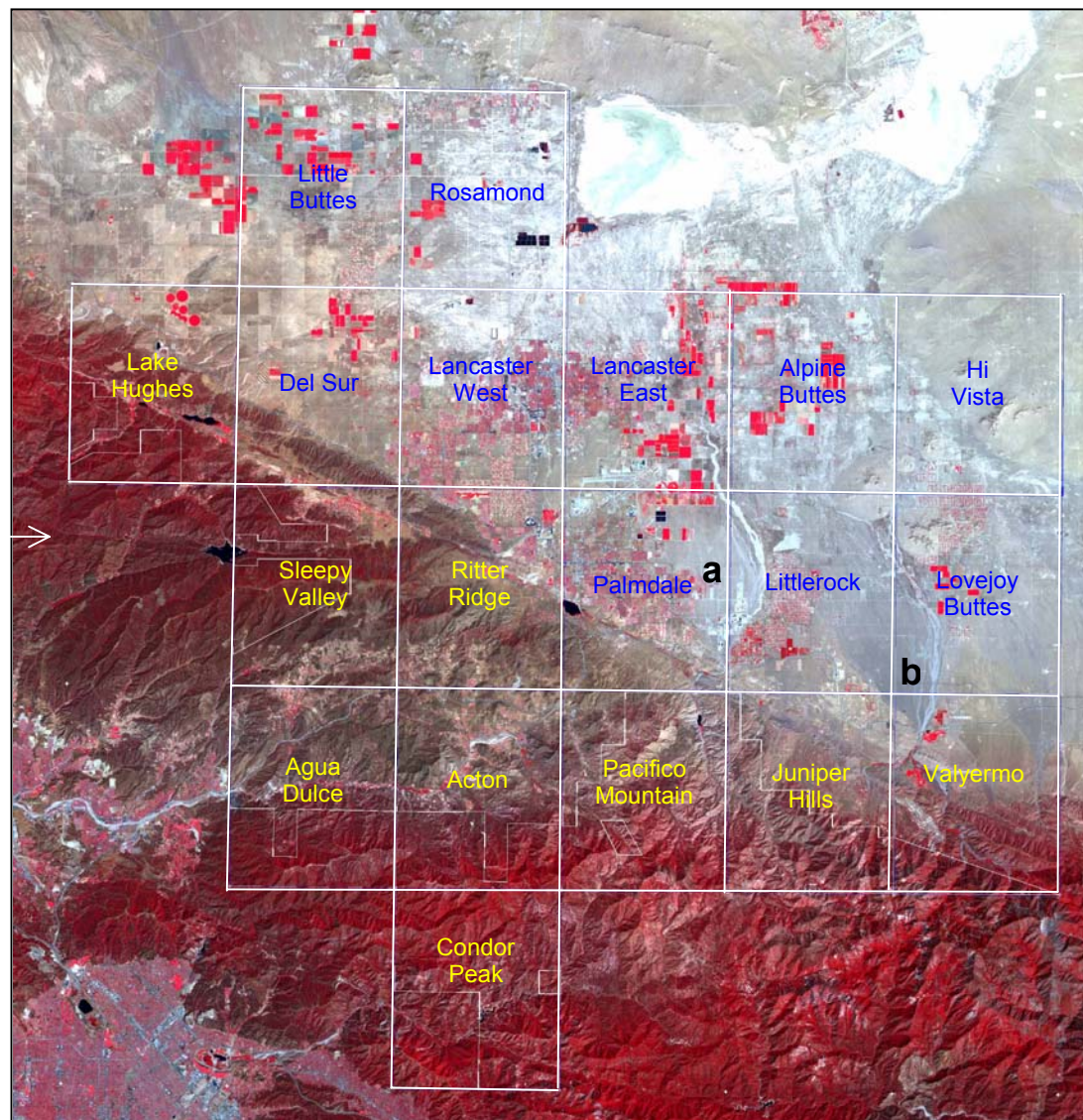
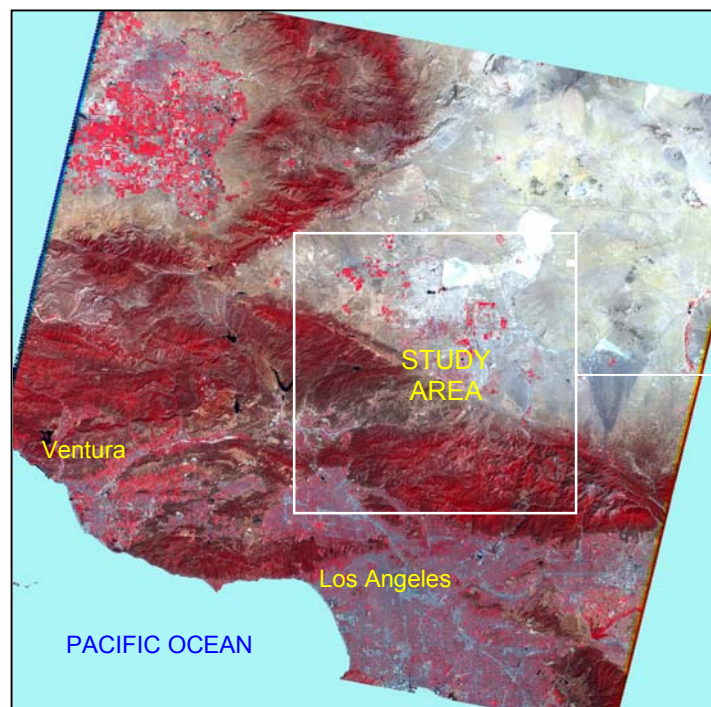


**FIGURE 1** – Overview of the study area as represented by the nineteen 7.5-minute quadrangles wholly or partially zoned for seismic hazards (landslides and liquefaction) by SHMP staff. Two prominent alluvial fans that were important in the study are Little Rock (a) and Big Rock (b).

**Sensor:** Landsat 7 ETM MSS

**Algorithm:** False Color Composite

**Band Order:** 4, 3, 2

the San Gabriel Mountains. Much of the northeastern part of the study area is a relatively flat plain, punctuated in a few places by small buttes that rise abruptly from the landscape. The southwestern part has moderate to high relief and is dominated by the prominent SE-trending low ridges (Portal Ridge, Ritter Ridge) that parallel the San Andreas Fault Zone and by the main massif of the San Gabriel Mountains. The boundary between these two parts varies in topographic character. It is abrupt in places where gently inclined alluvial fans and bajadas, variously dissected, abut the belt of SE-trending ridges. In other places, the intersection of alluvium and bedrock topography is more gradual.

Geologically, the area is characterized by two main environments. The San Gabriel Mountains consist largely of Mesozoic and older crystalline rocks (plutonic, schist, gneiss) with local exposures of younger Tertiary sedimentary and lesser volcanic rocks. Antelope Valley is underlain dominantly by unconsolidated alluvium, which surrounds several inliers (buttes) of plutonic rock in the eastern part; in the very northeast at Hi Vista is a broad, low-relief pediment (Mount Mesa) underlain by granitic rock. The east-southeast-trending San Andreas Fault Zone is the dominant structural feature of the study area; it forms the approximate physical boundary between Antelope Valley and the main San Gabriel Mountains in this region.

Vegetation is present in various compositions and densities, depending largely on elevation, orientation of slope, longitude, and to some extent, underlying lithology. The influence of oceanic moisture is apparent in the western part of the area as indicated by the presence of grasses. As one proceeds eastward, however, vegetation becomes more sparse and assumes a "desert" character (creosote, cactus, sagebrush, Joshua trees, etc.) in the fan areas of Antelope Valley; Dan Ponti (USGS, personal communication, 2002) concluded that the Joshua trees grew on older alluvial material. At higher elevations along the front of the San Gabriel Mountains, small trees (juniper, pinyon pine) and shrubs can reach high densities, especially on north-facing slopes. Although casual oblique views across the landscape at ground level suggest that vegetative cover may be substantial, vertical views of these same areas indicate that the percentage of cover may be much less than expected.

Despite its aridity, the surface of the study area has been substantially changed by cultural activity for many years. Urbanization in the Palmdale-Lancaster region is conspicuous and widespread, and there are large tracts of land to the west and east of this region that have been modified through agriculture and subdivision of the land into undeveloped parcels.

## **POTENTIAL APPLICATIONS OF REMOTE SENSING IN THE SEISMIC HAZARDS MAPPING PROGRAM**

The principles behind remote-sensing are rooted in a highly complex application of physics and statistics. The products derived from remote-sensing, however, can be readily applied by geologists who need only a basic understanding of these principles. Correspondingly, the main outcome of this project was to determine what potential ways, if any, remote sensing could be applied by technical staff in SHMP to aid their mapping and interpretation of geologic features related to seismic hazards. Another outcome was for all technical staff to start applying remote-sensing imagery to their projects as part of their routine geologic “toolbox.”

Use of remote-sensing imagery is founded on the spatial and spectral properties of spaceborne and airborne sensors. Spatial properties (represented by the size of each pixel in an image) determine to what level physical detail of the Earth’s surface can be seen. Spectral properties refer to the amounts and types of electromagnetic energy reflected or emitted from different materials at the Earth’s surface. Measurements of this energy (recorded by each pixel in the image) can help to discriminate or even identify surface materials such as masses of rock or alluvium, which can ultimately help define zones for earthquake-induced landslides and liquefaction.

Potential applications of remote-sensing imagery initially considered in our research for this project included the following:

- Assist cartographic registration of digital versions of geologic maps with underlying digital base maps. This application was especially important in this project because of difficulty in registering the digitized versions of the maps by Ponti and others (1980, 1981).
- Refine previous geologic contacts as portrayed on published and unpublished geologic maps.
- Subdivide previously mapped geologic units into new subunits (e.g., subdivide alluvial fans or plutonic bodies).
- Map new geologic units (i.e., rock bodies not recognized or delineated on published or unpublished geologic maps).
- Verify or refine previously mapped landslides or recognize new landslides.
- Increase the efficiency of both determination and collection of landslide attributes and the transfer of photographically interpreted landslides to base maps used for the project.
- Delineate currently active channels on alluvial fans.
- Define areas of shallow groundwater through distribution of vegetation and soil moisture.
- Enhance the use of stereographic pairs of traditional aerial photographs via the added spectral information of multispectral sensors, which can

show better contrast and discrimination of surface materials than the photographs.

- Improve the effectiveness of public and technical presentations on the results of zoning projects conducted by the Seismic Hazard Mapping Program.

As the project evolved, we concentrated our evaluation of the use of remote-sensing imagery on the following specific geologic applications:

- 1) **Delineation of contacts between bedrock and unconsolidated Quaternary deposits.** These boundaries are important because they separate geologic terrains that SHMP evaluates for *landslide zones* (bedrock) and *liquefaction zones* (unconsolidated deposits).
- 2) **Discrimination of alluvial deposits (fans, modern stream channels, etc.) from one another.** This discrimination is important because susceptibility to liquefaction (expressed through *liquefaction zones*) may vary from one type or generation of deposit to another.
- 3) **Discrimination of bedrock units from one another.** This discrimination is important because each bedrock unit has inherent shear strengths that are one of the criteria used to define *landslide zones*.
- 4) **Recognition and delineation of landslides.** Recognition and mapping of landslides are important for both *landslide zones* and the companion *landslide inventory*.
- 5) **Verification of cartographic registration of digital geologic maps.** Acceptable co-registration of previously mapped geology with base maps used in the project is essential for definition of *liquefaction zones* and *landslide zones*.
- 6) **Representation of previously mapped geologic contacts.** The more accurate the spatial representation of geologic contacts is, the higher the quality of the interpreted *liquefaction zones* and *landslide zones* derived from them.

Emphasis in this study was placed on the component units of Quaternary sediment within Antelope Valley and on the contacts between the unconsolidated Quaternary sediments and older bedrock units along the southwest edge of Antelope Valley in the vicinity of the San Andreas Fault Zone. Less time was devoted to evaluation of the imagery for discrimination of bedrock units in the San Gabriel Mountains and for recognition of landslides in the mountainous terrain of the study area.

## DATA ACQUIRED AND EVALUATED

To evaluate the use of remote sensing technology for enhancement of the zoning process by SHMP staff, we required three categories of data from the study area: geologic/soils maps, remote-sensing imagery, and field observations.

### Geologic/Soils Maps

Four different sets of published geologic maps (those by Ponti and others, Barrows, Dibblee, and Noble) and two sets of soils maps (Carpenter and Cosby, 1926; Woodruff and others, 1970), which individually covered all or parts of the study area were obtained to assist in interpretation and evaluation of the imagery. Each map is listed in the references section below. Except for the soils map of Carpenter and Cosby (1926), all of these maps were originally prepared at 1:24,000-scale or larger, although the maps of Ponti and others (1980, 1981) were ultimately published at 1:62,500. An advantage of the older soils map is that it was prepared in the 1920s, before most of the urbanization took place in the study area.

Challenges posed to us by these maps included: 1) comparing five different sets of maps, each of which was prepared for a different purpose and with corresponding differences in nomenclature, 2) matching different levels of detail, again depending on original purpose and scale, and 3) reliability of cartographic registration of them to base maps. Except for Noble (1954) and the soils maps, all maps were converted to digital form to allow overlay on the imagery. An index of these digital maps is shown in Figure 2.

### Remote-Sensing Imagery

Originally, the project was to evaluate three Landsat 7 ETM images obtained by SHMP, but as we proceeded in the study we recognized that use of other sets of imagery would enhance the evaluation. These sets are briefly described below and summarized in Table 1; graphic displays of each type of imagery are also presented. Some sets cover the study area entirely, some do not.

**Aerial Photographs:** Several stereo sets of different vintages and resolutions covering parts of the study area (Figure 3).

**ASTER (Advanced Spaceborne Thermal Emission and Reflection Radiometer):** One satellite multispectral scene (acquired in July 2001) at 15-, 30-, and 90-meter spatial resolutions (14 bands total – 3 VNIR; 6 SWIR; 5 TIR), which covers nearly all of the study area (Figure 4).

**Digital Elevation Models (DEM):** Two sets of DEMs were obtained (Figure 5), one from the USGS at 10-meter spatial resolution and covering the entire study area, and the other from Intermap Technologies Incorporated (by means of

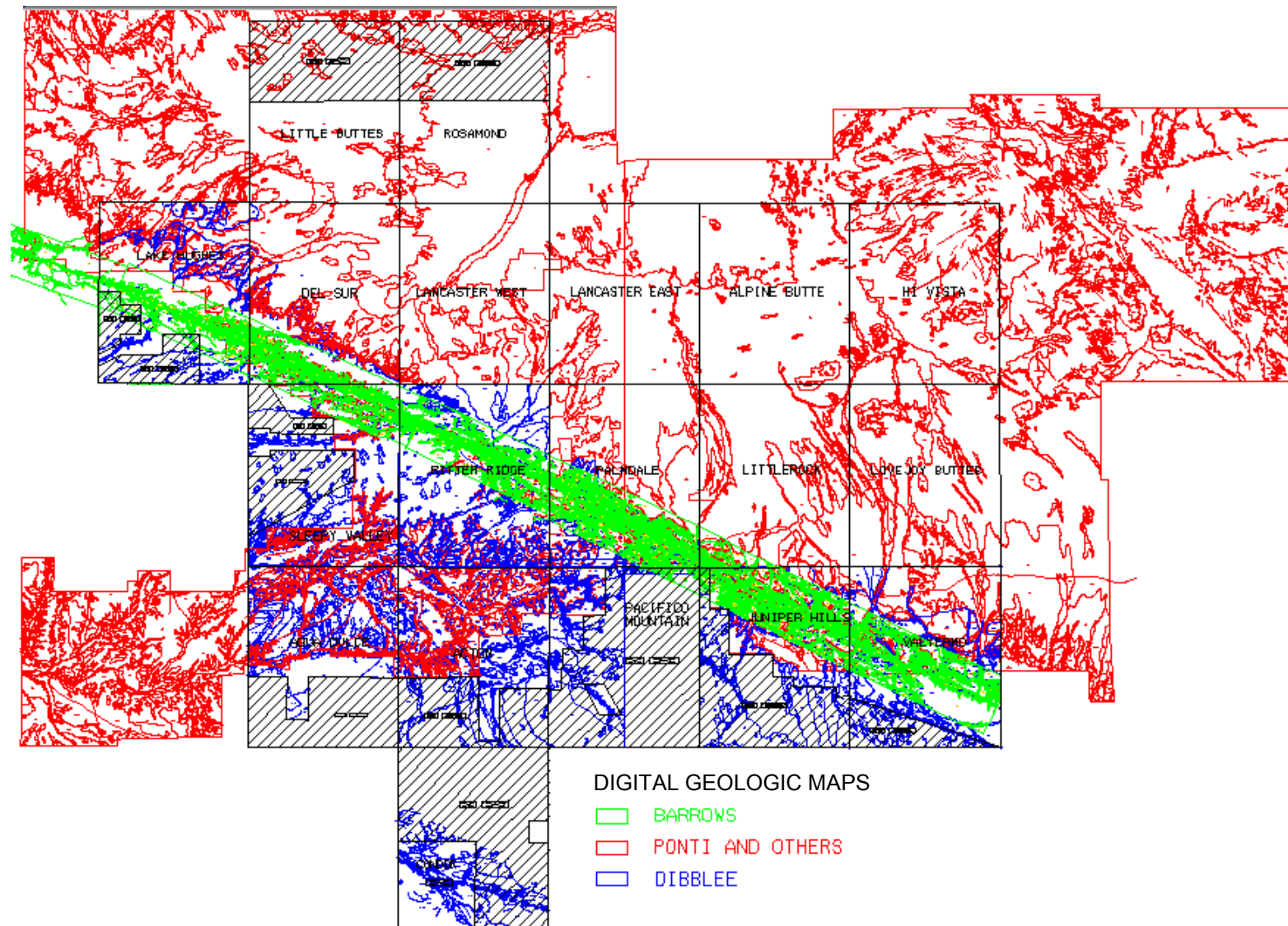


**FIGURE 2** – Index to the published geologic mapping used for SHMP zoning of the 19 quadrangles and for assistance in evaluation of remote-sensing imagery. Diagonal lines represent areas not zoned.

REMOTE-SENSING DATA	RESOLUTION (meters)	NUMBER OF BANDS	DATE
ASTER	15, 30, 90	14	2001
DOQQ	1	NA	1990s
INTERMAP DEM	5	1	2001
INTERMAP RADAR	2.5	1	2001
LANDSAT 7 ETM MSS	30	6	1999, 2000
LANDSAT 7 ETM PAN	15	1	1999
SPOT	10	1	1998-2000
USGS DEM	10	1	1970-1990s

**TABLE 1** – Brief summary of specifications of sensors, products of which were evaluated in this study.

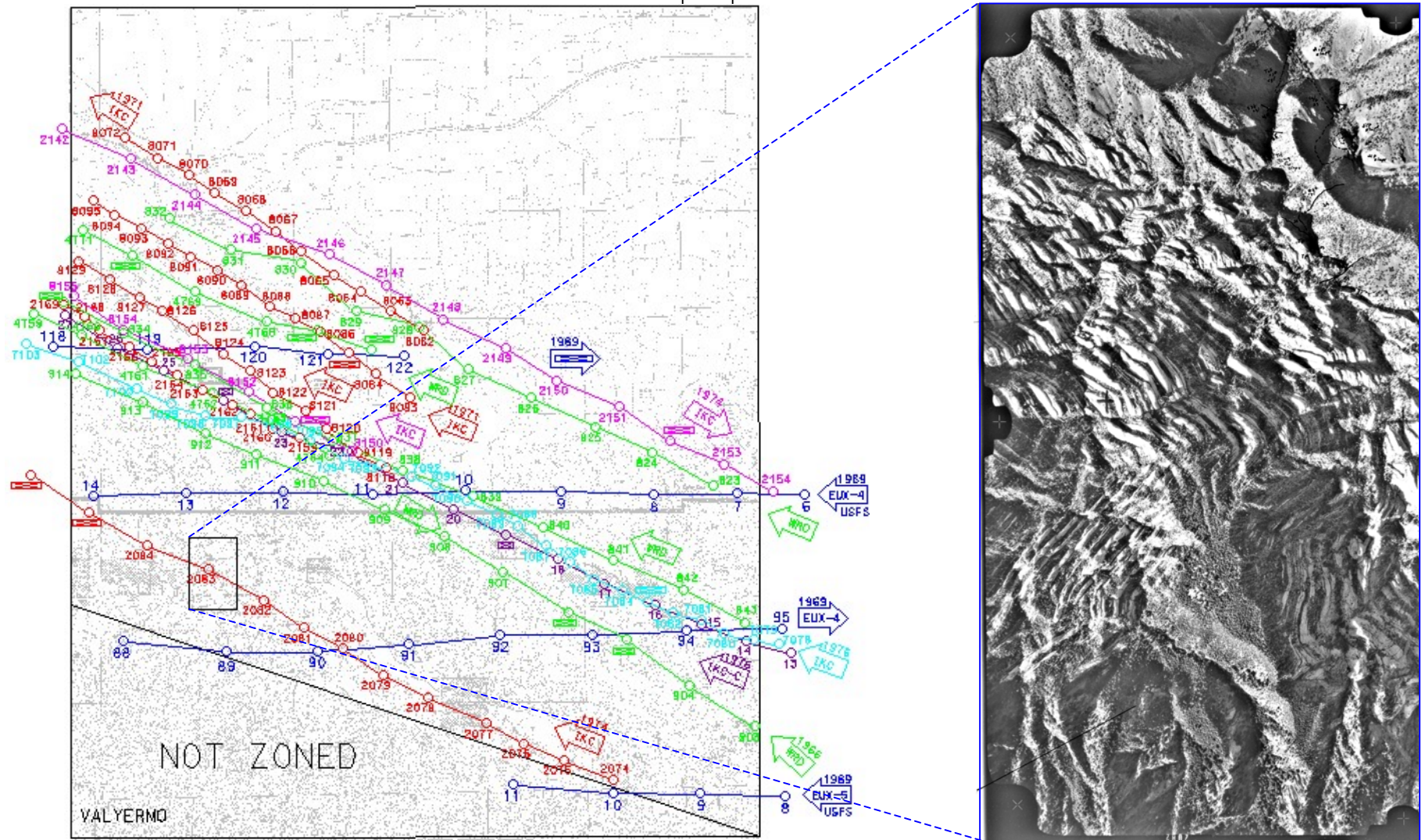
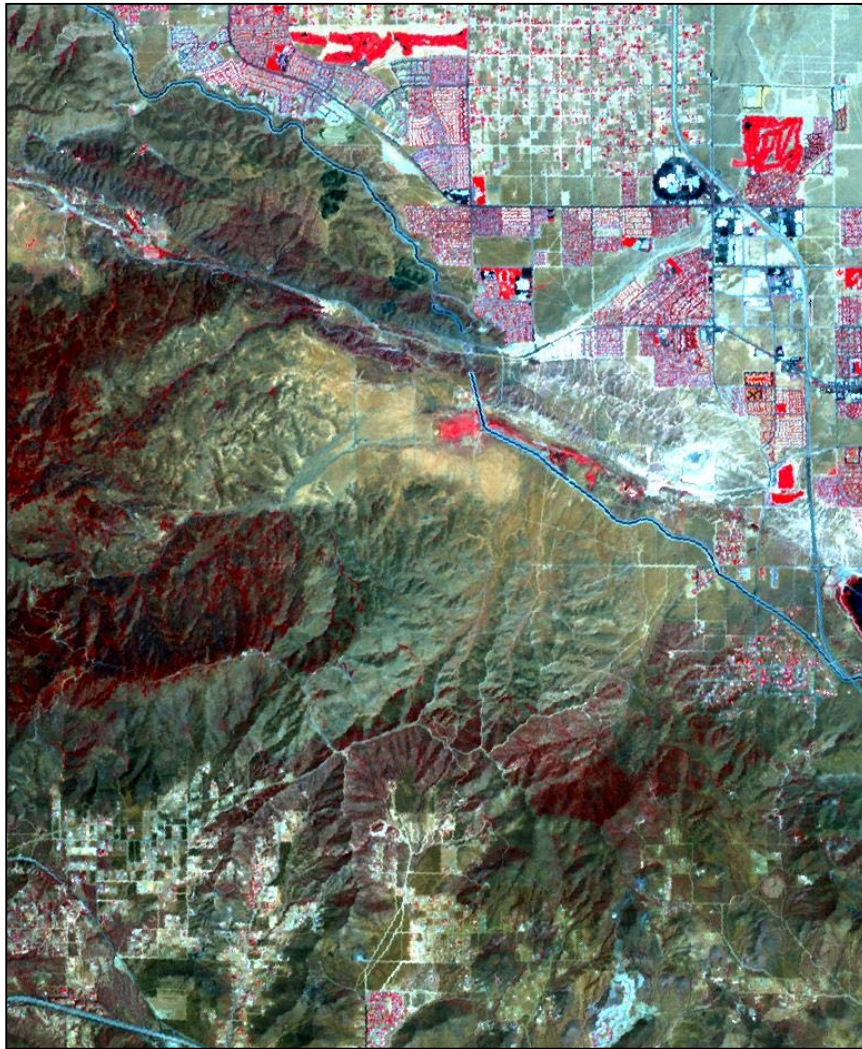
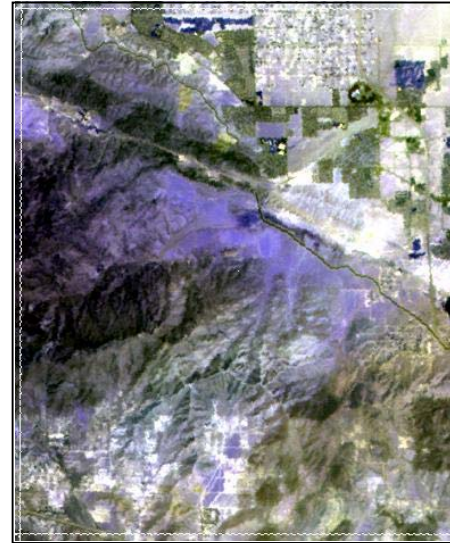


**FIGURE 3** – Examples of a portion of an aerial photograph (Devils Punchbowl in Valyermo Quadrangle) and indexes to flight lines and principal points of aerial photographs on the Valyermo 7.5-minute quadrangle.



(a)



(b)



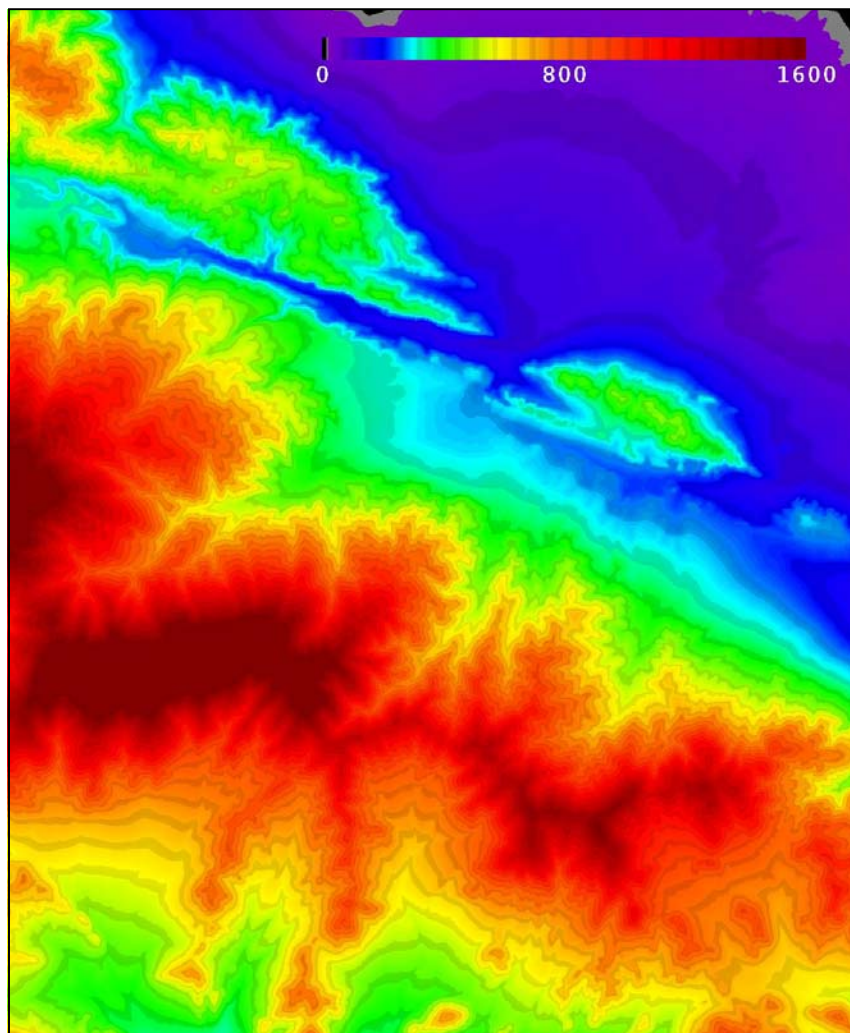
(c)

**FIGURE 4** – Examples of the three groups of ASTER bands, collected over the Ritter Ridge 7.5-minute quadrangle. a) VNIR at 15-meter resolution, b) SWIR at 30-meter resolution, and c) TIR at 90-meter resolution.

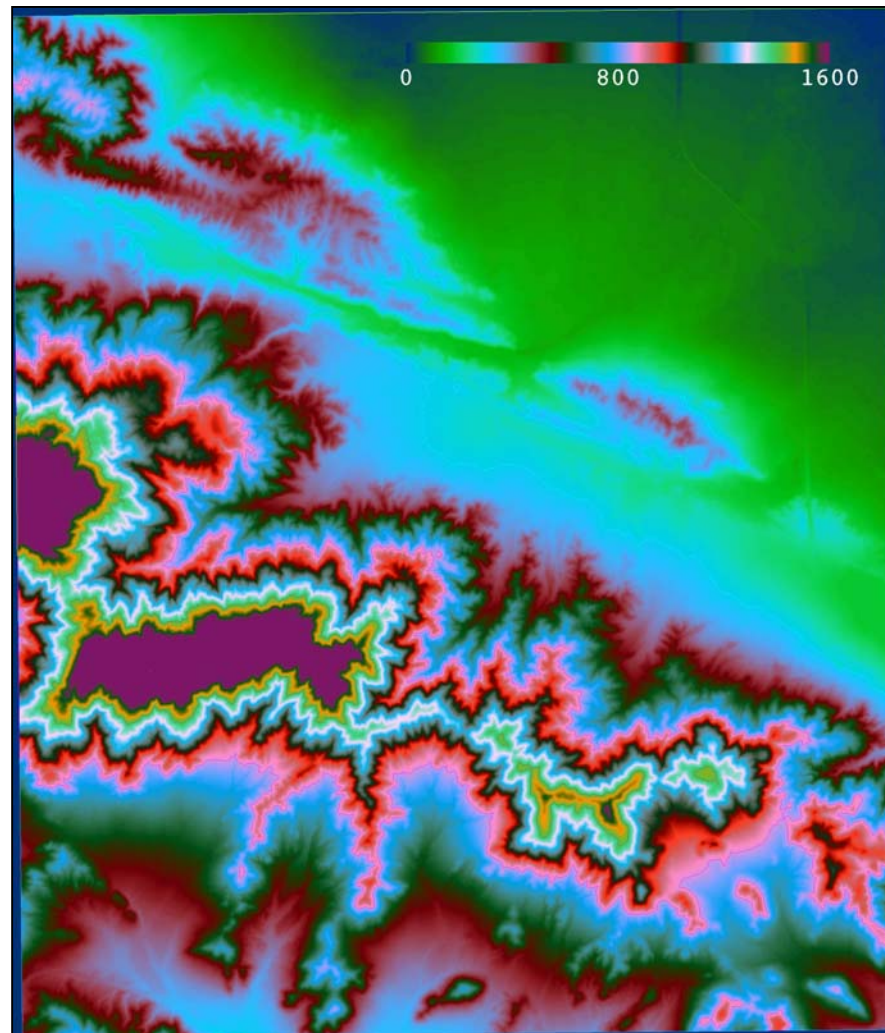
**Sensor:** ASTER

**Algorithm:** False Color Composite

**Band Order:** a) 3, 2, 1, b) 1, 2, 3, c) 1, 2, 3



(a)



(b)

**FIGURE 5** – Examples of digital elevation models, produced for Ritter Ridge Quadrangle. a) USGS, 10-meter spatial resolution. b) Intermap Technologies, 5-meter spatial resolution. Scale bars indicate elevations in meters.

**Sensor:** (a) Airborne Cameras, (b) SAR

**Algorithm:** Grayscale; Color Table (Rainbow)

airborne X-band Synthetic Aperture Radar) at 2.5-meter spatial resolution and covering the following USGS 7.5-minute quadrangles:

Agua Dulce  
Acton  
Lake Hughes  
Lancaster East  
Littlerock  
Palmdale  
Ritter Ridge  
Valyermo

The two sets were used to generate shaded-relief images.

**Digital Orthophoto Quarterquads:** Panchromatic images at 1-meter spatial resolution (derived from aerial photography, thus there were no raw data to process) covering the entire study area (Figure 6).

**Landsat 7 ETM (Enhanced Thematic Mapper):** Two satellite multispectral scenes (acquired on 9/20/1999 and 9/6/2000) at 30-m spatial resolution and one panchromatic image (acquired on 9/20/1999) at 15-m spatial resolution. Each scene covers the entire study area (Figure 7).

**Radar:** Commercially-obtained airborne X-band Synthetic Aperture Radar (SAR) images in GeoTIFF at 2.5-meter spatial resolution covering the following quadrangles (Figure 8a):

Agua Dulce  
Acton  
Lake Hughes  
Lancaster East  
Littlerock  
Palmdale  
Ritter Ridge  
Valyermo.

**SPOT:** Mosaic of satellite panchromatic images at 10-m spatial resolution covering the entire study area (Figure 8b).

We researched the archives of AVIRIS (Airborne Visible and Infrared Imaging Spectrometer, operated by the Jet Propulsion Laboratory for NASA) for lines covering the study area, but found only a few sets from 1996 that were over the alluvial plain near Lancaster. This area was of less interest to us for geologic evaluation. Also, data from this vintage of flights have suspect reliability as to geographic control.

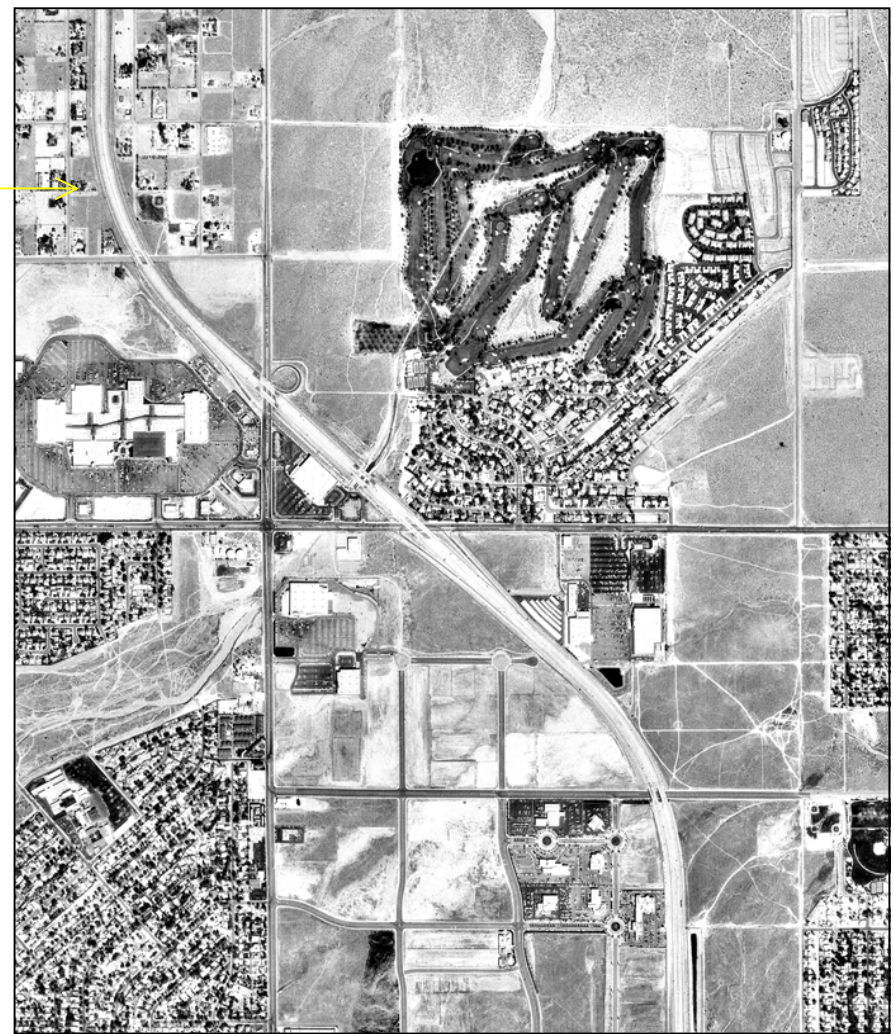


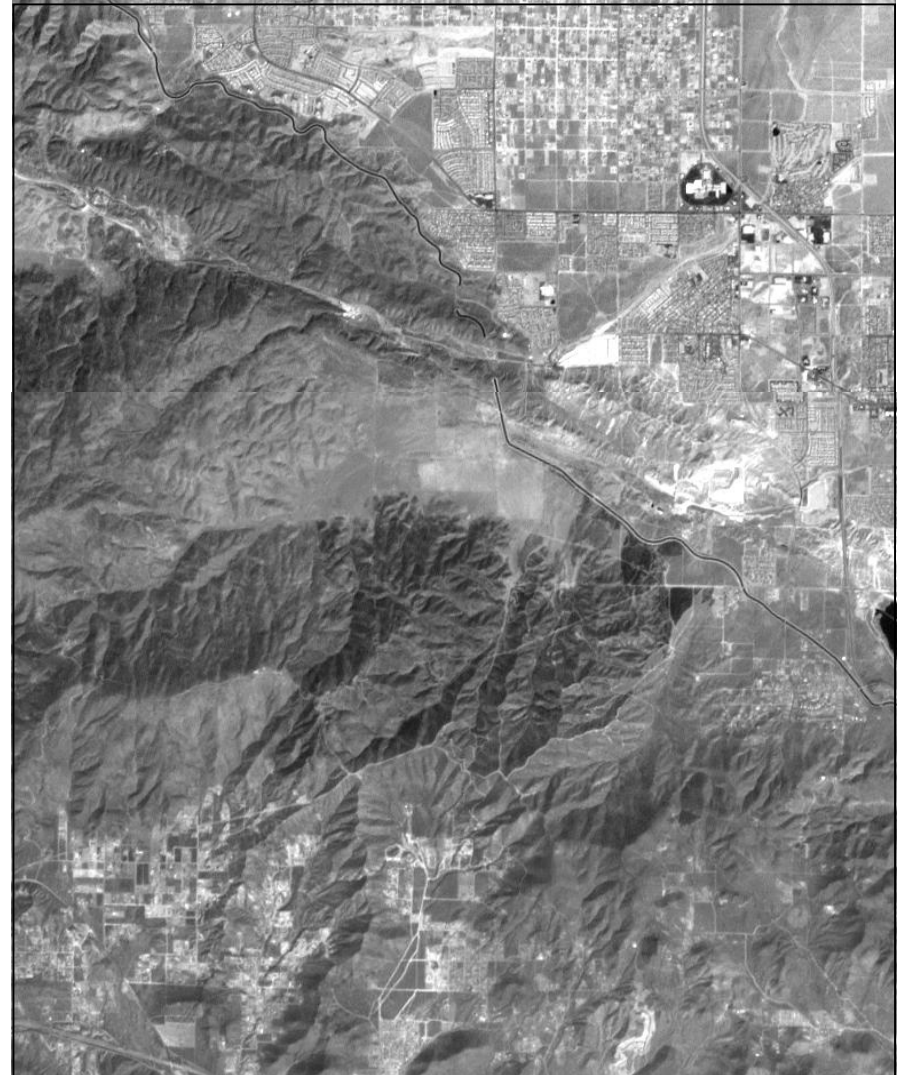
**FIGURE 6** – Example of a mosaic of four USGS digital orthophoto quarterquads covering Ritter Ridge Quadrangle. The inset demonstrates the high spatial resolution (1-meter) of the imagery.

**Sensor:** Airborne Cameras

**Algorithm:** Grayscale



(a)



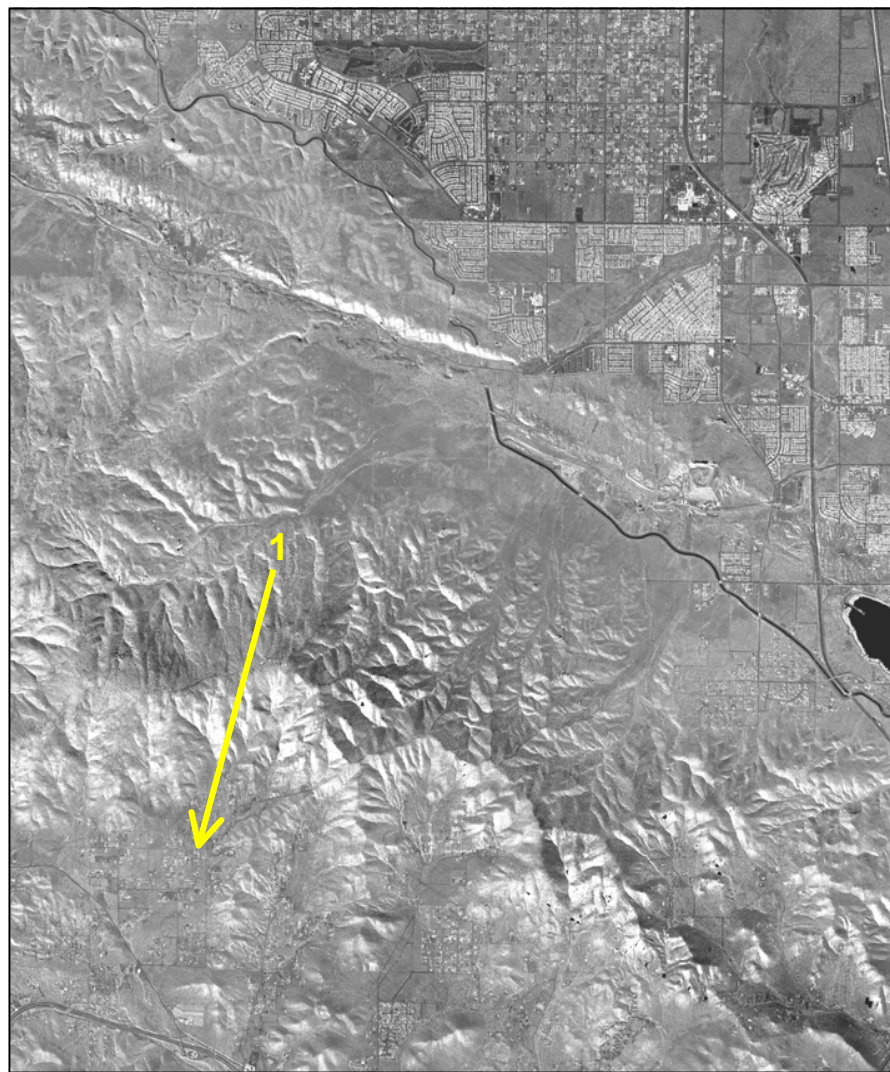
(b)

**FIGURE 7** – Examples of Landsat 7 ETM multispectral 30-meter (a) and panchromatic 15-meter (b) imagery covering Ritter Ridge Quadrangle. As one zooms in on both images, the difference in their spatial resolutions becomes more conspicuous.

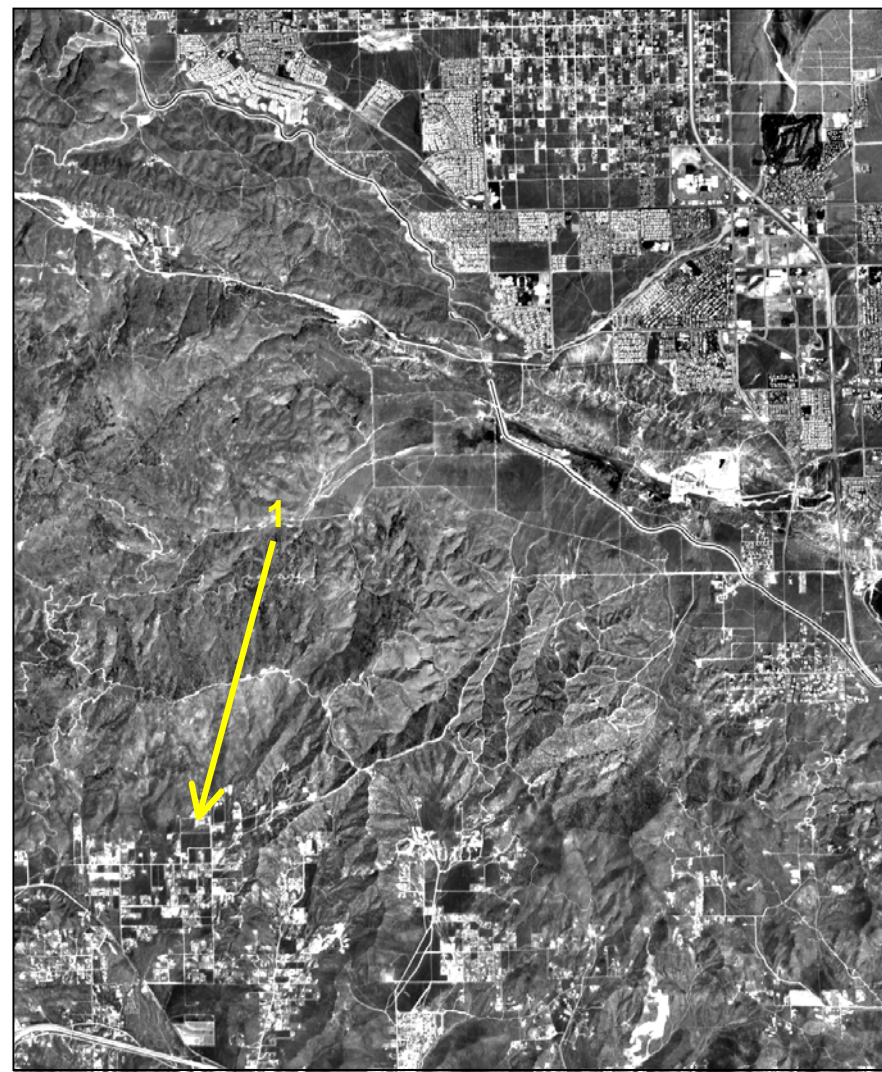
**Sensor:** Landsat 7 ETM

**Algorithm:** (a) Color-Infrared Composite, (b) Grayscale

**Band Order:** (a) 4, 3, 2



(a)



(b)

**FIGURE 8** – Examples of an Intermap Technologies X-band radar image at 2.5-meter spatial resolution (a) and a SPOT panchromatic image at 10-meter spatial resolution (b) covering Ritter Ridge Quadrangle. The look direction of the radar is from southwest to northeast. The difference between low-angle illumination recorded from an airplane (a) and high-angle illumination from a satellite (b) is apparent. The SPOT image provides a more “complete” view (topography, cultural features) of the quadrangle, but the radar image allows better discernment of topography in many places where cultural features are subdued by the display (1).

**Sensor:** (a) SAR, (b) SPOT

**Algorithm:** (a), (b) Grayscale

## Field Observations

We spent a few weeks total visiting the study area to observe conditions and characteristics of the ground surface. Done in reconnaissance (the entire study area) and in detail (specific locations in selected quadrangles), this work was designed to identify and verify features displayed on the imagery. Photographs were taken of typical landscapes and features of the area to document topography, rock/soil exposure, vegetative cover, and cultural modifications for later use in the office; a selected group of photographs that represents the study area is presented in Appendix B.

## PROCEDURES OF EVALUATION

Our approach to evaluation of the remote-sensing tools and imagery available to SHMP for the northern Los Angeles County area is summarized as follows:

### Pre-Evaluation Research of Geologic Characteristics

First, we reviewed and evaluated the usefulness and quality of the existing geologic/soils maps. The maps served in general as a means of comparison to help identify areal features shown on the imagery and as a “check” for spectral features on the images where fieldwork was not conducted.

We initially conducted reconnaissance of the entire study area, then we selected specific areas and quadrangles where utility of the imagery could be best tested. These areas and quadrangles included:

**Valyermo Quadrangle** – probably the best region in the study area for variety of terrain, landscape, and lithology. It was also studied by Perez for geologic compilation and landslide inventory.

**Juniper Hills Quadrangle** – adjacent to, and thus similar to, Valyermo Quadrangle. It was also studied by Perez for geologic compilation and landslide inventory.

**Ritter Ridge Quadrangle** – good example of landslide terrain associated with high-relief areas underlain largely by Pelona Schist. It was also studied by Perez for geologic compilation and landslide inventory.

**Region of inselbergs in eastern part of study area** – includes inliers of granitic bedrock such as Lovejoy Buttes, Saddleback Butte, and Alpine Butte as well as good examples of associated pediments and bedrock-alluvium transitions.

**Range front (transition zone) in Del Sur-Lake Hughes area** – example of abrupt transitional boundaries between bedrock ridges along San Andreas Fault Zone and alluvial fans and plains of Antelope Valley. This environment contrasts with that of the more-gradual bedrock-alluvium transitions of the Valyermo-Juniper Hills area.

## Evaluation of Sensor Characteristics

We briefly evaluated the sensors for the following characteristics of their products:

- Availability of images (number of archive scenes, different times of year, etc.)
- Spatial resolution of images
- Spectral resolution of images
- Cost of products
- General applicability to the study area

## Methods of Processing the Imagery

Following our review of the geology and soils data, we applied standard digital processing to the remote-sensing data and imagery to extract information for interpretation of the geology of the study area. We did not perform corrections to the ASTER scene.

All imagery was processed and observed on ENVI (versions 3.5 and 3.6.), a standard off-the-shelf commercial software package. Another commercial image-processing package, ILWIS (version 3.1), was used to generate anaglyph stereo and epipolar stereo images, which were viewed with either a mechanical stereoscopic viewer (ScreenScope) or anaglyph glasses directly on a computer monitor. Finally, MapInfo, a desktop GIS, was used occasionally to display images when rapid panning and a range of zoom views were required.

As needed during preparation of the imagery for evaluation and for use by SHMP staff, “subsetting” (extraction of portions of scenes), conversion of projection to the State Plane coordinate system (NAD27, California Zone V), and warping were conducted on the remote-sensing data to allow overlaying of vector data on the images for analysis.

We applied the following *basic displays, transformations, topographic modeling, classification, and combination images* to the package of remote-sensing data described above. Examples of each are presented in a set of companion figures that encompass the Valyermo 7.5-minute quadrangle; to give the reader some familiarity with the geology of this quadrangle, a geologic map of the quadrangle (Dibblee, 2002c) is presented in Figure 9.

***Basic Displays – bands are displayed singly or in combination in either grayscale or color without any mathematical manipulation of the digital data.***

- **Single-Band Grayscale (Figure 10a)** – applied to data from several sensors including the Intermap radar files, DOQQ, SPOT, and band ratios,

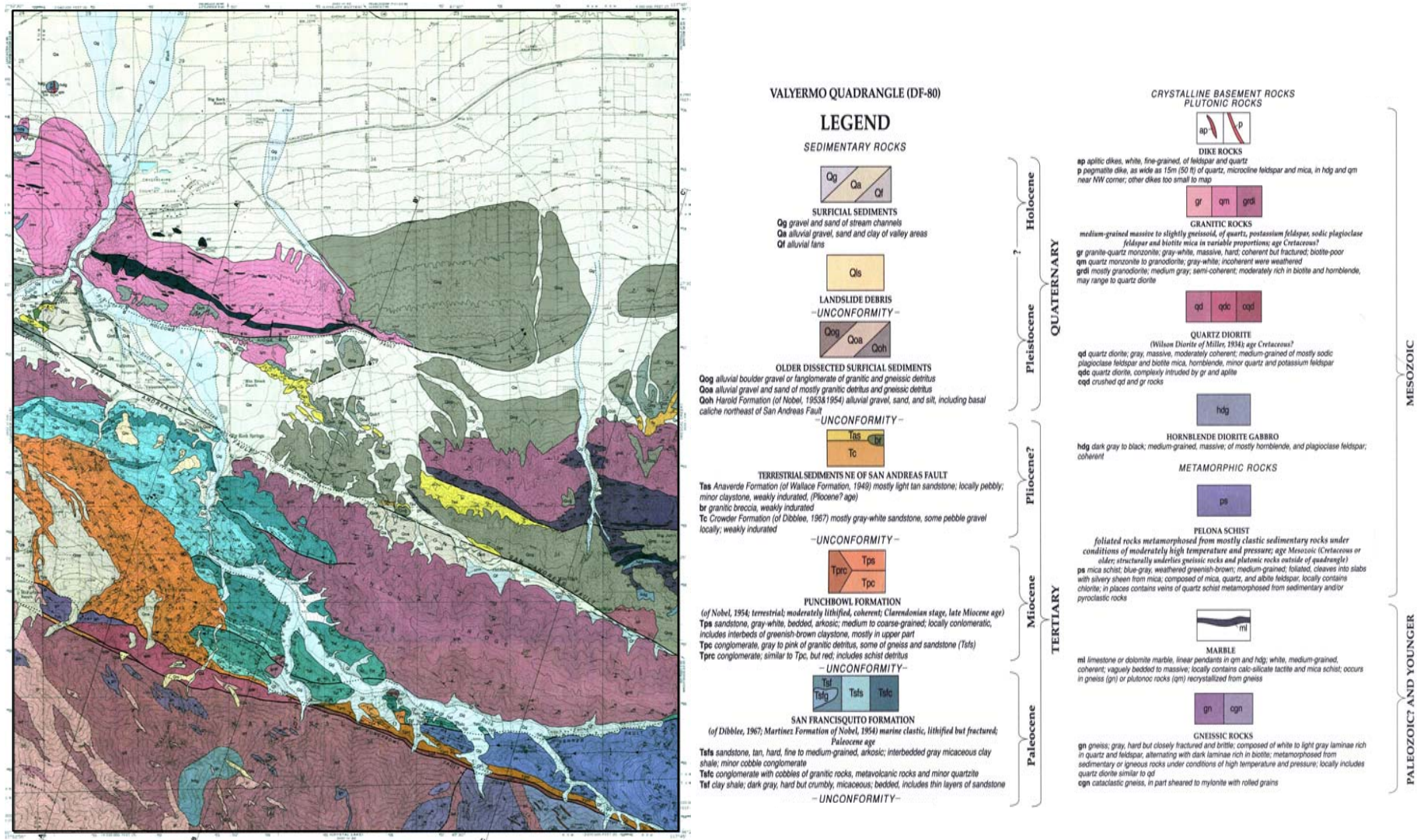
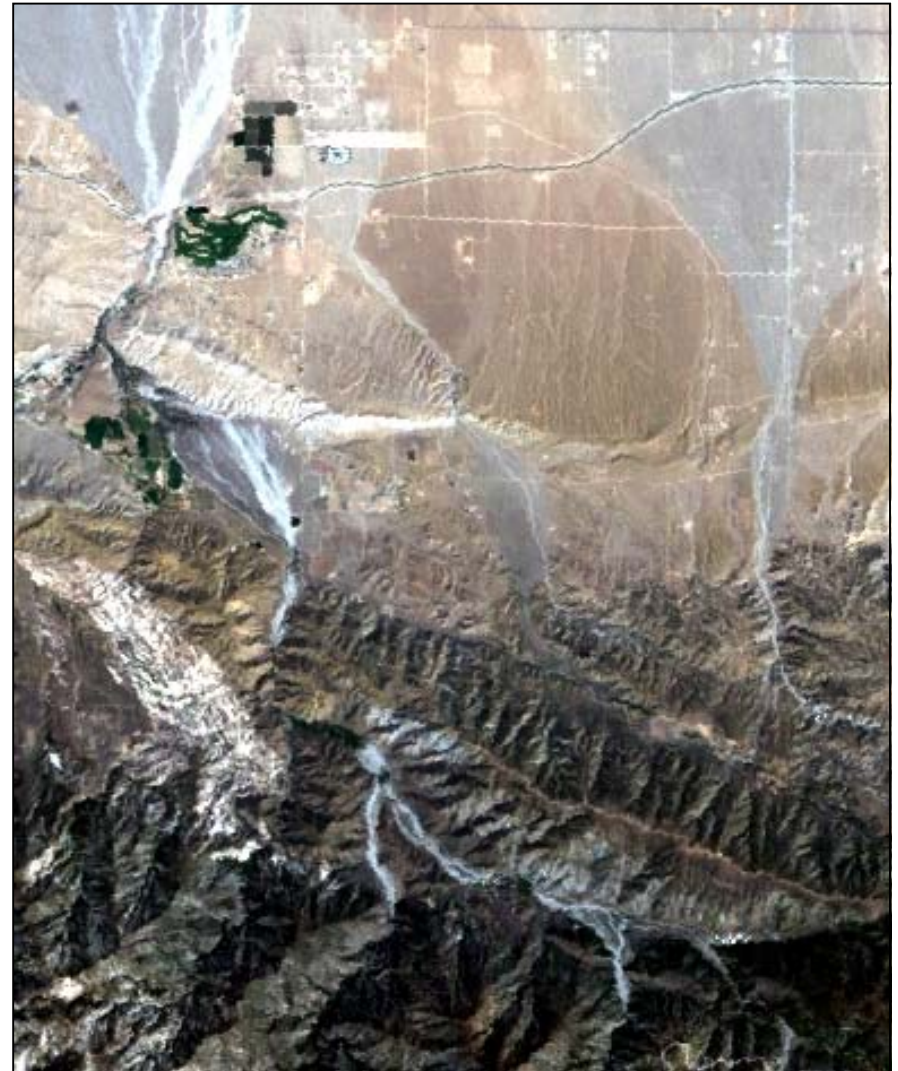


**FIGURE 9 –** Geologic map of Valyermo Quadrangle after Dibblee (2002c).



(a)



(b)

**FIGURE 10** – Basic displays of Valyermo Quadrangle as a) single-band grayscale image and b) true-color composite image. The true-color image has been “contrast-stretched” to improve detail and differentiation of features, which were highly subdued in the original non-enhanced version of the image.

**Sensor:** Landsat 7 ETM

**Algorithm:** (a) Grayscale, (b) True-Color Composite

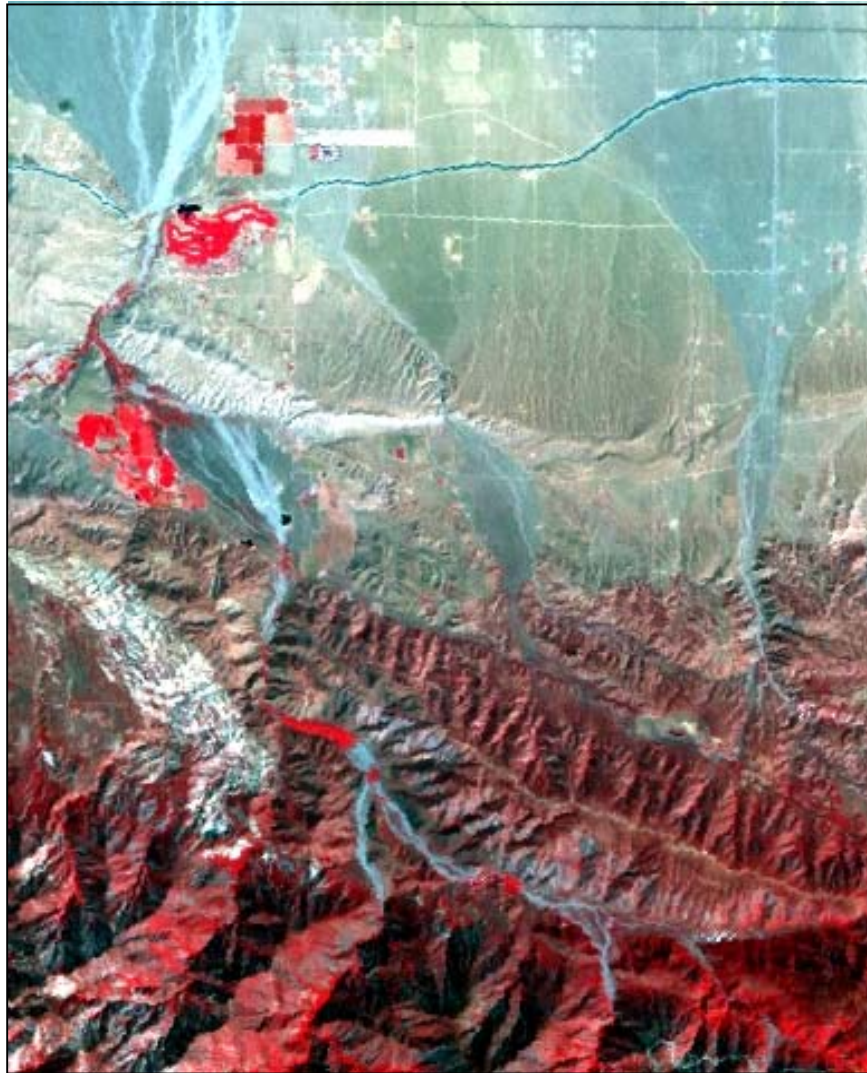
**Band Order:** (a) 5, (b) 3, 2, 1

as well as Landsat and ASTER panchromatic, this display is the simplest form of processing in that the data from only one band are displayed as an image.

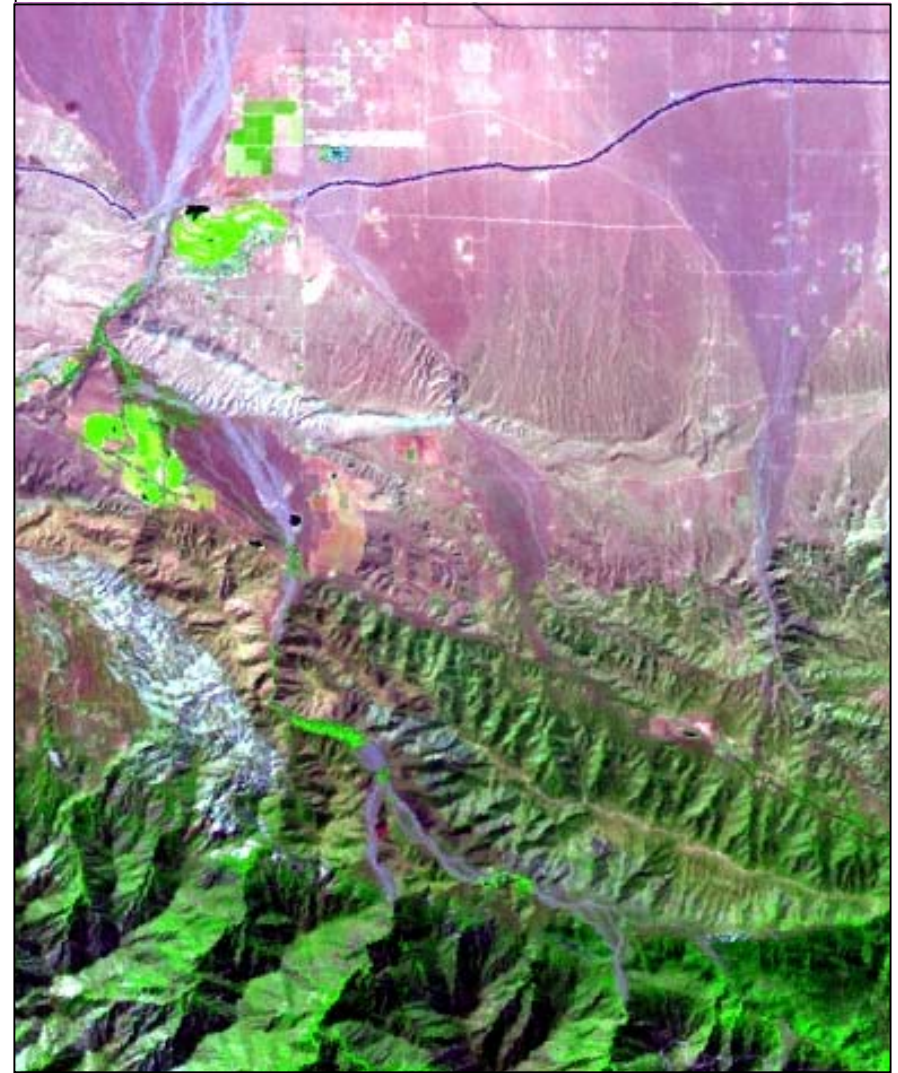
- **True-Color Composite (Figure 10b)** – limited to Landsat 7 only, this image displayed the study area as it would appear to the human eye if observed from the air. Data from Bands 1, 2, and 3, which represent the wavelength intervals for blue, green, and red, respectively, are combined to generate the image.
- **Color-Infrared Composite (Figure 11a)** – applied to both ASTER and Landsat 7, this composite is equivalent to the “false-color infrared” of conventional aerial photography. It combines the green and red bands of the visible part of the spectrum and a near-infrared band.
- **False-Color Composite (Figure 11b)** – applied to both ASTER and Landsat 7, these images resulted from various combinations of three bands at a time, each band being assigned either red, green, or blue. The above two composites (true-color and color-infrared) are specific examples.
- **Color Mapping (Figure 12)** – application of color, via color tables, to any grayscale image (native or derivative) to enhance subtle differences that are less obvious when viewed in shades of gray. For example, color tables were applied to the SPOT panchromatic and Intermap radar images to bring out textural differences.

***Transformations*** – image-processing operations that “transform” the data by mathematical algorithms into other forms or space. The main purpose of transformation is to improve visual presentation of the data so that the image is more easily interpreted and thus more information can be extracted.

- **Image Sharpening (Figure 13)** – applied to Landsat 7 and ASTER, this process merges an image of lower spatial resolution with an image of higher spatial resolution. The result is an image that shows multispectral properties at higher detail.
- **Band Ratios (Figure 14)** – applied to the six Landsat 7 bands and the various sets of ASTER bands, these algorithms use one band as the numerator and another band as the denominator in a mathematical ratio for each pixel. The result is an image that reduces the effects of topography and enhances the spectral differences between bands.
- **Principal Components Analysis (PCA) (Figure 15a)** – applied to ASTER and Landsat 7, this mathematical procedure involves transforming the original data values from a standard X-Y coordinate system into a new coordinate system that increases the “variance” of the data (see Lillesand and Kiefer, 2000, p. 518). This transformation is important for three reasons: 1) Reduces the dimensionality of the dataset, 2) segregates noise that is present in the bands, and 3) produces new “bands,” or



(a)



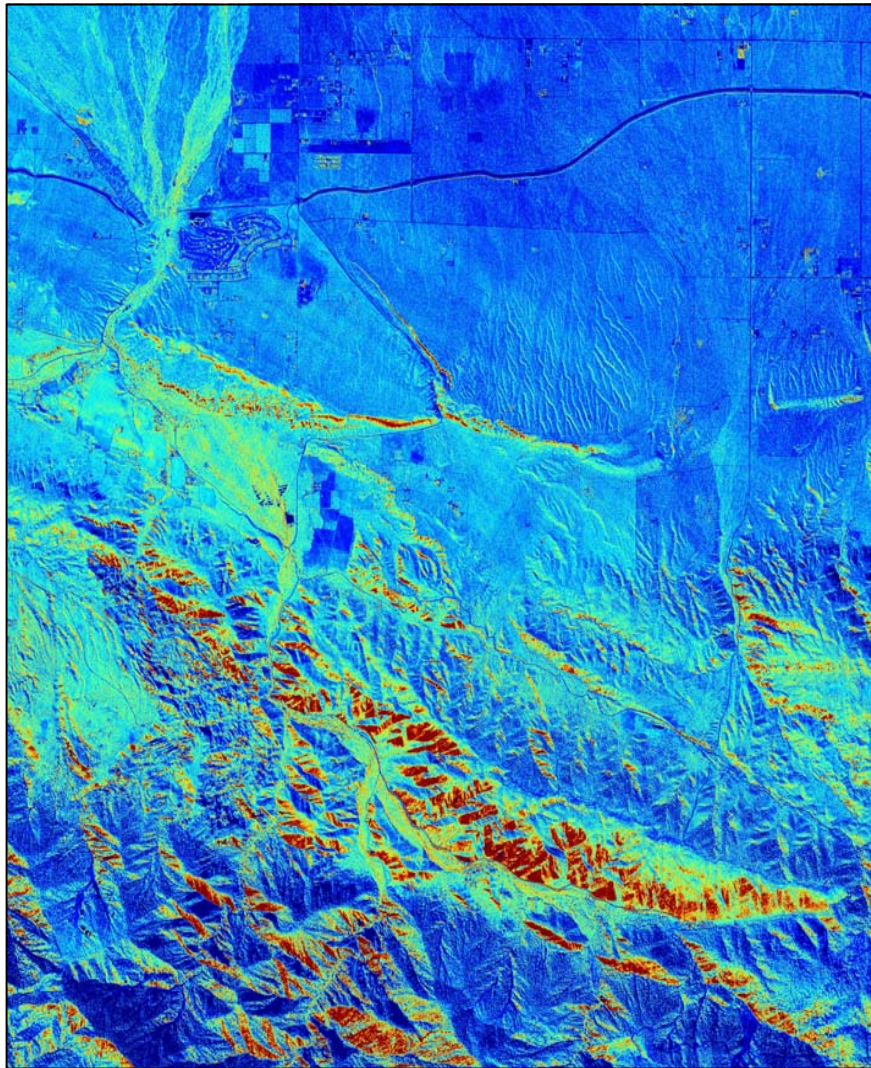
(b)

**FIGURE 11** – Basic displays of Valyermo Quadrangle as a) color-infrared composite image and b) false-color composite image.

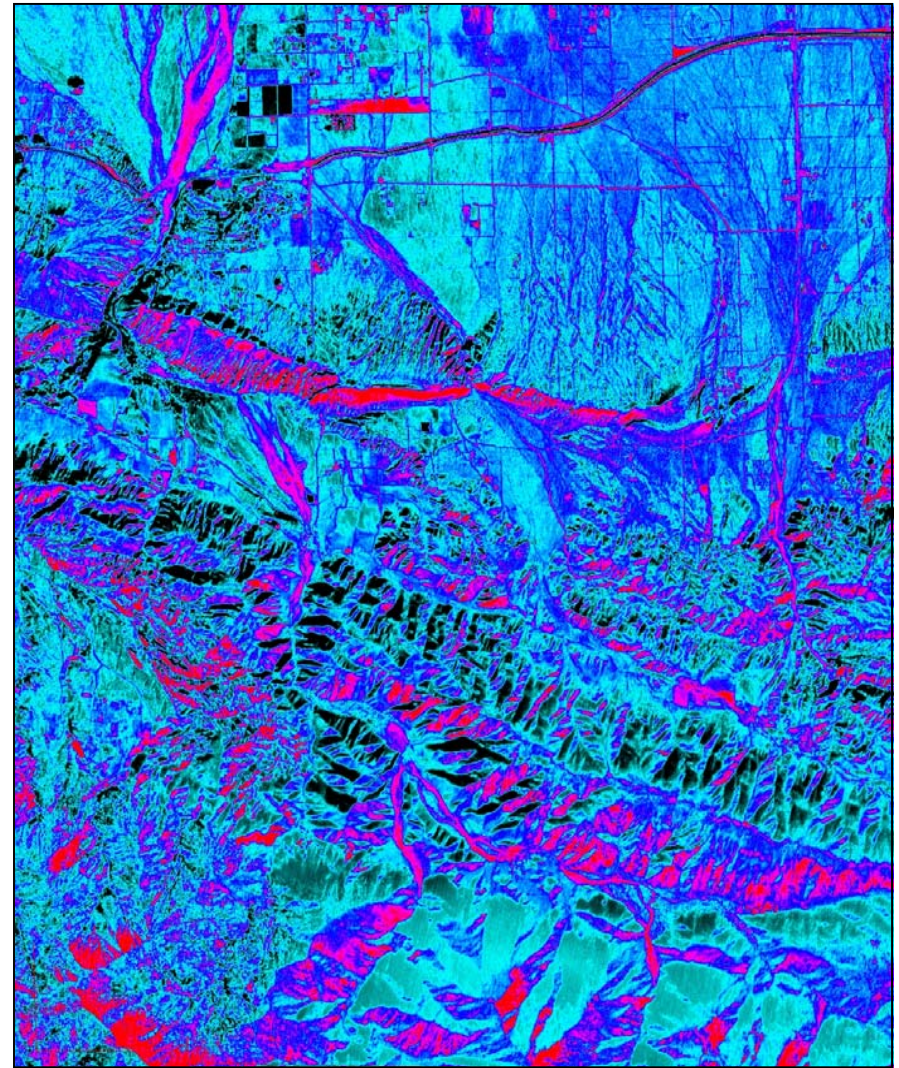
**Sensor:** Landsat 7 ETM

**Algorithm:** a) Color\_infrared Composite b) False-Color Composite

**Band Order:** a) 4, 3, 2, b) 1, 2, 3



(a)

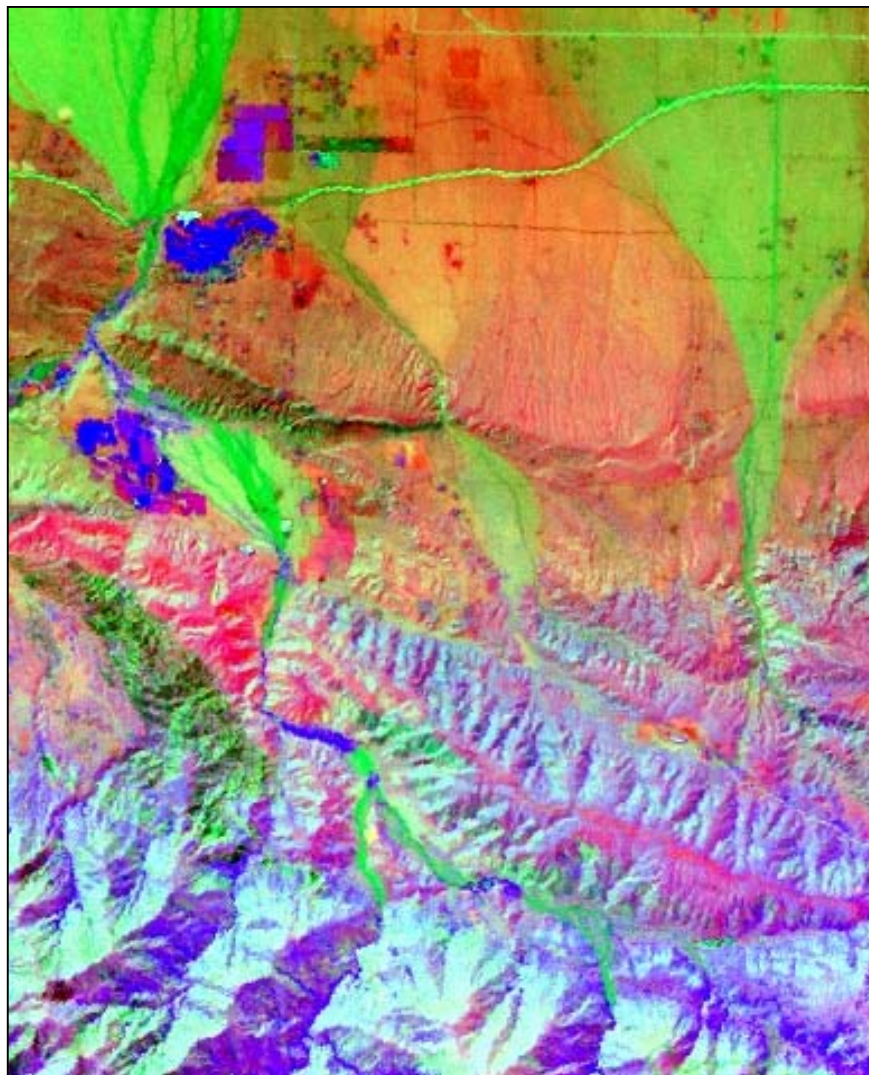


(b)

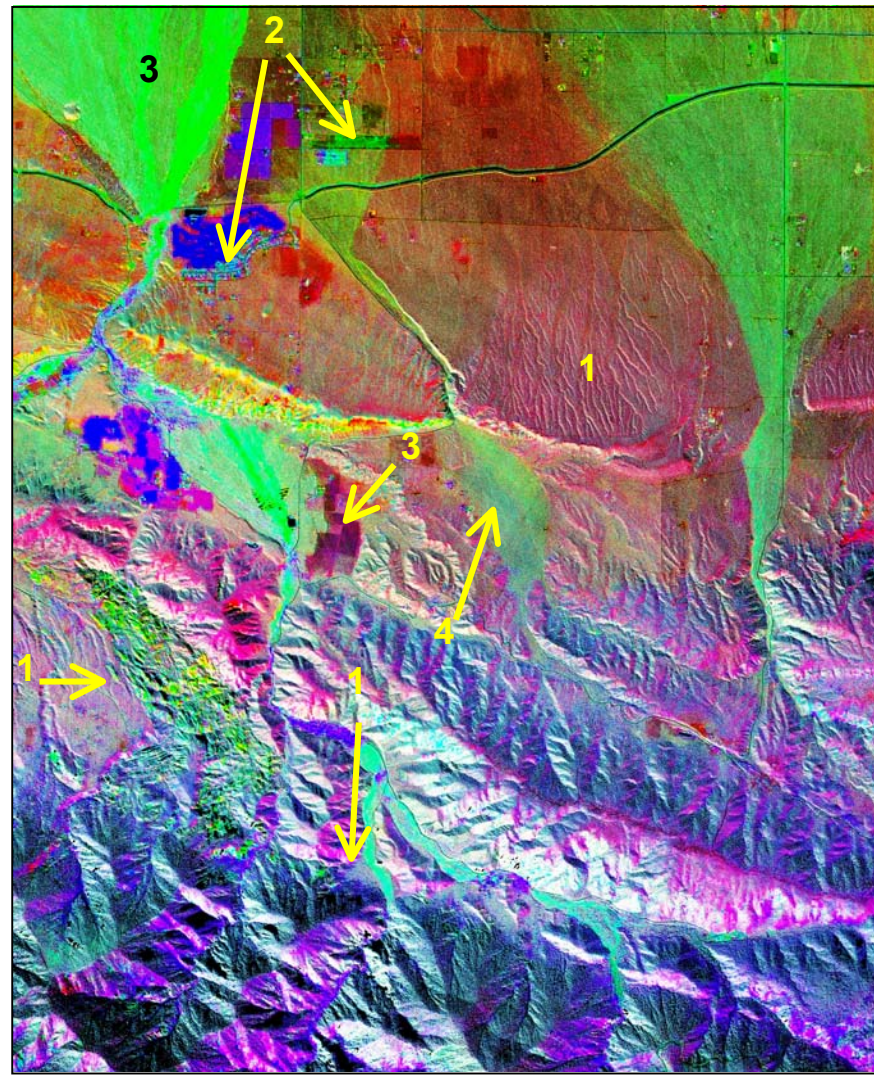
**FIGURE 12** – Basic displays of Valyermo Quadrangle using color mapping on a) Intermap Technologies X-band radar image and b) SPOT panchromatic image.

**Sensor:** (a) SAR, (b) SPOT

**Algorithm:** Grayscale; Color Table (Red-Blue)



(a)



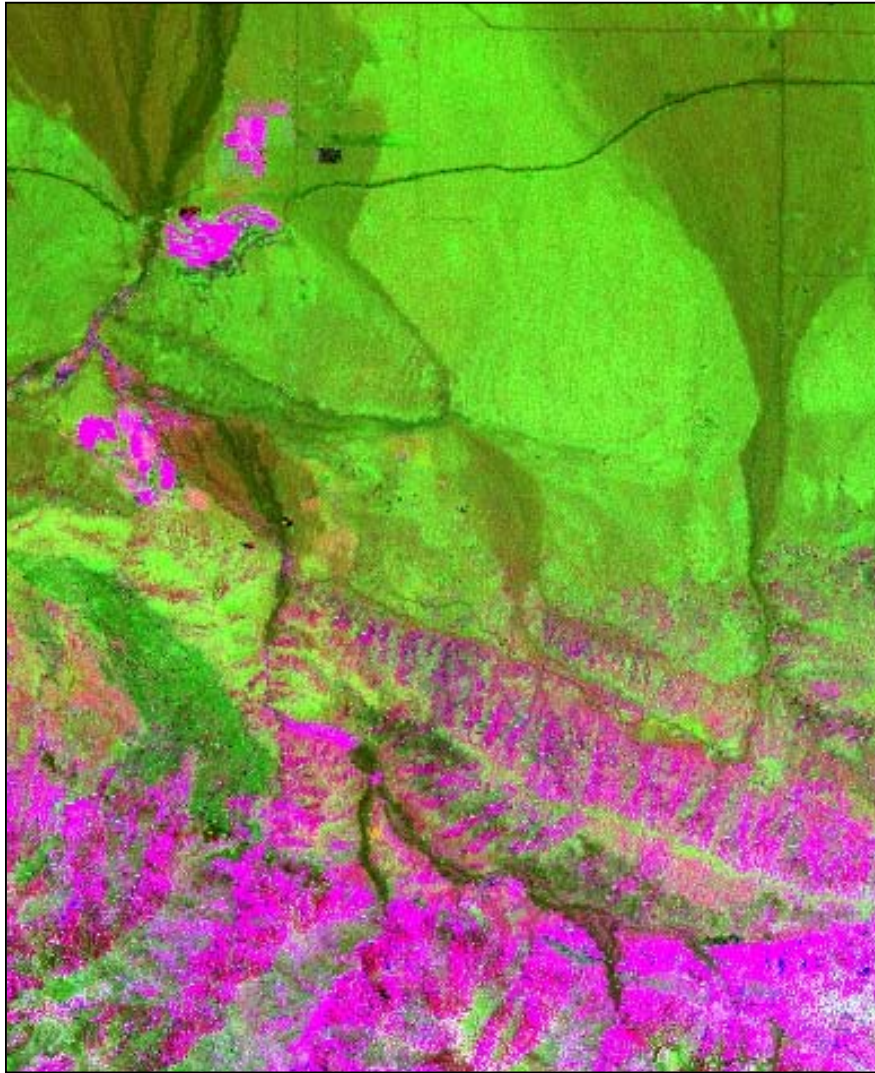
(b)

**FIGURE 13** – Display of Valyermo Quadrangle using image-sharpening transformation of a low-resolution image (a) with a high-resolution image (b). In (b), sharper topographic and cultural detail are observable at (1) and (2), respectively. This image also demonstrates some gain (3) and loss (4) of spectral information from the transformation.

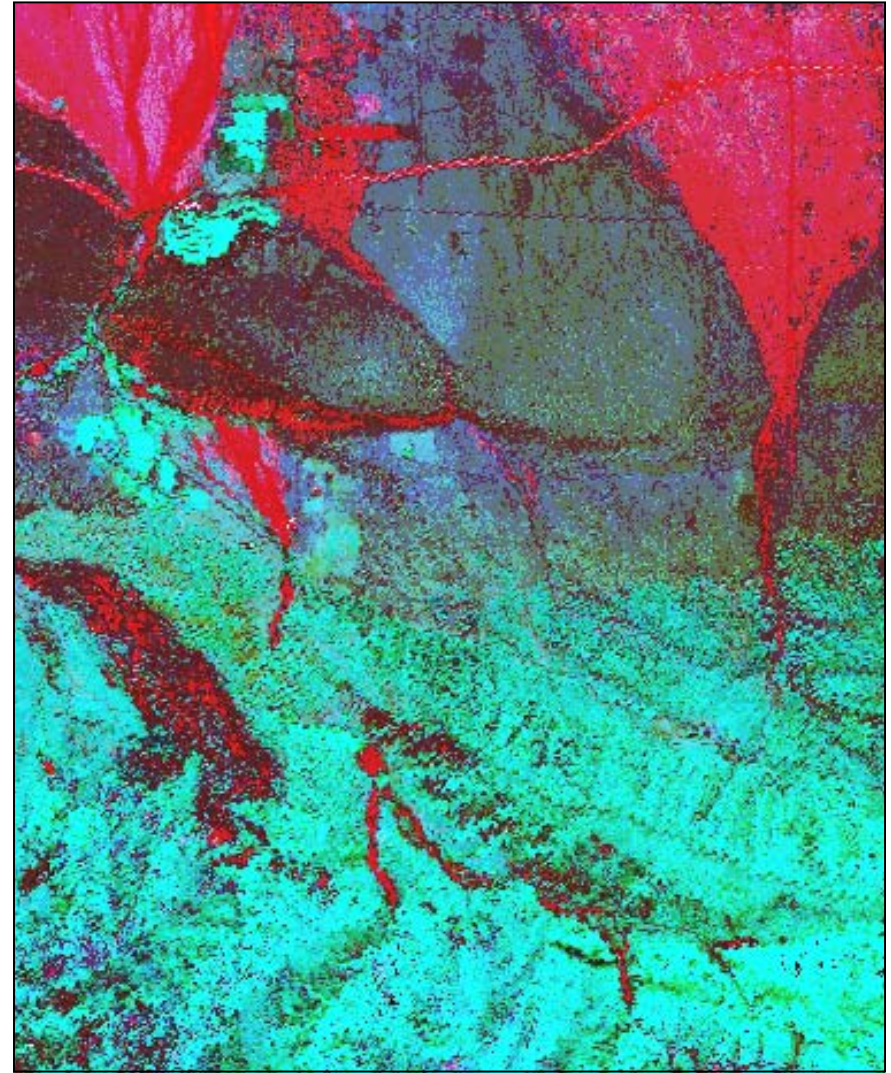
**Sensor:** a) Landsat 7 ETM, b) Landsat 7 ETM plus SAR

**Algorithm:** a) False-Color Composite, b) Image Sharpening, Color Normalization

**Band Order:** 4, 3, 2



(a)



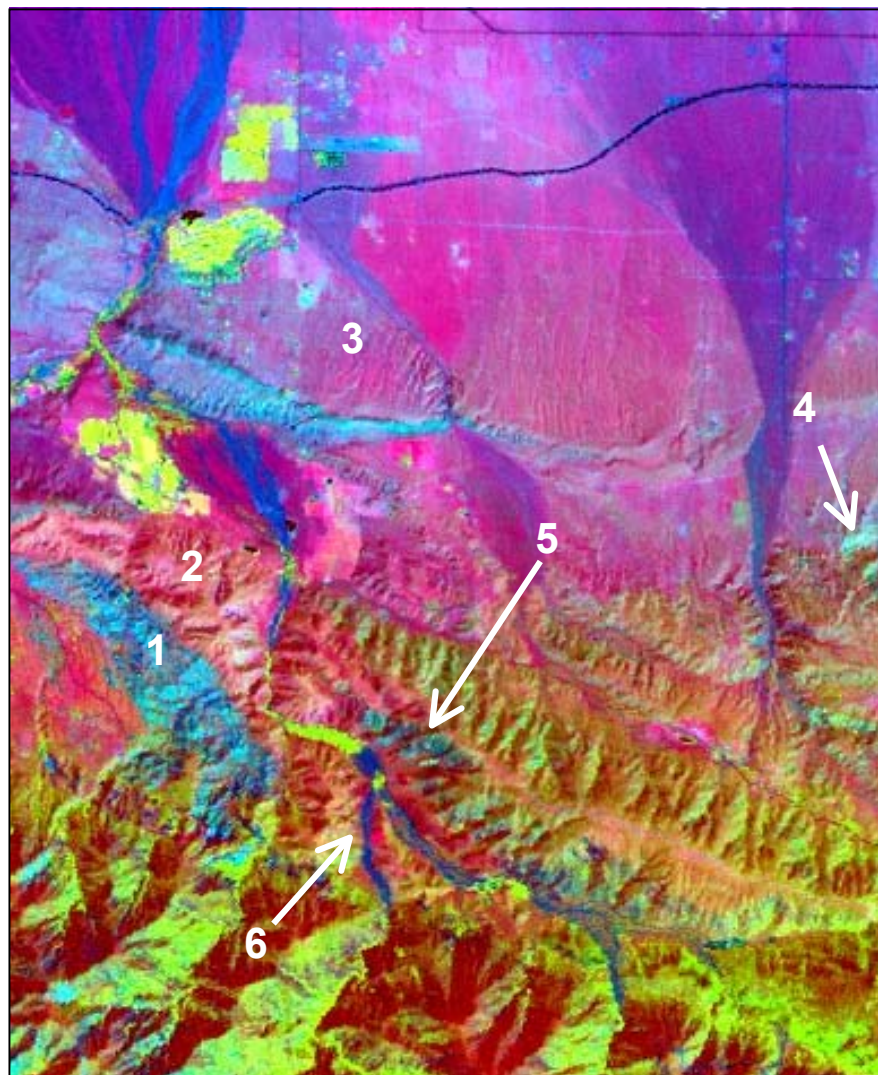
(b)

**FIGURE 14** – Display of Valyermo Quadrangle using a single band-ratio transformation (a) and a complex band-ratio transformation (b). The capability of band-ratioing to subdue topography is apparent.

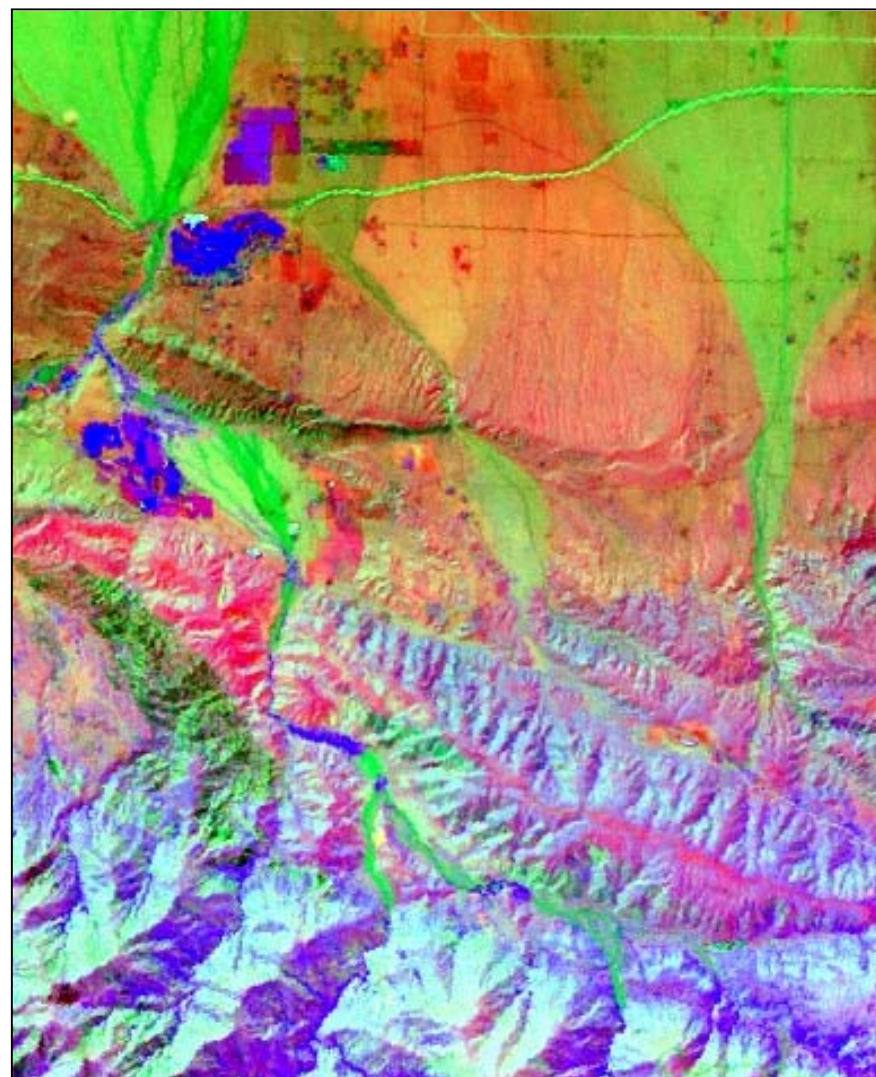
**Sensor:** Landsat 7 ETM

**Algorithm:** Band Ratios

**Band Order:** a) 5/3, b) 2/4, 5/3, 7/3



(a)



(b)

**FIGURE 15** – Display of Valyermo Quadrangle using a principal-components transformation (a) and a minimum-noise-fraction transformation (b). Examples of geologic features include: 1) Devils Punchbowl Formation (blue), 2) San Francisquito Formation (pink), 3) possible slopewash (pink) over granitic rock (blue), 4) Tertiary sedimentary rock (blue), 5) possible quartz diorite bodies (blue), and 6) modern alluvium (dark blue).

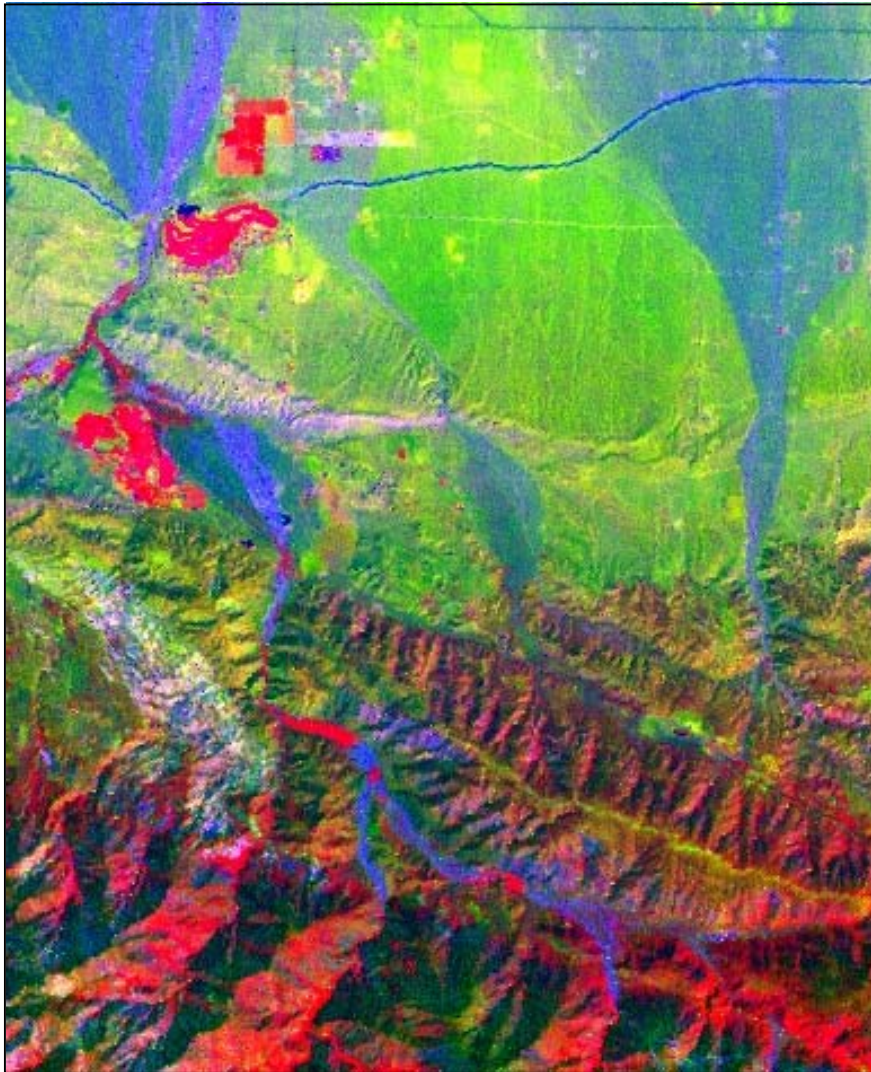
**Sensor:** Landsat 7 ETM

**Algorithm:** a) Principal Component Analysis, b) Minimum Noise Fraction

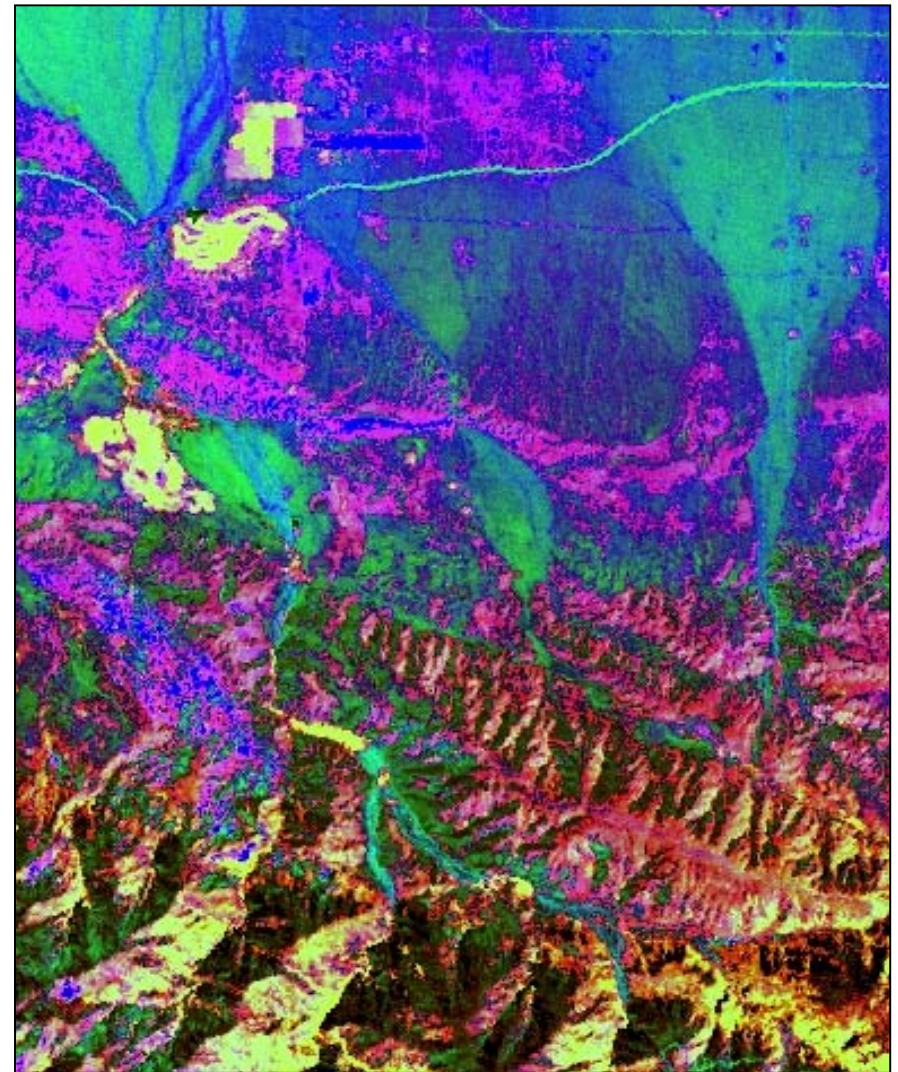
**Band Order:**

“components,” that are uncorrelated, meaning the bands convey information that is different from one band to the next. The first two bands (Principal Component 1 and Principal Component 2) contain nearly all of the “variance” in the data.

- **Minimum Noise Fraction (MNF) Rotation (Figure 15b)** – applied to ASTER and Landsat 7, it differs from standard principal components analysis mentioned above in that it consists of two cascaded principal component transformations rather than one. In the first transformation, noise is decorrelated and rescaled. In the second transformation, the noise-“whitened” data are processed by standard principal components analysis. The main purpose of MNF is removal of noise from the useful (signal) data, which results in improved spectral properties of the image. An additional purpose is to determine the dimensionality of the data.
- **Decorrelation Stretch (DS) (Figure 16a)** – applied to ASTER and Landsat 7, this process produces images that commonly show more vivid color. The original multispectral data collected by the sensor are generally “highly correlated”, which means that the data do not differ much from band to band; as a result, the overall color of an image is typically represented by bland pastels, which do not aid interpretation. Decorrelation stretch uses principal components analysis to recalculate the data in a way that reduces this high correlation. It differs from the principal components analysis described above in that it “stretches,” or exaggerates, the differences in the less-correlated data, so that saturation of colors in the image are increased to help interpretation.
- **Color Transform (Figure 16b)** – applied to ASTER and Landsat 7, these transformations convert an RGB image to different color “spaces” such as HSV (hue-saturation-value, which is known also as IHS for intensity-hue-saturation) and HLS (hue-lightness-saturation) and then back to RGB space for viewing. The advantage of different color spaces over conventional RGB displays is that they tend to make colors in the derived images more intense (saturated) and more similar to what is perceived by the human eye. This transformation converts a bland, pastel-dominated image (RGB) into a more vivid image that allows for improved discrimination of patterns and features. Also, these transforms can be used to merge lower-resolution data from a multispectral sensor with higher-resolution data from a panchromatic sensor.
- **Saturation Stretch (Figure 17)** – increases the saturation of colors of three RGB input bands to enhance the color contrast of an image. It differs from a decorrelation stretch by the process of transformation: rather than using principal components, this algorithm is a simple transformation from RGB space to HSV color space (hue-saturation-value bands). It differs from a standard color transform by applying a stretch on the saturation band to fill the entire range of saturation.
- **Synthetic Color Image (Figure 18)** – transforms a grayscale image into a color image; it is commonly used with single-band radar data. It differs from the “color mapping” described above by applying “high-pass” and



(a)



(b)

**FIGURE 16** – Display of Valyermo Quadrangle using a decorrelation-stretch transformation (a) and a color transform (b). In places in the northern two-thirds of the quadrangle, the color-transform image shows strong color-differentiation of details that are not as conspicuous on the decorrelation-stretch image.

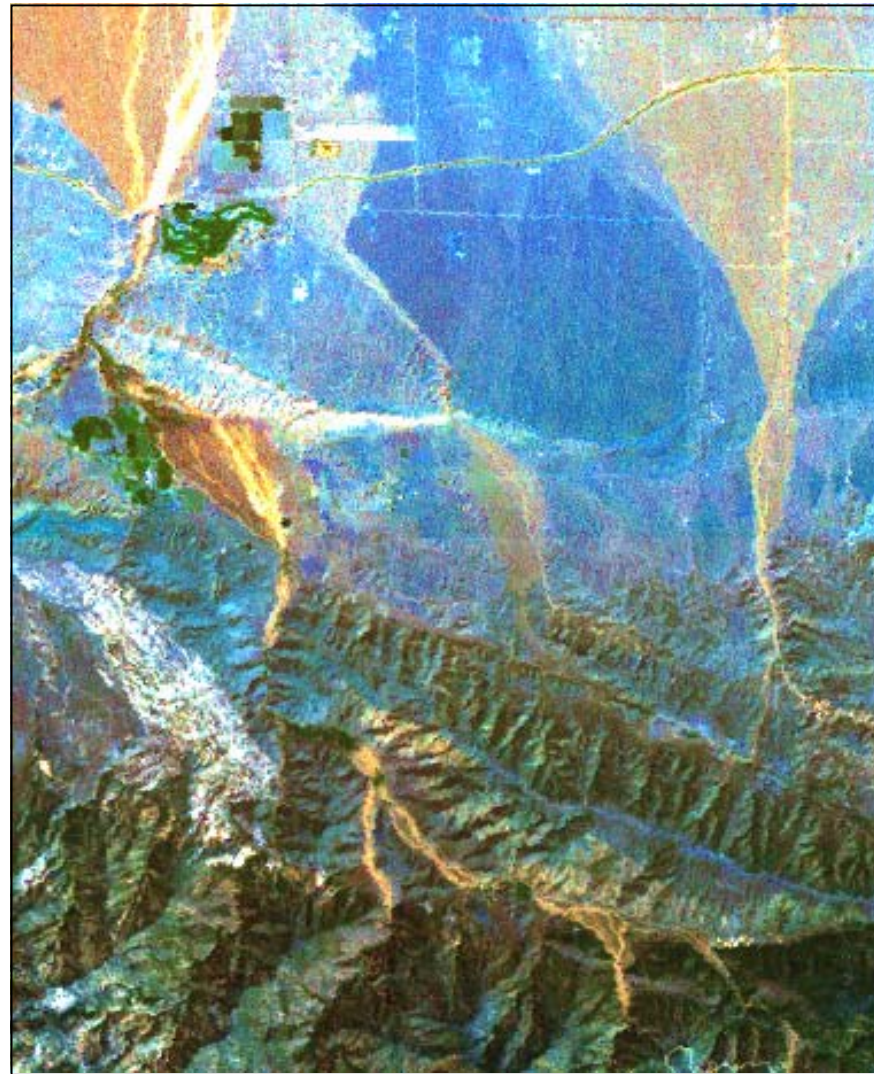
**Sensor:** Landsat 7 ETM

**Algorithm:** a) Decorrelation Stretch, b) Color Transform

**Band Order:**



(a)



(b)

**FIGURE 17** – Display of Valyermo Quadrangle showing a true-color composite (a) that has been transformed by a saturation stretch (b).

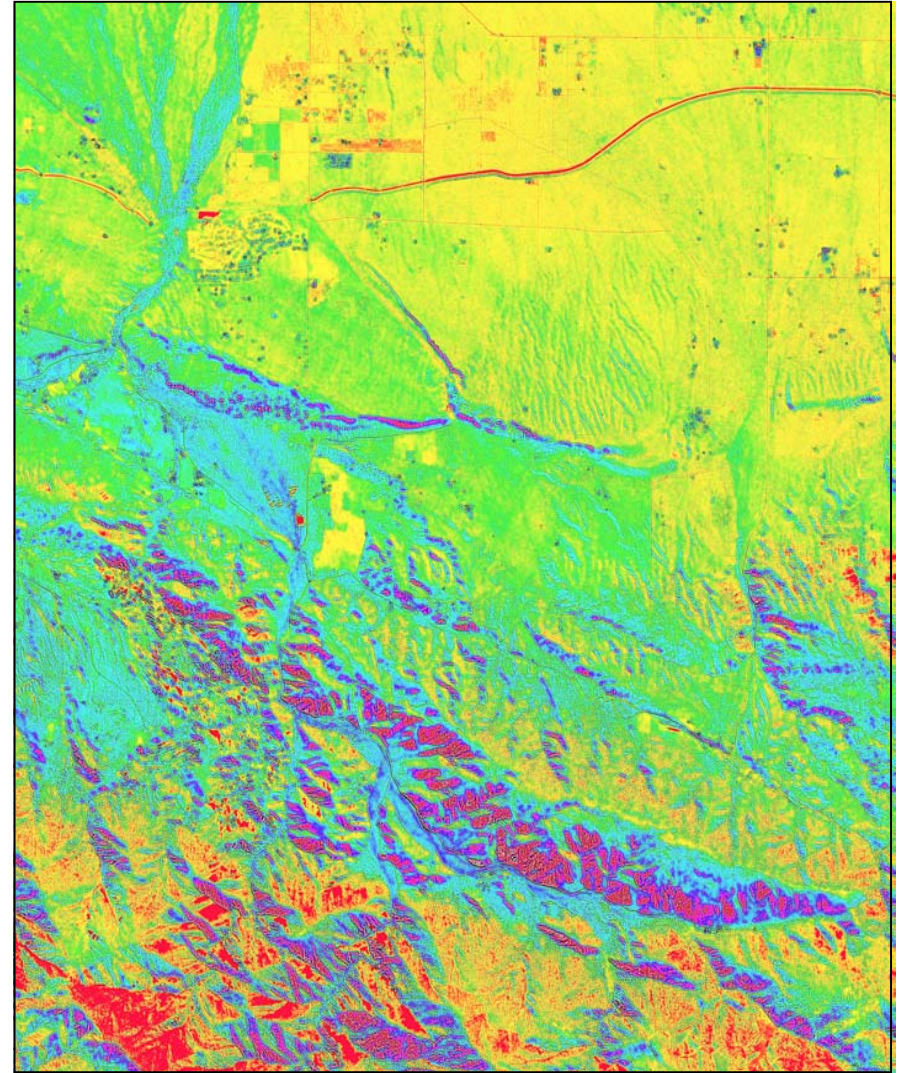
**Sensor:** Landsat 7 ETM

**Algorithm:** a) True-Color Composite, b) Saturation Stretch

**Band Order:** 3, 2, 1



(a)



(b)

**FIGURE 18** – Display of Valyermo Quadrangle by transforming a grayscale Intermap Technologies X-band radar image (a) into a synthetically colored image (b). In the synthetic color image, topography is subdued, and there is a noticeable loss of textural and cultural detail.

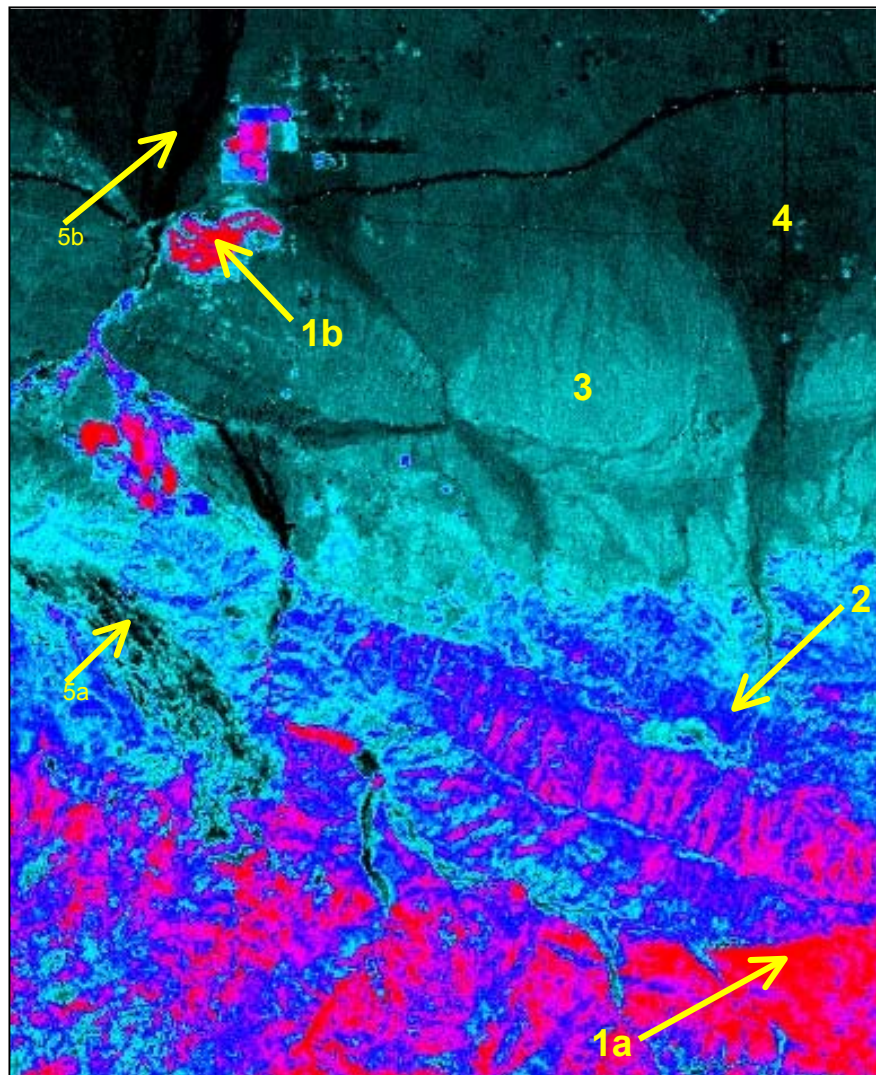
**Sensor:** SAR

**Algorithm:** a) Grayscale, b) Synthetic Color Image (Color table: Hue Sat Lightness 2)

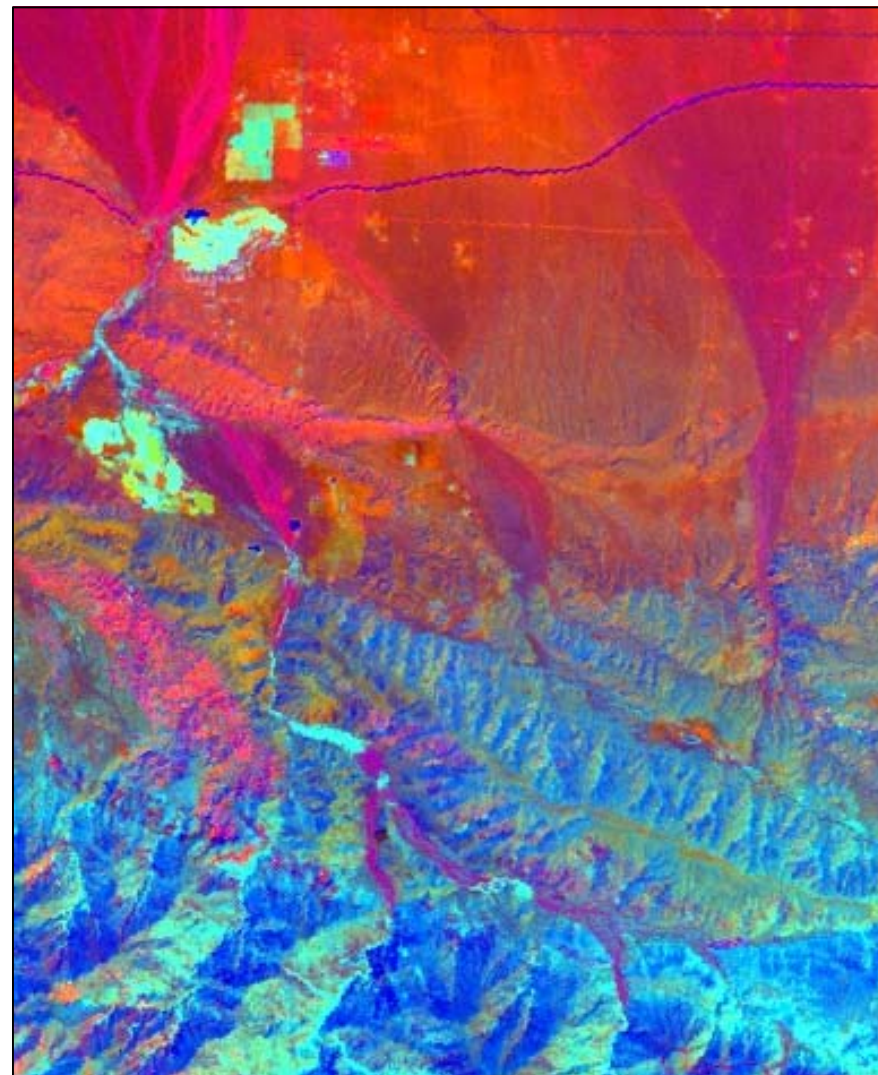
- “low-pass” filters to the grayscale image to separate high- and low-frequency information. In radar, high-frequency features are commonly caused by small-scale topography, whereas low-frequency features are caused by scattering from lithology and vegetation.
- **Normalized Difference Vegetation Index (NDVI) (Figure 19a)** – applied to Landsat 7, this algorithm is designed to show the distribution of healthy green vegetation in an image by ratioing of Bands 3 (red) and 4 (near-infrared); green vegetation shows high reflectance in Band 4, whereas bare rock and soil typically produce an index near zero because reflectance values of both materials are similar in both bands.
  - **Tasseled Cap (Figure 19b)** – applied to Landsat 7 data as a more sophisticated vegetation index than NDVI, this transformation uses an orthogonal rotation of the band data to produce three components that can be mapped in RGB color space: *Brightness* (red), which equates with soil, *Greenness* (green), which equates with amount of green vegetation, and *Third* (blue), which equates with soil and canopy features, including moisture.

**Topographic Modeling – potentially improves interpretation of images by adding a 3-dimensional effect to them.**

- **Shaded Relief (Figure 20)** – these grayscale images were derived from both the USGS 10-meter and the Intermap 5-meter DEM data sets. They appear as though the observer were looking down vertically, with shadows cast from an artificially-created sunlight angle that creates a sense of topography.
- **3-D Surface View (Figure 21)** – applied as an overlay of ASTER data on a 3-D surface derived from either the USGS or Intermap DEMs, this image allows one to view the selected area from different non-vertical elevations and directions. It is equivalent to a traditional oblique-view photograph.
- **Hill Shade (Figure 22a)** – a process of fusion that drapes a color image from one sensor over a shaded-relief image derived from a DEM. It adds a 3-D topographic effect to a color image, which can be a basic or transformed display.
- **Anaglyph (Figure 22b)** – a stereo image that consists of two slightly different perspectives of the same scene, which are displayed in contrasting colors (typically blue and red). When viewed with a set of eyeglasses of correspondingly colored filters, a three-dimensional image is seen. A set for the Valyermo Quadrangle was generated from the Intermap DEM data.
- **Epipolar Stereo (Figure 23)** – this imagery is the digital version of the conventional stereo pair of aerial photographs. Two aerial photographs with overlap are scanned and resampled to remove rotation and scale differences. Each point on the left image is restricted to lie on a given line on the right image, which is termed the “epipolar” line. The stereo pair is



(a)



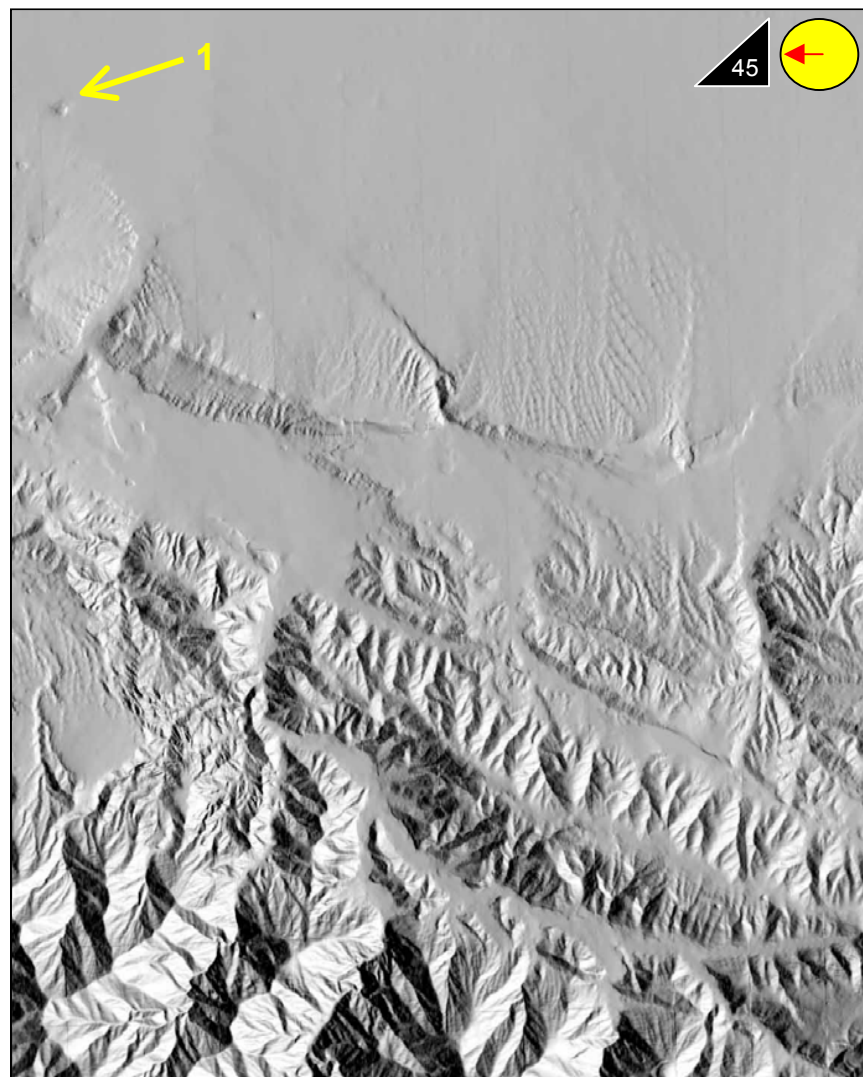
(b)

**FIGURE 19** – Display of Valyermo Quadrangle using NDVI transformation (a) and tasseled cap transformation (b). Five main vegetation regimes are apparent in the NDVI image: 1a) abundant green vegetation and 1b) irrigated vegetation; 2) moderate vegetation; 3) scattered vegetation; 4) sparse vegetation; and 5a) bare rock and 5b) active stream channels.

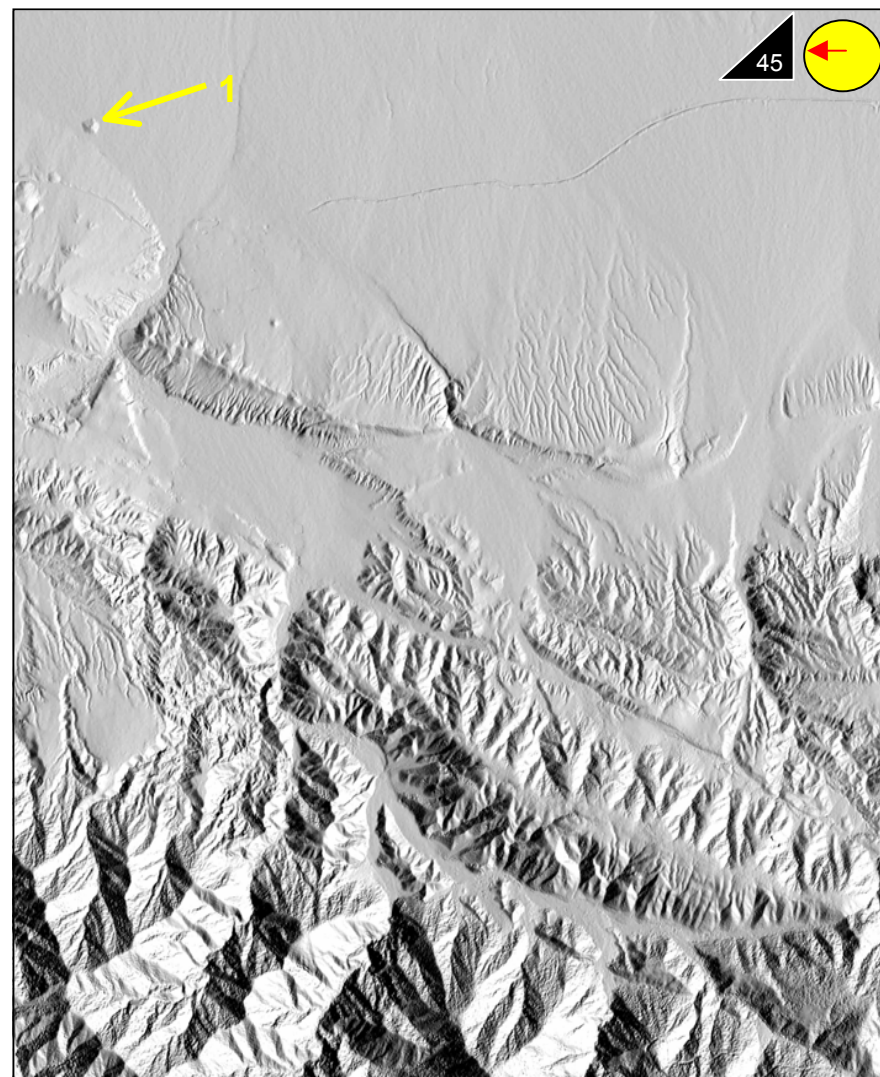
**Sensor:** Landsat 7 ETM

**Algorithm:** a) NDVI, b) Tasseled Cap

**Band Order:** a) 3, 4



(a)



(b)

**FIGURE 20** – Display of Valyermo Quadrangle as shaded-relief images generated from USGS DEM at 10-meter resolution (a) and Intermap Technologies DEM at 5-meter resolution (b). The fine texture of drainage is more apparent in (b). The bedrock inlier at (1) was obvious immediately when observing these images; the inlier was not shown on one of the published geologic maps used for zoning.

**Sensor:** a) Airborne Cameras, b) SAR

**Algorithm:** Shaded Relief

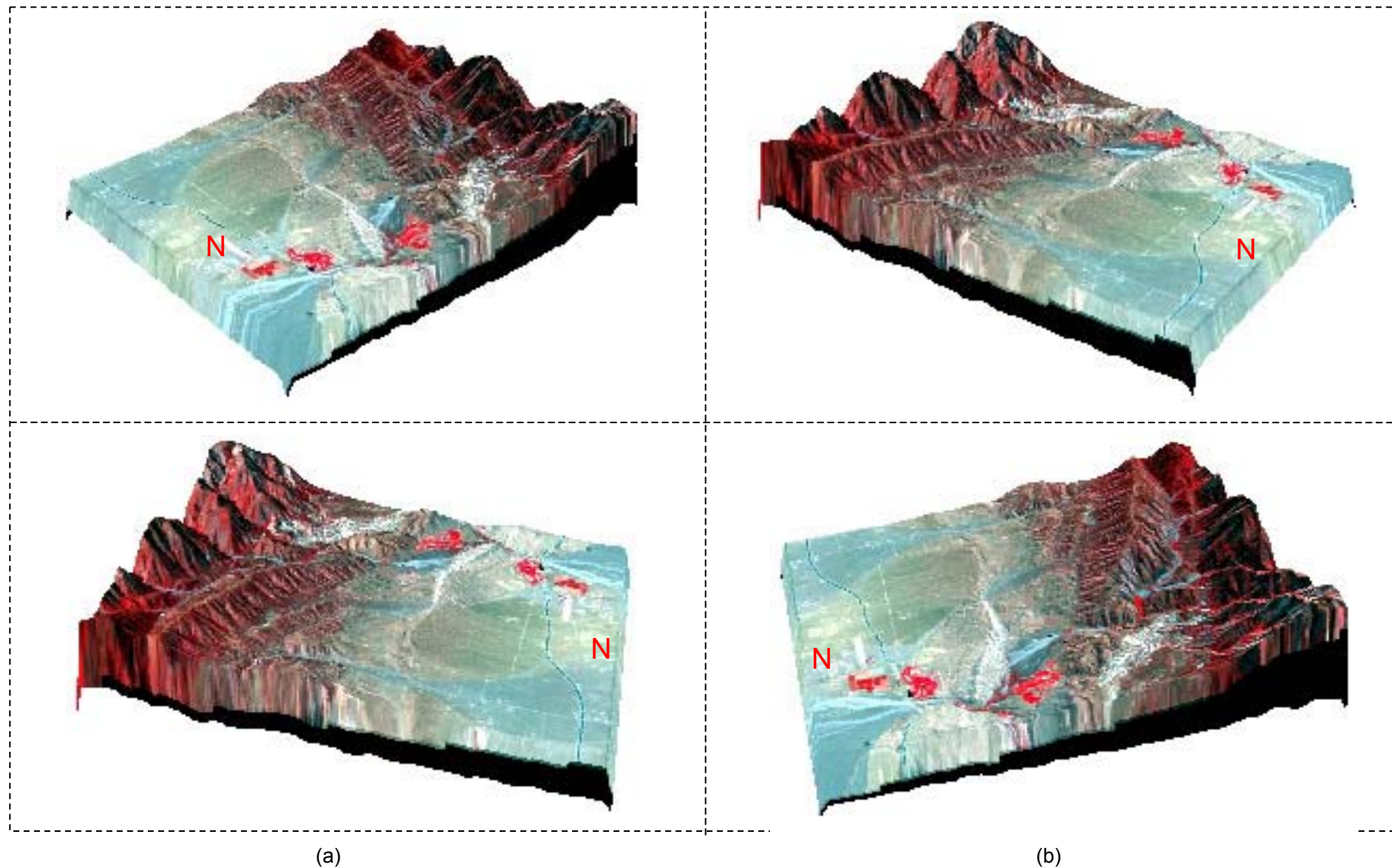


**FIGURE 21** – Display of Valyermo Quadrangle as 3-D surface views. “N” indicates the north direction of the quadrangle.

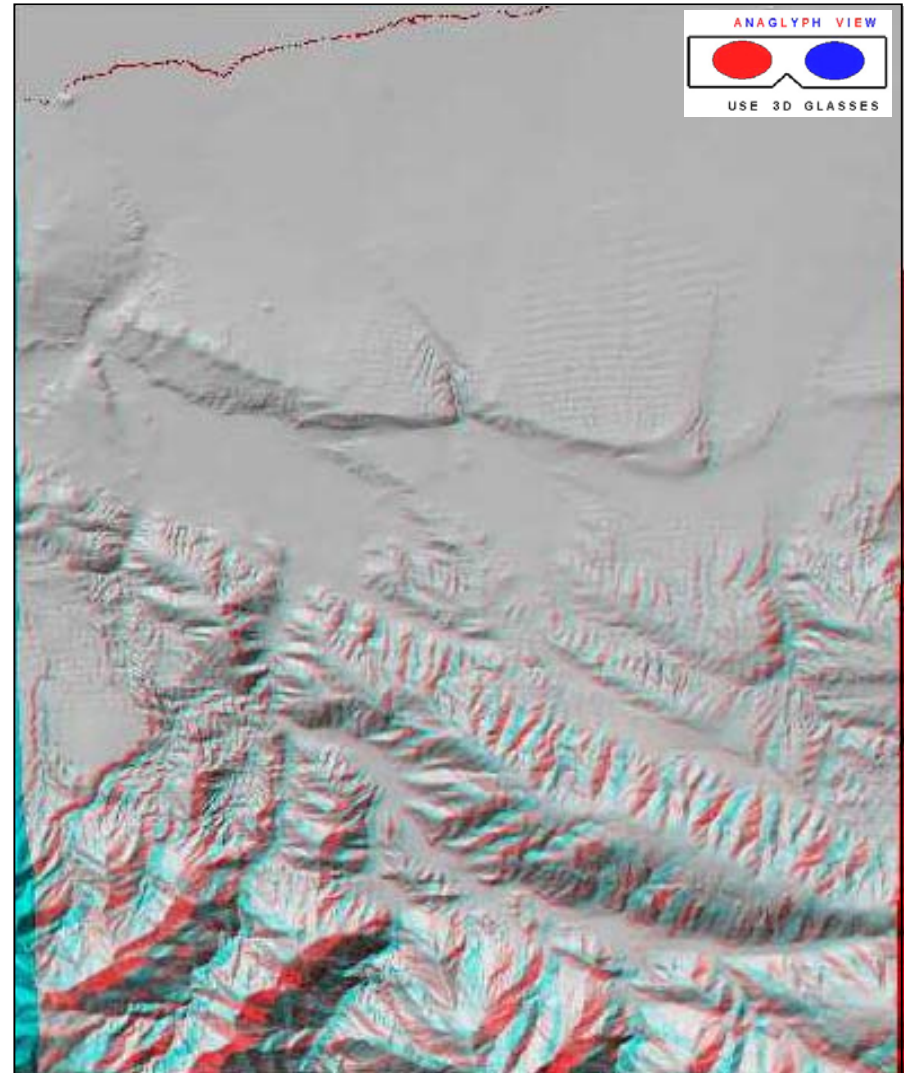
**Sensor:** Landsat 7 ETM and USGS DEM

**Algorithm:** 3-D Surface View: Color\_Infrared Composite draped over USGS DEM

**Band Order:** 4, 3, 2



(a)



(b)

**FIGURE 22** – Display of Valyermo Quadrangle as a hill-shade image that drapes multipsectral information over shaded-relief (a) and an anaglyph image that can be viewed in stereo with anaglyph glasses (b).

**Sensor:** Landsat 7 ETM and USGS DEM

**Algorithm:** a) Hill Shade Image : Color-Infrared Composite draped over USGS DEM

**Band Order:** a) 4, 3, 2

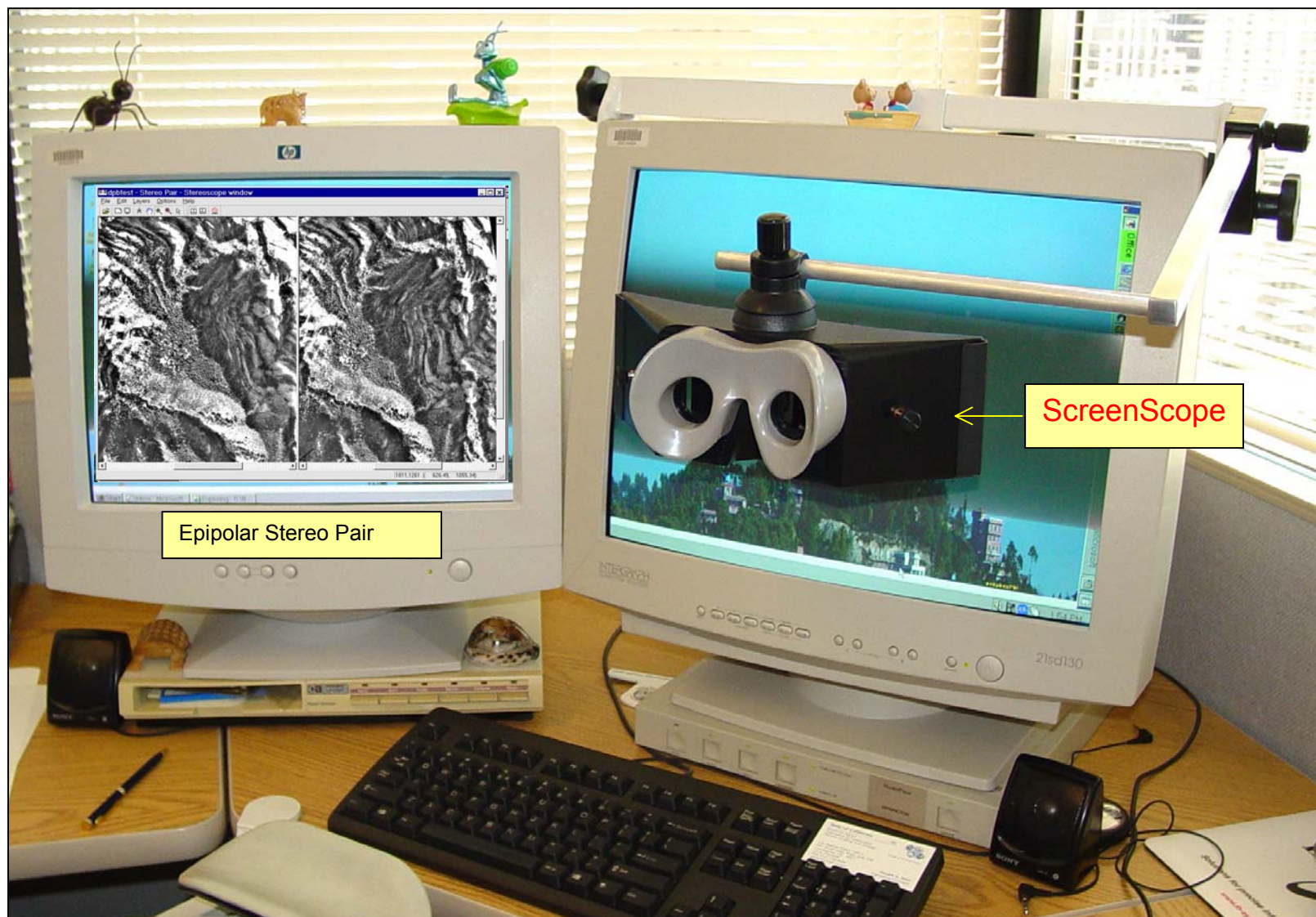


**FIGURE 23** – Hardware set-up to view epipolar stereo imagery, the digital equivalent to conventional stereo pairs of aerial photographs. The stereo images on the left computer monitor are of Devils Punchbowl in Valyermo Quadrangle.

thus calculated and displayed on the computer monitor; panning and zooming over the entire scene can be done without losing stereoscopy. A set covering the Devils Punchbowl area near Valyermo was generated from conventional aerial photographs.

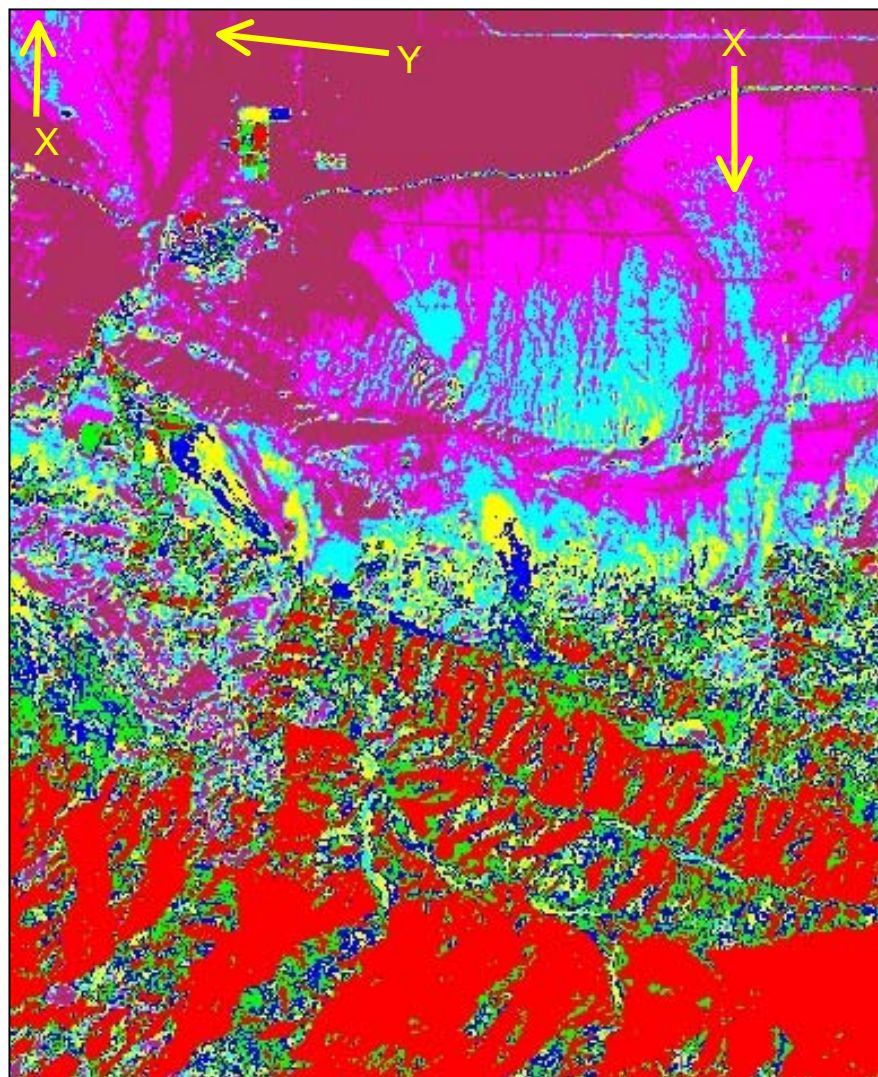
***Classification – the process of grouping pixels of an image into categories, or “classes,” according to their similarity. This process works well for pixels composed of discrete surface materials, but not as well for pixels composed of a wide mixture of materials, which causes noise and ambiguity in the resulting image.***

- **Unsupervised Classification (Figure 24)** – was applied to Landsat 7 using both the ISODATA classifier and the K-means classifier. “Unsupervised” means that the computer is allowed to do all the clustering of data (pixels) into a specified number of classes, so that each class represents a set of like pixels and thus, by extension, like surface materials and properties.

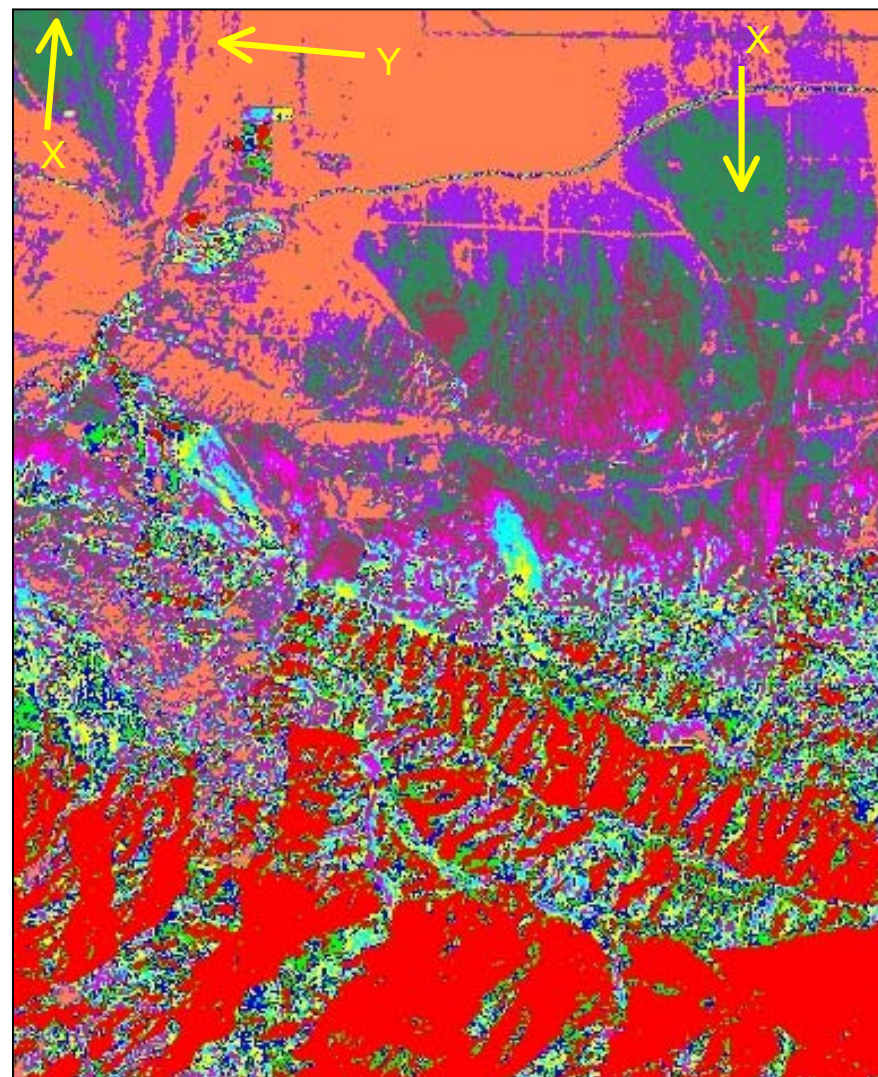
***Combination Images – images prepared by merging bands of data from more than one sensor to produce a single image that displays useful properties from each of the sensors. Image sharpening and hill shade, described above, are special cases of this processing. The goal of this approach is to see if discrimination and identification of geologic features may be improved over use of data from single sensors only. Besides image sharpening and hill shade, other combination images prepared included the following:***

- **ASTER VNIR Combined With ASTER SWIR As Band Ratios (Figure 25)** – combination of the spectral properties of a range of bands that have different spatial resolutions (15-m versus 30-m).
- **Landsat TM 432 Fused With Intermap Radar (Figure 26)** – combination of the spectral properties of a range of bands (Landsat TM) with surface roughness (radar).
- **ASTER TIR (Band 13) Fused With Intermap Radar (Figure 27)** – combination of the spectral properties of single thermal-infrared band (ASTER) with surface roughness (radar).

***Other processing*** of the remote-sensing data that we did not have time to accomplish, but which we believe is worth investigating in the future include:



(a)



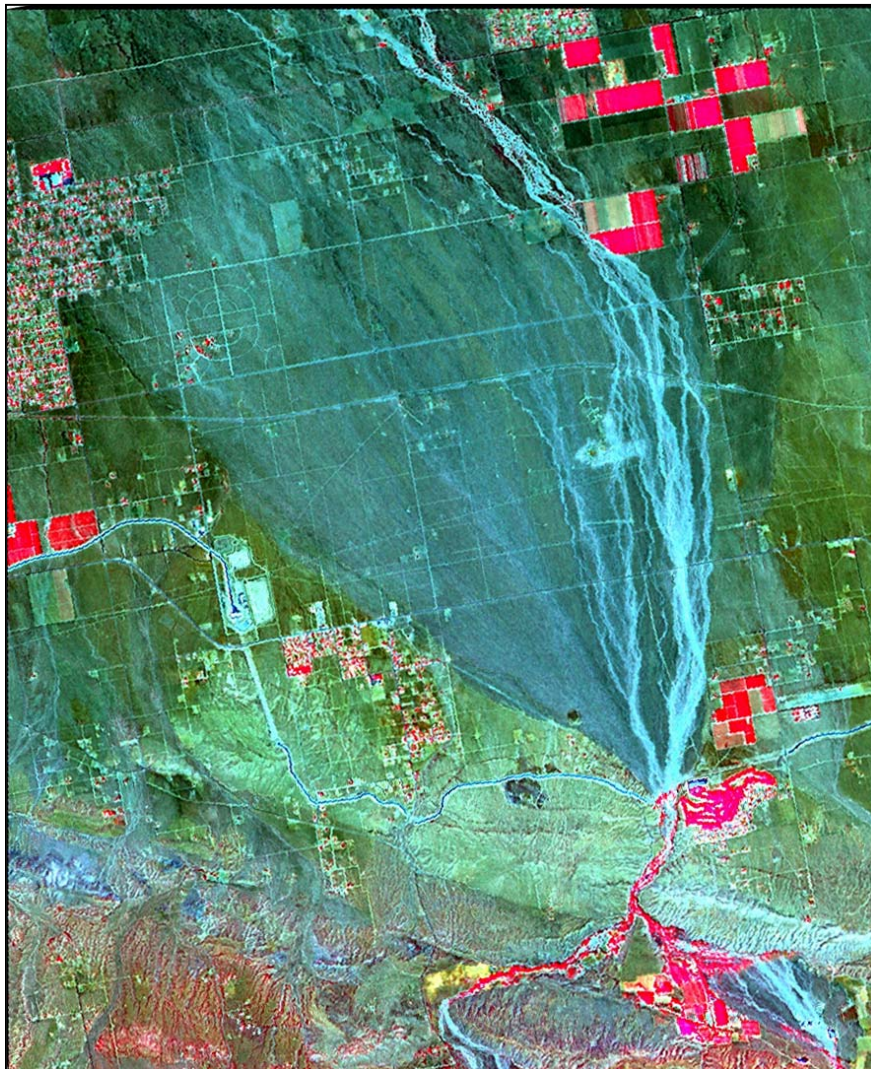
(b)

**FIGURE 24 –** Unsupervised classification of Valyermo Quadrangle by ISODATA classifier (a) and K-means classifier (b). Number of classes for each image = 10. “x” marks locations of discrepancies between the two classifiers, “y” marks locations where both classifiers did not discriminate adequately.

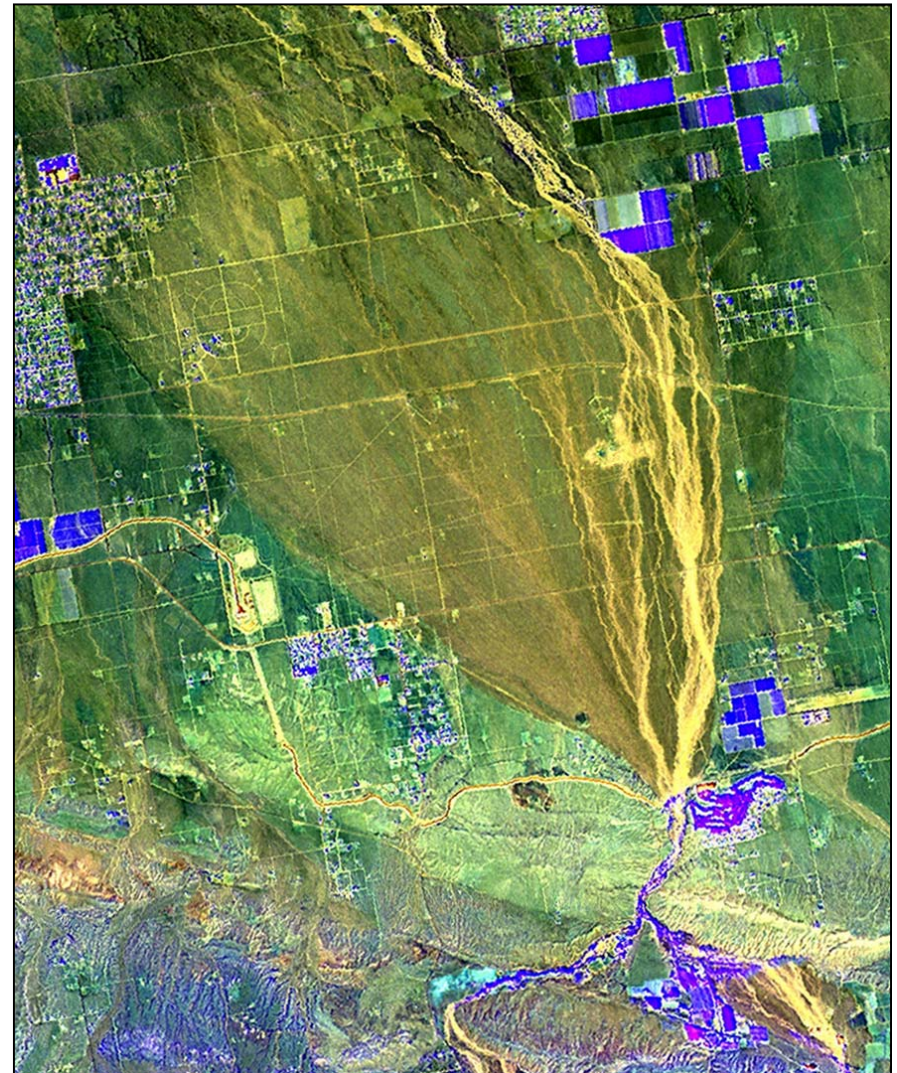
**Sensor:** Landsat 7 ETM

**Algorithm:** Unsupervised Classification: 10 Classes

**Band Order:**



(a)



(b)

**FIGURE 25** – Combination images of Big Rock fan north of Valyermo using band ratios that comprise data of two different spatial resolutions (15-meter and 30-meter).

**Sensor:** ASTER

**Algorithm:** Layer Stacking: SWIR and VNIR

**Band Order:** VNIR/SWIR

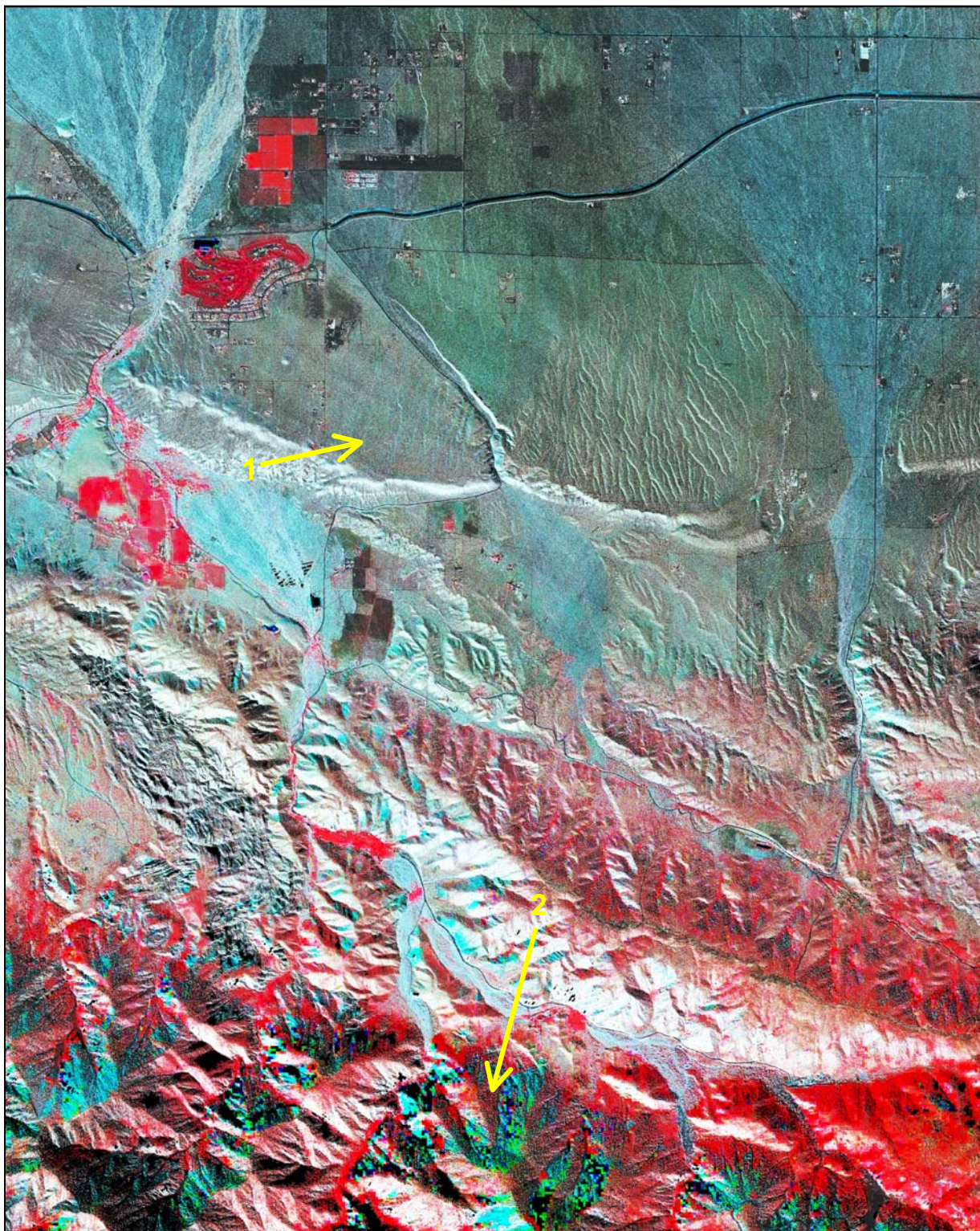


**FIGURE 26** – Combination image of Valyermo Quadrangle composed of a low-resolution multispectral image with a high-resolution radar image. Loss of textural detail of drainage is shown at (1); compare this location to that on Figure 20. Loss of spectral information is shown at (2).

**Sensor:** Landsat 7 ETM and SAR

**Algorithm:** Image Sharpening: Color Normalization

**Band Order:** 4, 3, 2

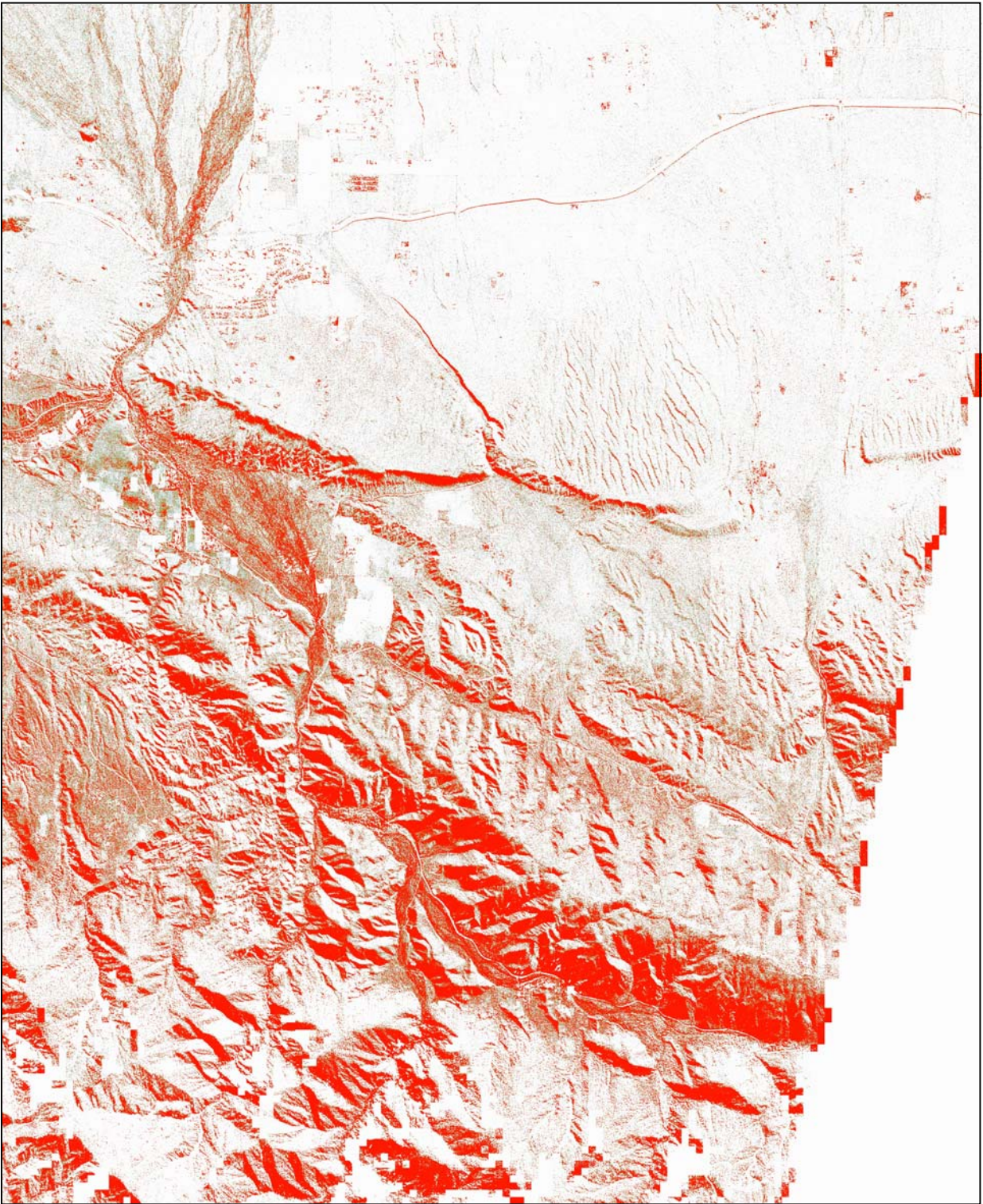


**FIGURE 27** – Combination image of Valyermo Quadrangle composed of a single low-resolution thermal-infrared band with a high-resolution radar image.

**Sensor:** ASTER TIR and SAR

**Algorithm:** Image Sharpening: Color Normalization  
Color Mapping: Color table-Hazel

**Band Order:** 13

- **Stereo Pairs of Satellite Images** – these are available for ASTER in Normal (N) and Back (B) for Band 3.
- **Supervised Classification** – instead of the computer grouping the pixels into classes, the geologist chooses “training sites” in the image and then instructs the computer to assign all pixels to classes based on these sites.
- **Spectral Analysis Tools** – these are sophisticated means of attempting to identify the component surface materials (“endmembers”) that make up the pixels in images. Generally they are most effective when evaluating “hyperspectral” rather than multispectral data.
- **Complex algorithms** – algorithms that are composed of more-complicated mathematical formulas and/or derivative components of imagery from other algorithms (see conclusions section for additional discussion).

### Methods of Evaluating the Imagery

After any image-processing was completed to produce derivative images, we analyzed and evaluated the images for geologic features using one or more of the techniques described below.

- Viewed the images on-screen to discern patterns, features, and boundaries. This process is termed “scientific visualization,” which is defined as visually exploring data and information in such a way as to gain understanding and insight into the data (Jensen, 1996).
- Compared these results to the published geologic and soils maps either visually or by overlaying vector lines of the geology on top of the images.
- Plotted selected images and then checked/verified the actual surface materials and features in the field.
- Visually compared two or more sets of different imagery with the image being evaluated to aid interpretation of features observed. For example, when we evaluated images generated from ASTER, we would compare them to features on DOQQs or Landsat 7 ETM.

Part of our strategy in evaluation was to not just focus on parts of the study area where the dominant exposure is rock and soil, but to also to observe characteristics of vegetation and topography, which often provide clues to the underlying rock and soil. Most projects in SHMP are conducted in areas that have moderate to high vegetation cover and ranges of topographic conditions.

## **RESULTS OF EVALUATION**

The procedures described above led to numerous interpretations, decisions, adjustments in direction of the project, and finally, conclusions and recommendations. Our results of evaluation of remote sensing as a tool to aid preparation of zoning maps in SHMP are tempered by two facts:

1) the limitations in experience of the two project geologists in remote sensing, and 2) recognition that remote-sensing data and imagery have their own inherent limitations regardless of the experience of the interpreters; that is, interpretation of some of the features on the imagery will always be ambiguous no matter what algorithms are applied.

In general, our analysis revealed discrepancies as well as reasonable agreement between specific features portrayed on the geologic maps (e.g., contacts) and corresponding features on the remote-sensing images. Highlighting the discrepancies can help the project geologists select sites to investigate in the field or re-evaluate concerning final geologic boundaries for zoning.

### **Geologic/Soils Maps**

The most important data derived from the geologic maps were the contacts between bedrock and unconsolidated Quaternary deposits. Next in importance were the subdivision of the bedrock units into lithologic type (rock strength is determined for these units, which is an important quantity in the process of zoning for landslides) and discrimination and delineation of the alluvial deposits. The soils maps were applicable mainly in the low-lying alluvial areas of Antelope Valley. These maps were useful to some degree in providing alternative interpretations of the boundaries between bedrock and unconsolidated Quaternary deposits of the study area and for internal differentiation of the alluvial materials.

### **Sensor Characteristics**

The results of our evaluation of sensor characteristics are presented in Table 2. The increasing number of X's equates with the more desirable attributes of availability and resolution (a positive). The increasing number of "\$" signs equates with increasing cost of product (a negative). In other words, the utility of sensors improves as cost for imagery goes down, the number of available archive scenes gets larger, and refinement of spatial and spectral resolution increases. Considering these factors, no one sensor that we obtained data from possessed all of the most desirable characteristics. Nonetheless, all sensors offered something useful for SHMP applications. ASTER was determined to be the best single sensor overall for its versatility in the four categories evaluated.

SENSOR	AVAILABILITY	SPATIAL RESOLUTION	SPECTRAL RESOLUTION	COST	APPLICABILITY TO STUDY AREA	ADDITIONAL COMMENTS
<b>Aerial Photographs (conventional)</b>	XXXXX	XXXXX	X	\$\$\$	Useful as a cross-check when analyzing lower-resolution satellite imagery, particularly for vegetation cover. Best for landslide analysis and mapping.	Availability and quality are variable. Still a useful tool because of stereo viewing. No multispectral information.
<b>ASTER</b>	XXXX	XX	XXXX	\$	Most versatile sensor when considering all properties (resolution, cost, availability, etc.). VNIR and SWIR bands useful through PCA, MNF for discrimination of some surface materials (bedrock subunits, alluvial fans, etc.).	Several advantages over Landsat include spatial and spectral resolution, and cost, which is nominal. Availability of archive scenes is much more limited, however.
<b>Digital Elevation Models (USGS DEM)</b>	XXXX	XXX	X	\$0	Could generate shaded-relief and hill-shade images for every quadrangle in study area. Useful for analysis of landslide terrain, some geologic boundaries, georegistration of geologic maps.	Reliable product available at 10-m for about half of California; data are free. Resolution not as high as Intermap, but consistency of feature information is better.
<b>Digital Elevation Models (Intermap DEM)</b>	XXX	XXXX	X	\$\$\$\$\$	High cost limited use to 8 quadrangles. Shaded relief and hill-shade useful for some contacts between bedrock and unconsolidated Quaternary deposits. Useful for analysis of landslide terrain, georegistration of geologic maps, some contacts between bedrock and unconsolidated Quaternary deposits.	Superior resolution to USGS, but some surface features are missing compared to USGS (inconsistent coverage of California because generated from separate airborne radar campaigns). Expensive for one quadrangle.
<b>Digital Orthophoto Quarter-Quads (DOQQ)</b>	XXXXX	XXXXX	X	\$0	Useful as a cross-check when analyzing lower-resolution satellite imagery, particularly for vegetation cover. Less useful than aerial photographs because no stereo available.	Every quadrangle is available, but quality varies because of vintage of aerial photography used to generate images. Already have a complete statewide set, so data are free. Spatial resolution excellent.
<b>Landsat 7 ETM</b>	XXXXX	X	XXX	\$\$	One scene covered entire study area (ASTER needed three scenes). Good for smaller-scale viewing, but severely degraded at 1:24,000. Multispectral useful through many algorithms to highlight bedrock and unconsolidated Quaternary deposits. Too coarse to use for refinement of geologic boundaries (other imagery is better).	Large archive to allow inspection during different seasons. Cost has come down significantly. Spatial resolution is a limitation for mapping at 1:24,000, although can sharpen with other imagery. Spectral resolution limited, but superior to panchromatic.
<b>Radar (Intermap)</b>	XXX	XXXX	X	\$\$\$\$\$	High cost limited use to 8 quadrangles. Useful for sharpening (increasing spatial resolution) of other imagery. Of mixed value in discerning geologic boundaries depending on signal return. Cultural features not as apparent.	Good spatial resolution, but limited by inconsistency in return signal (some features obscured by selection of look-direction). Expensive for one quadrangle. Should not be used by itself for interpretation.
<b>SPOT Panchromatic Mosaic</b>	XXXXX	XXX	X	\$0	Good for textural analysis of landscape and finding cultural features. Sharper detail than ASTER and Landsat 7 ETM because of higher spatial resolution.	Already have 1998-2000 mosaic at 10-meter resolution, so data are free. Disadvantage is panchromatic rather than multispectral. Prepared in Teale Albers projection, which is not commonly built into software projection files for on-the-fly conversion.

**TABLE 2** – Summary of properties of sensors as they apply to SHMP projects. The higher the number of Xs for a given property, the more valuable the sensor. The higher the number of \$ signs, the more expensive the product from a sensor, which translates to potentially lower likelihood of use.

## **Remote-Sensing Imagery**

The following sections summarize the results of our evaluation of the usefulness of the different algorithms for the six specific geologic applications pertinent to SHMP as described above. These results are also presented in Table 3.

### **Basic Displays**

#### **Single-Band Grayscale (Figure 10a):**

Although lacking the vividness of color imagery, single-band grayscale images were sometimes superior to color images because of their display of the textural detail of topography. This display can be valuable for discerning drainage patterns, degree of dissection of the topography, and surface roughness, which can aid in differentiating alluvial deposits, both spatially and temporally. Also, panchromatic products commonly have higher spatial resolution than the companion multispectral products from a given sensor and thus can be used to “sharpen” the detail of multispectral images through image-sharpening transformations as discussed previously.

#### **True-Color Composite (Figure 10b):**

Without image enhancement, the true-color Landsat 7 ETM 321 image is dark and bland, dominated by shades of brown, gray, pink, and dark green. It is difficult to discriminate features and surface materials, and contrast is poor to average. With enhancement, however, the image improves to make the colors more “real” to the human eye, similar to a color aerial photograph. This type of image was useful for initial evaluation of the study area, that is, to recognize 1) topography, 2) dominant natural surface cover (vegetation versus soil/rock), and 3) cultural development. It is useful as a tool of introduction to the study area prior to fieldwork by the geologist.

#### **Color-Infrared Composite (Figure 11a):**

The main value of these images is in determination of degrees of vegetation cover. The near-infrared bands used in these images are very sensitive to vigorous green vegetation, and when they are assigned the color red in the composite image, areas of vegetation are more striking in these images than in the true-color images described above. In the study area, the images were valuable in establishing whether the signal displayed in other imagery results from rock/soil or from vegetation. They were also useful in delineating areas of urbanization and cultivation.

**APPLICABILITY OF EVALUATED REMOTE SENSING IMAGERY IN CHARACTERIZING VARIOUS GEOLOGIC PHENOMENA IN NORTHERN LOS ANGELES COUNTY**

GEOLOGIC MAPPING/HAZARD ZONING APPLICATIONS	REMOTE-SENSING DATA / ALGORITHM																					
	Basic Displays					Transformations										Topographic Modeling				Classification		
	Single-Band Grayscale	True Color Composite	Color Infrared Composite	False Color Composite	Color Mapping	Image Sharpening	Band Ratios	Principal Component	Minimum Noise Fraction	Decorrelation Stretch	Color Transform	Saturation Stretch	Synthetic Color	NDVI	Tasseled Cap	Shaded Relief	3D Surface View	Hill Shade	Stereo Anaglyph	Epipolar Stereo	U-Class	
																					Isodata	K-means
1. Delineation of contacts between bedrock and unconsolidated Quaternary deposits	Yellow	White	Yellow	Yellow	White	Green	Yellow	Green	Green	Green	White	Yellow	White	Red	Red	Green	White	Green	Red	Green	White	White
2. Discrimination of alluvial deposits(fans, modern stream channels, etc.) from one another	Yellow	Red	Yellow	Yellow	Red	Green	Yellow	Green	Green	Green	Red	Red	Red	Red	Red	Yellow	White	Green	Red	Green	Red	White
3. Discrimination of bedrock units from one another	White	White	Red	Red	White	Green	Green	Green	Green	Green	White	Yellow	White	White	White	Red	White	Yellow	White	Yellow	White	White
4. Recognition and delineation of landslides	Red	White	Red	White	White	Yellow	White	White	White	White	White	White	White	Red	Red	Green	Red	Yellow	Red	Green	White	White
5. Verification of cartographic registration of digital geologic maps	Red	White	White	White	White	Yellow	White	White	White	White	White	White	White	White	White	Green	White	Yellow	White	Green	White	White
6. Representation of previously mapped geologic contacts	Red	Red	Yellow	Yellow	Red	Green	Yellow	Green	Green	Green	Red	Red	White	Red	Yellow	Green	White	Green	Red	Green	White	White

Applicability:

H	High
M	Moderate
L	Low
VL	Very Low

**TABLE 3** – Summary of evaluation of different remote-sensing imagery for six specific SHMP technical applications in the northern Los Angeles County study area.

The highlighting of vegetation in this type of image also has an important temporal element that potentially could aid mapping of landslides. As seasons change, moisture conditions and growth cycles of vegetation change also; analysis of images taken at different times of the year might thus aid delineation of landslides from non-landslide terrain through analysis of these changes. Although the present study area was not especially favorable for such testing, it might be applicable in more temperate, vegetated study areas such as the San Francisco Bay Area. In such climates, the different vigor in vegetation growth and annual dynamics between landslide and non-landslide areas may be detectable as changes in brightness on these types of images.

#### **False-Color Composite (Figure 11b):**

The two main advantages of this type of imagery are the versatility in rearranging color combinations (e.g., 234 compared to 432) of the bands as well as the numerous band combinations available (6 bands in Landsat 7 ETM; for example, 543 or 754). These combinations allow potential experimentation with a large variety of possible individual images; several were observed to highlight particular features of interest such as active stream channels and boundaries between alluvial fans. Furthermore, use of the sets of SWIR bands in Landsat 7 ETM (5 and 7) and ASTER (4-9) can be sensitive to groups of minerals and thus sometimes aid in lithologic discrimination.

#### **Color Mapping (Figure 12):**

This process was a useful complement to analysis of single-band grayscale images mainly through its enhancement of the differences in brightness throughout the different images (e.g., SPOT, radar). Areas of heavy vegetation versus areas dominated by rock and soil, for example, were more readily distinguishable when color-mapped than when viewed via grayscale alone.

### **Transformations**

#### **Image Sharpening (Figure 13):**

The main use of this transformation is to improve the spatial resolution of a given image so that features in the image stand out more sharply. Higher resolution is not significantly noticeable when images are viewed at small scales; for example, a Landsat image (30-meter resolution) won't look substantially different from an ASTER image (15-meter resolution) when

they are “zoomed-out.” The difference will appear dramatic, however, when an unsharpened Landsat image and the same Landsat image sharpened with SPOT or Intermap radar are viewed at large scale (“zoomed-in”). Correspondingly, the sharpened images can help the geologist refine (digitize) geologic contacts interpreted from the associated multispectral data of the lower-resolution image to greater locational accuracy and detail. In the study area, such contacts included those between bedrock and unconsolidated Quaternary deposits, between alluvial fans, and along active alluvial channels. We did observe, however, that sharpening of some multispectral images with the Intermap radar caused degradation of the multispectral information; that is, the high-brightness areas of the radar locally obscured, or overwhelmed, the display of the multispectral colors.

### **Band Ratios (Figure 14):**

One of the obvious advantages of this type of transformation is the reduction in topographic effect in the Valyermo Quadrangle. Regarding discrimination of lithologic units, it is apparent that some units and features are conspicuous while others are subdued in comparison to their appearances in other types of imagery.

Although we looked at only a small number of ratio combinations for the study area, we recognize that band ratios have good potential for highlighting some lithologies through recognition of distinct mineral groups (e.g., clays, carbonates, abundance of quartz). The sets of SWIR bands in Landsat 7 ETM and ASTER are particularly useful because of their sensitivity to mineralogy; because of its greater number of bands and its narrower bandwidths, ASTER has more potential use in discrimination than Landsat 7 ETM. The set of TIR bands in ASTER also have potential, but we believe at this time that the coarse spatial resolution (90 meters) severely limits its applicability for mapping at scales of 1:24,000 and larger. The main problem is that such large pixels are commonly composed of spectral signatures from many different materials on the ground.

Additional research on band ratios that use the TIR suite for this study area might reveal useful results for local sites, especially if integrated into combination images perhaps as “complex” rather than “simple” ratios. Along this line, approaches similar to those offered by Rowan in his presentation at the ASTER workshop (April, 2003) for use of ASTER TIR would be a worthwhile avenue to research.

### **Principal Components (Figure 15a), Minimum Noise Fraction (MNF) Rotation (Figure 15b), Decorrelation Stretch (Figure 16a):**

We have combined discussion of these three transformations because of their overall similarity in construction (they all are fundamentally derived from principal components) and results. All produced dramatically vivid images of the study area and were among the most useful imagery for purposes of discrimination of surface materials and features.

These transformations were performed on both ASTER VNIR and SWIR bands as well as Landsat 7 ETM bands. They were useful in all six SHMP geologic applications, especially discrimination of active alluvial channels and fans and discrimination of bedrock units (Figures 28, 29, 30). Usefulness did, however, vary throughout the study area depending on vegetation cover.

As with false-color composites, we found that it is essential to process the sensor bands in different color combinations to highlight particular features of interest. For example, several geologic units in the Valyermo Quadrangle are discriminated better in MNF 312 (Figure 28) than in MNF 213 (Figure 29) and vice versa.

### **Color Transform (Figure 16b):**

As a tool for enhancement of geologic interpretation of the study area, this transformation was of variable use. The sample image in Figure 16b exhibits a complexity that is not as easy to interpret compared to other imagery evaluated.

### **Saturation Stretch (Figure 17):**

This transformation is useful in its ability to enhance the color contrast in a bland image that has high correlation among its component bands (Figure 17). Its value is that surface materials are more vividly contrasted so that the boundaries among them are more obvious.

### **Synthetic Color Image (Figure 18):**

In the application of this transformation to the Intermap radar image of Valyermo Quadrangle (Figure 18), we determined that it showed excellent detail of active alluvial channels along Big Rock fan, but did not clearly display distinct geologic units in other selected locations.

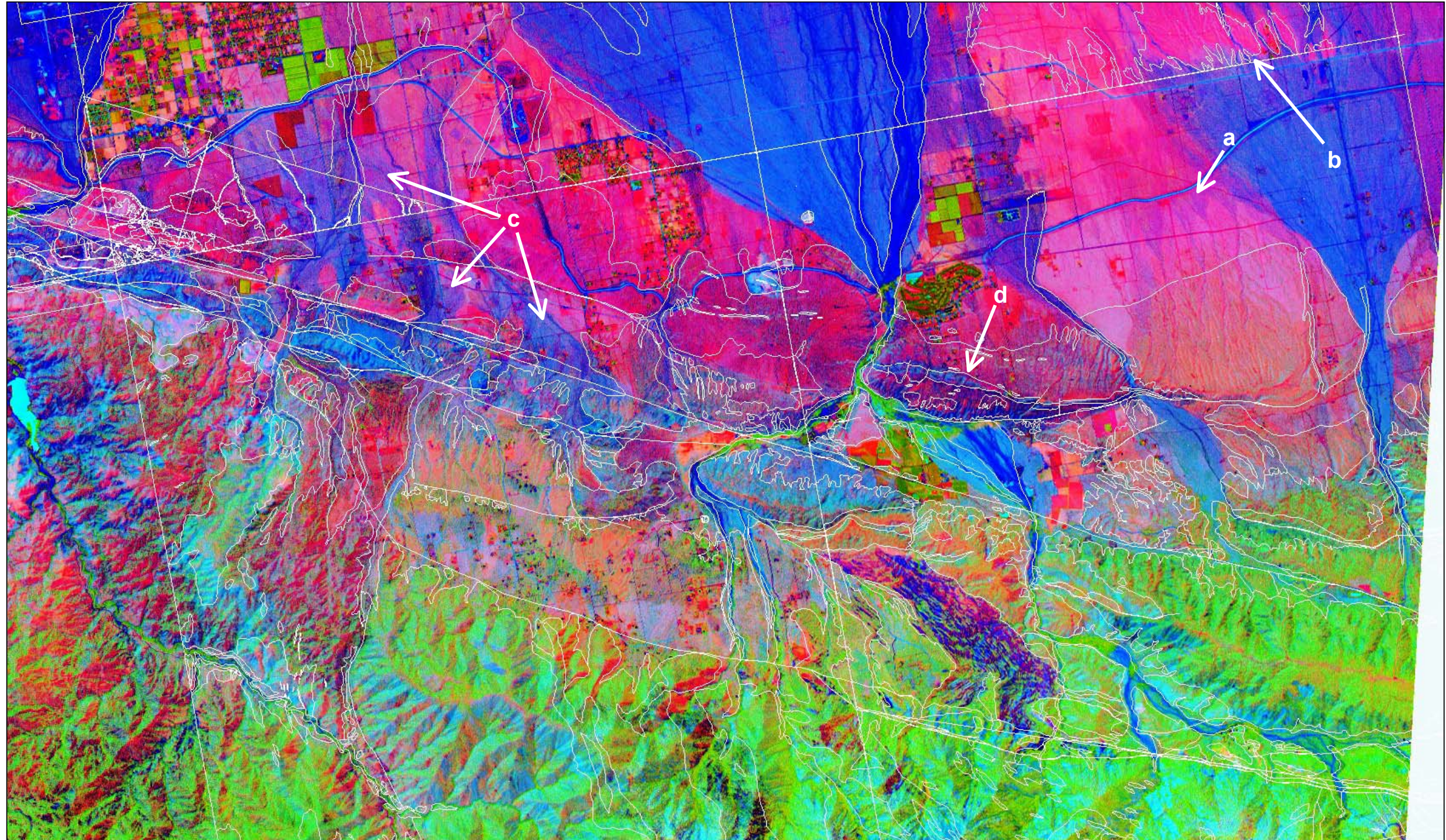
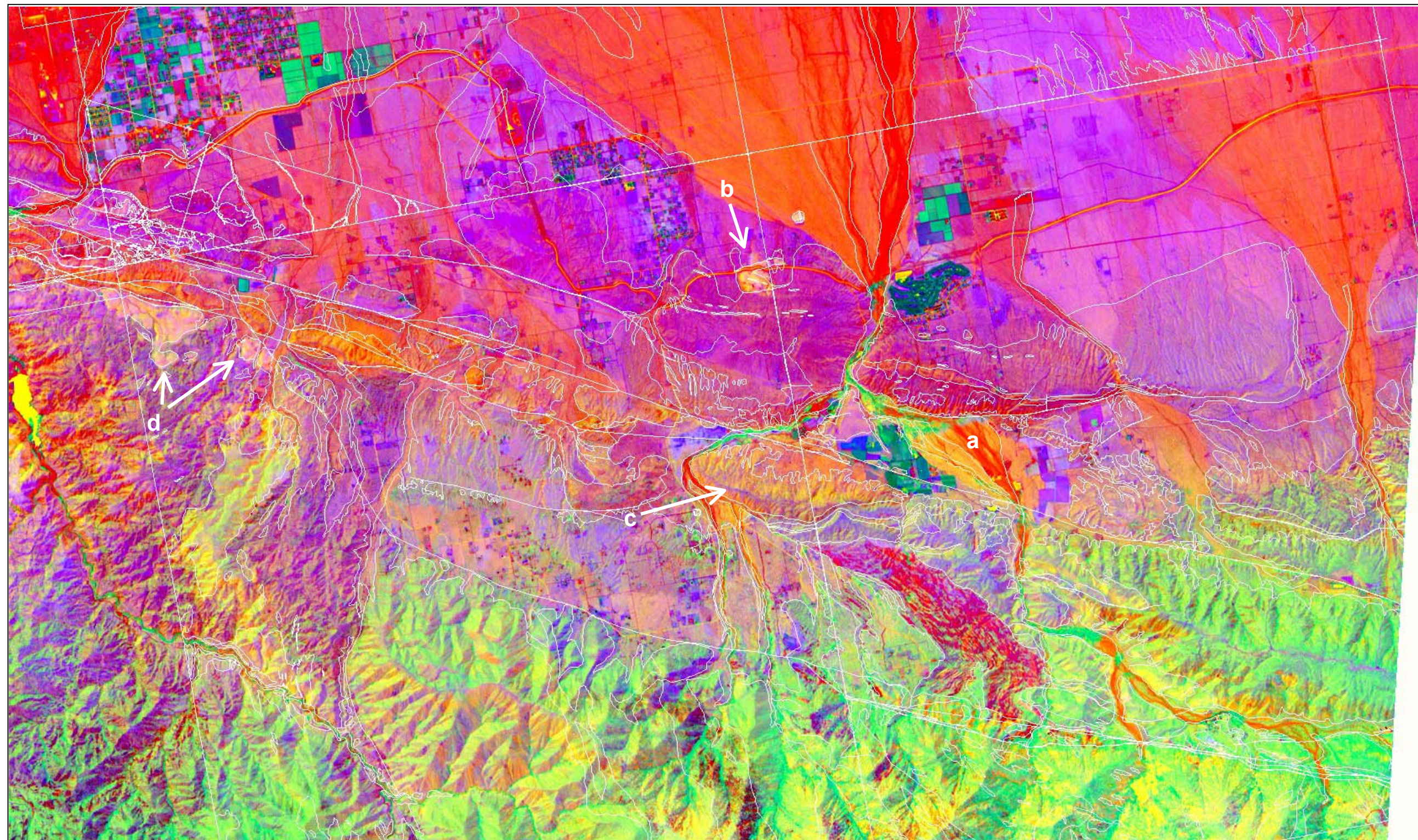


FIGURE 28 – Image of portions of Littlerock, Lovejoy Buttes, Valyermo, and Juniper Hills quadrangles, with overlay of geologic contacts (white) of Dibblee (2002a, 2002c) and Ponti and Burke (1980). Examples of geologic information include: a) differentiation of older alluvial-fan material, b) potential to refine the mapped alluvial contacts (white lines on pink) and evidence of a structural boundary that may be a groundwater barrier, c) younger alluvial deposits, and d) a carbonate pendant (blue) within granitic rock (pink).

Sensor: ASTER

Algorithm: Minimum Noise Fraction

Band Order: MNF3, MNF1, MNF2



**Figure 29** - Same type of transformation, area, and geologic overlay as in Figure 31 except that the color combination is different to demonstrate how one needs to vary color combinations to highlight specific features. Examples of geologic information include: a) finely-detailed modern alluvial deposits, b) body of gabbro (yellow) within granitic terrane (lavender), c) linear geologic unit (lavender) not obvious in aerial photographs, and d) Tertiary volcanic rocks (pink).

**Sensor:** ASTER

**Algorithm:** Minimum Noise Fraction

**Band Order:** MNF2, MNF1, MNF3

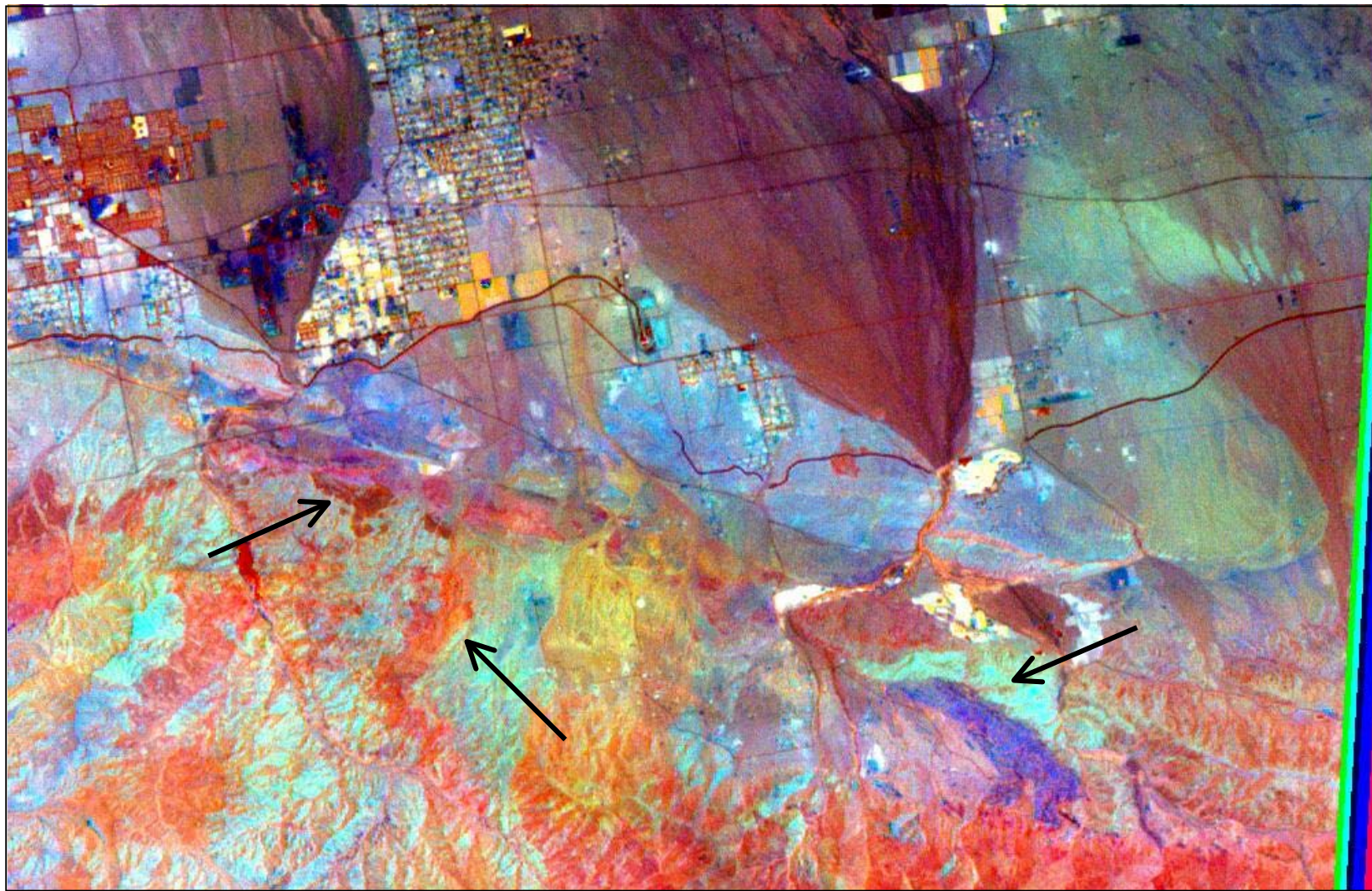


**FIGURE 30** – Image of portions of Littlerock, Lovejoy Buttes, Valyermo, and Juniper Hills quadrangles. Although the spatial resolution is lower (30-m versus 15-m), color contrasts between some lithologic units (arrows) are more vivid in this image than in Figures 28 and 29.

**Sensor:** ASTER

**Algorithm:** Principal Components Analysis

**Band Order:** PC2, PC3, PC4 OF 6 SWIR BANDS

### **Normalized Difference Vegetation Index (NDVI) (Figure 19a):**

Similar to the color-infrared composite imagery, the strength of this imagery is its emphasis on vegetation cover. It is superior to the color-infrared in that it reduces the effect of topography and, through color-mapping, it brings out differences in vegetation cover more sharply. In Valyermo Quadrangle, it was useful in discriminating bare rock/soil areas from areas that are sparsely to heavily vegetated (Figure 19a). This determination can aid interpretation of whether the spectral signals in an area are dominated by rock/soil or vegetation. Regarding evaluation of landslides, this study area is not as favorable for application of NDVI, but evaluation of temperate regions (e.g., San Francisco Bay Area) might see more effective use of this algorithm. Finally, the intensity of reflectance of green vegetation shown in an NDVI image might provide indirect evidence of the underlying hydrologic condition at local sites. This evidence might be useful in local evaluation of potential for liquefaction.

### **Tasseled Cap (Figure 19b):**

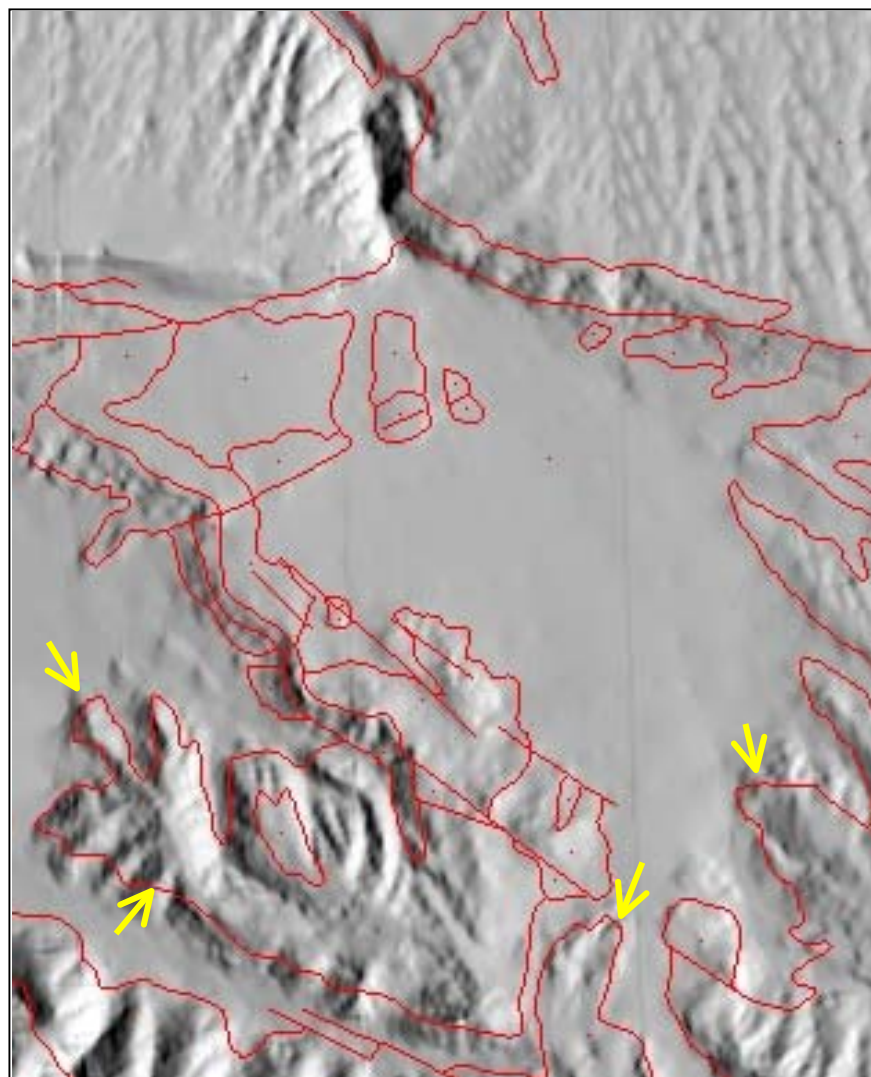
As a more-sophisticated algorithm than NDVI, there is higher potential to extract more information from this type of image regarding rock/soil, vegetation, and ground moisture. As shown in Figure 19b, there is more variegation because three components are displayed instead of one as in NDVI. Although we only briefly evaluated this transformation, we believe that the “Third” component, which contains information about moisture, may be a useful tool for evaluation of landslides in vegetated temperate areas, and thus deserves more research.

## **Topographic Modeling**

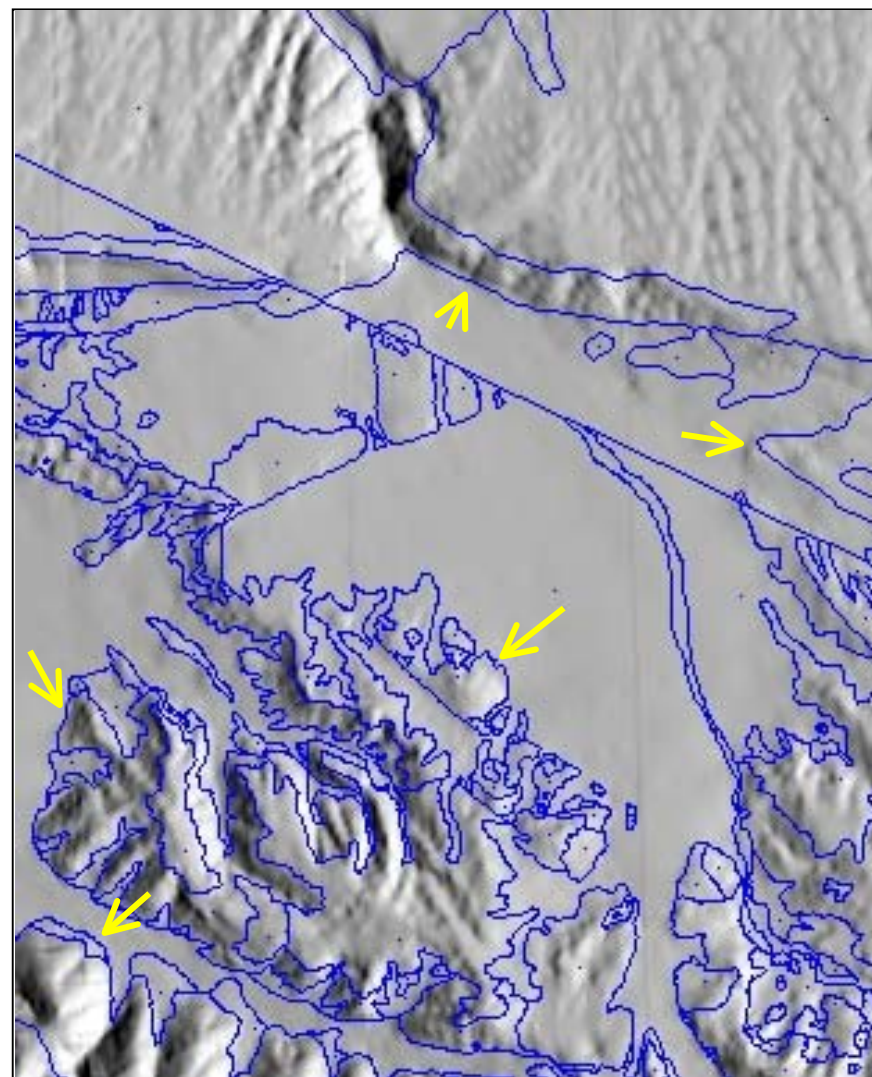
### **Shaded Relief (Figure 20):**

Shaded-relief images were among the most valuable of all imagery that we evaluated during this study. Because they depict the geomorphological expression of an area, features such as valleys, canyons, hills/mountains, flatlands, and mesas are easily recognizable. Overall, these images are a versatile tool for cartographic registration, evaluation of geologic features, and as “3-dimensional” back-layers for other imagery.

Shaded relief at the quadrangle level was helpful in verifying the cartographic registration of digital geologic maps with the SHMP base maps for the study area. Indeed, it was through use of this imagery that mis-registration of some maps was quickly recognized early in the study (Figure 31), and that corrections would have to be done to properly register these maps.



(a)



(b)

**FIGURE 31** – Demonstration of use of shaded-relief images to verify cartographic registration of digital geologic maps. In image (a), several examples are marked (arrows) where there are discrepancies between locations of mapped contacts of alluvium (red) and the expected geomorphic locations of the contacts as displayed on the underlying shaded-relief image, which serves as the correctly georeferenced base map. In image (b), the blue lines below the straight diagonal blue line represent contacts from a different geologic map, which is properly georeferenced. Arrows in (b) mark examples of contacts between bedrock and unconsolidated Quaternary deposits that are observable by differences in topography.

Recognition and evaluation of previously mapped contacts between bedrock and unconsolidated Quaternary deposits were enhanced in several locations where flat alluvial deposits abut against higher-relief hills of bedrock as abrupt breaks in slope (Figure 31b). These sudden changes in relief are observable also where flat, gently inclined pediment surfaces join the irregular remnant outcrops of inselbergs (Figure 32). Finally, an isolated hill of bedrock in Valyermo Quadrangle, which is conspicuously displayed on the shaded-relief image (Figure 20), was found to be missing on the digital geologic map and was then added to the final SHMP composite of geology for the area.

One of the mechanical strengths of shaded relief is the capability to vary the azimuth and inclination of illumination of the image. This feature allows highlighting of surface textures so that drainage patterns, geologic structures, and some erosion textures of bedrock can be readily discerned. The drainages, particularly through patterns of dissection of the surface, can help delineate subunits of alluvial deposits. Faults and joints, bedding and foliation (including attitudes of), and degrees of erodability, when illuminated properly, can aid discrimination of some geologic units from one another.

Finally, the recognition and mapping of landslides can be improved in both quality and efficiency with shaded-relief imagery (Figure 33). Through use of DEMs of sufficient spatial resolution that cover areas with landslides of large-enough size to be observed, evidence of landslides such as head scarps, hummocky topography, and anomalies in drainage can be discerned on these images, both in the office and in the field. The rapid distinction through shaded relief of bedrock hills, which may be susceptible to landslides, from low-relief areas can also help staff focus on what locations to collect data on shear-strength. Man-made features that might be susceptible to landsliding, such as open pits, quarries, and large roadcuts, can also be recognized on high-resolution shaded-relief images.

Regarding the mechanics of interpretation and mapping of landslides, shaded relief offers two potential tools. First, determination and collection of attributes, such as direction of movement, are improved by using the shaded-relief image as a back-layer of visual reference to the digital inventory map of landslides (Figure 34). Second, transfer of the boundaries of landslides from interpreted aerial photographs to the digital layer of the landslide inventory can be streamlined by allowing the geologist to bypass the steps of transferring the boundaries to a mylar quadrangle and scanning of that mylar; in other words, the geologist uses the shaded-relief image on-screen as a pseudo-stereo photopair to visually transfer his or her interpretations from the aerial photographs to the computer screen via heads-up digitizing.

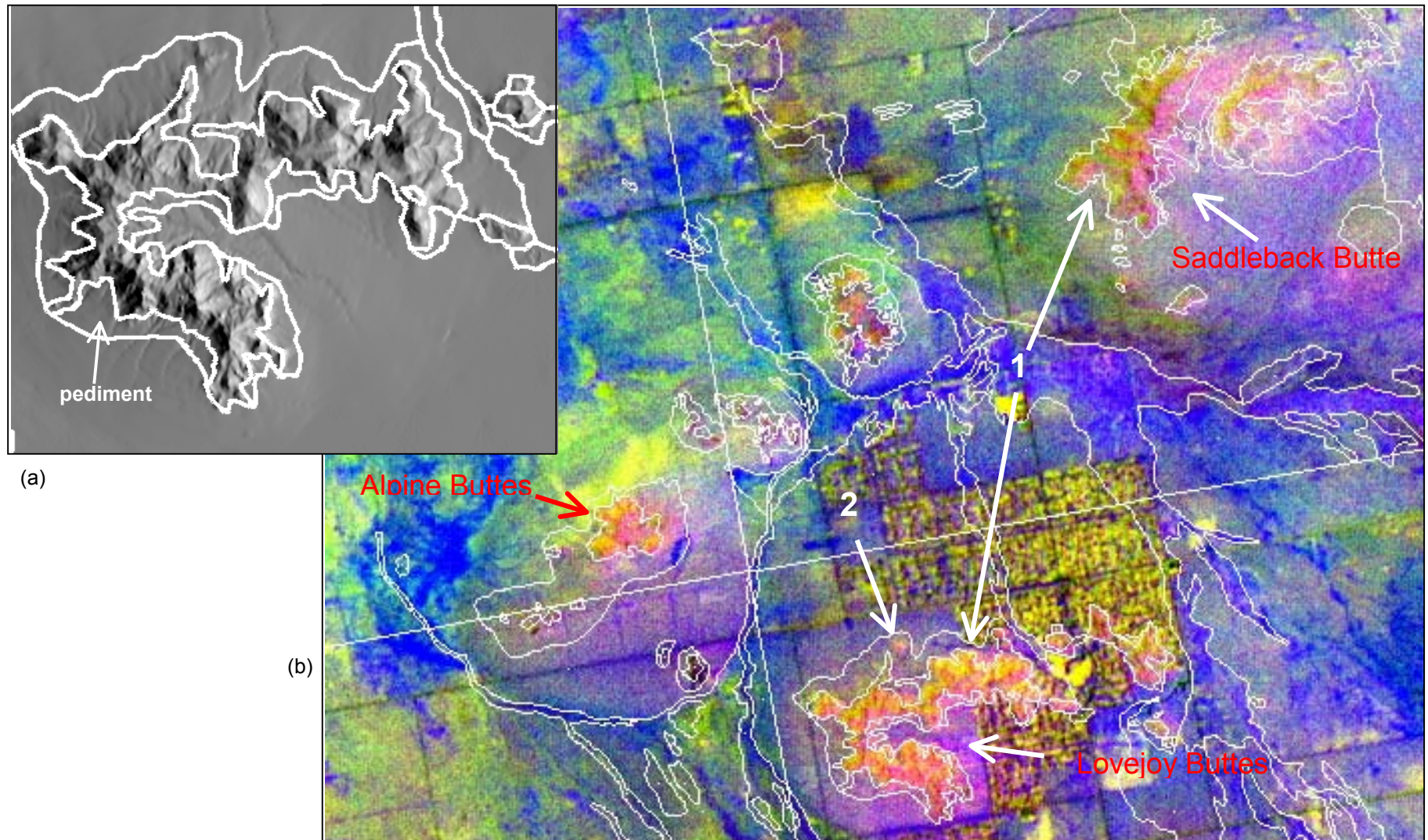
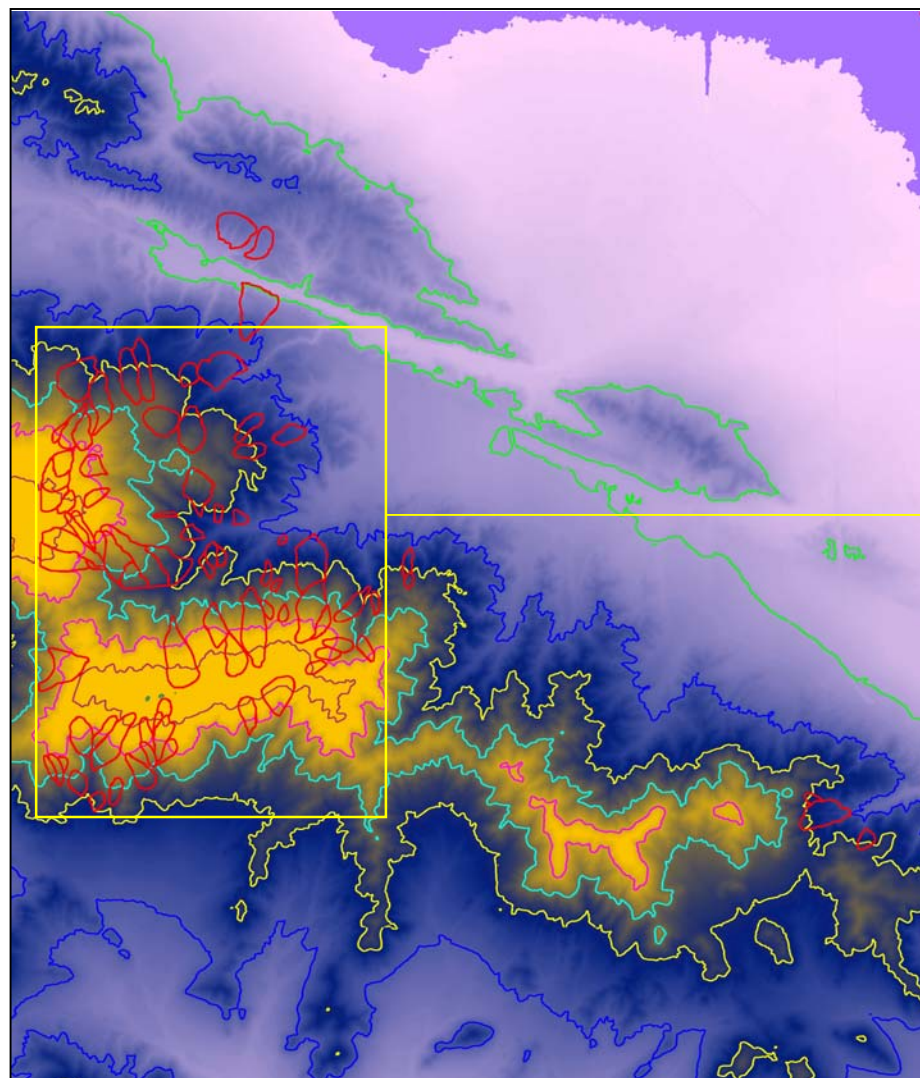


**Figure 32** - Portrayal of inselbergs in the Alpine Butte-Lovejoy Buttes area of Antelope Valley. White lines are geologic contacts of Ponti and Burke (1980). Shaded relief image (a) of Lovejoy Buttes shows change in topography from pediment to irregular outcrop. In (b), areas of non-pediment outcrop are observable spectrally in pink and yellow (1); a non-pediment outcrop (pink) at (2) is mapped as pediment.

**Sensor:** a) USGS DEM b) ASTER SWIR

**Algorithm:** a) Shaded Relief, b) Principal Components Analysis

**Band Order:**



(a)



(b)

**FIGURE 33** – Demonstration of landslide inventory draped over a DEM image (a) and a shaded-relief image (b) of Ritter Ridge Quadrangle. The shaded-relief image as a back-layer helps the geologist verify locations and boundaries of landslides and their potential directions (azimuth) of movement.

**Sensor:** SAR

**Algorithm:** a) Color Mapping: Color table-Haze, b) Shaded Relief

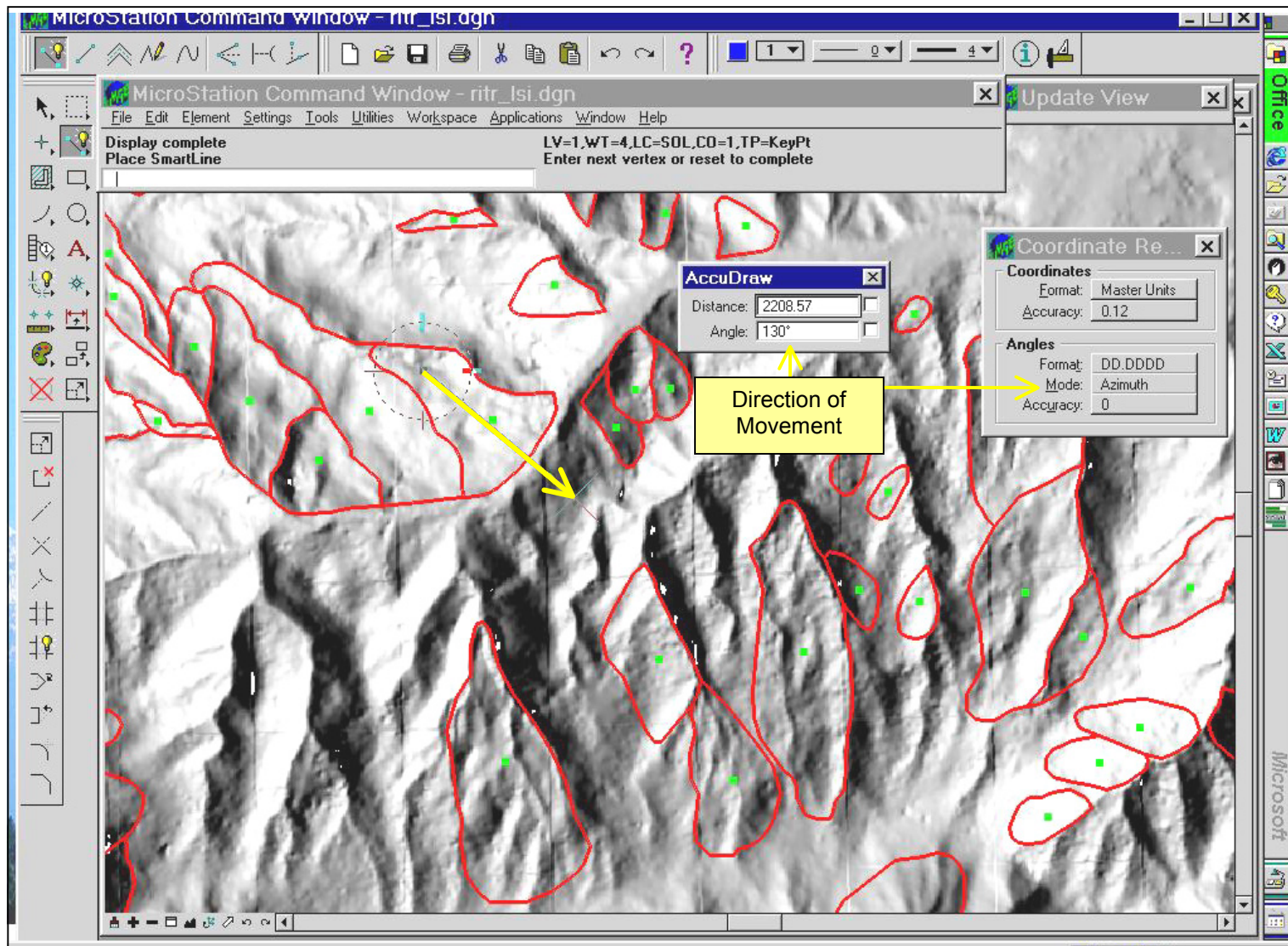


**FIGURE 34** – Demonstration of on-screen determination of direction (azimuth) of landslide movement by application of a shaded-relief back-layer and a built-in drawing tool that measures azimuth.

**Sensor:** SAR

**Algorithm:** Shaded Relief

Shaded relief has some advantages over digital radar images including 1) capability to vary the azimuth (“look” direction) and inclination of illumination, and 2) a “cleaner” appearance (illumination is even, not noisy). An advantage of radar, however, is that it contains information on surface roughness.

### **3-D Surface View (Figure 21):**

These images allow oblique viewing from all cardinal directions and inclinations; “fly-through” animation of the images is also an option. They are not particularly useful for mapping (planimetric imagery is more appropriate), but they are useful in public presentations and as introductory views for staff geologists as they begin their projects and prepare for fieldwork. For public presentations of seismic-hazard zones, an effective use of these images would be to drape a composite of the seismic-hazard zones over the 3-D relief to demonstrate how landslide hazards correspond to the high-relief areas and liquefaction hazards correspond to the low-relief areas or bottoms of drainages. This type of display more emphatically highlights areas that require the most attention from the public and government officials. Another advantage of the images is that the relief can be exaggerated to highlight subtleties in the landscape that would not be obvious at normal 1:1 portrayal, which can improve verification of locations and extent of landslides.

### **Hill Shade (Figure 22a):**

These images combine the best of the 3-dimensional effect of topography with spectral information. Figure 22a demonstrates more dramatically than Figure 11a how green vegetation corresponds with the landscape of Valyermo Quadrangle. Also noticeable is how the image is much “cleaner” appearing with use of the shaded relief, rather than radar (Figure 13), as the background.

### **Anaglyph (Figure 22b):**

This type of image complements shaded-relief in that it is an actual 3-D stereo view of an area. Contacts between low-relief modern alluvial deposits and surrounding high-relief bedrock as well as geologic structures that are revealed geomorphically are better-exhibited via stereo viewing. Another advantage of this type of image is that through the use of anaglyph glasses, an audience can simultaneously view the image during demonstration of features on the image. Compared to stereo pairs of conventional aerial photographs, which are often limited by their small areal coverage, an anaglyph can be generated to cover large areas, such

as entire quadrangles, which can be viewed rapidly in their entirety (Figure 22b).

### **Epipolar Stereo (Figure 23):**

After they have been georeferenced and orthorectified, the greatest value of these images is that they allow the geologist to do photo-interpretation, heads-up digitization, and annotation directly on-screen while viewing the images in stereo. Panning and zooming can be done without loss of stereoscopy. A disadvantage is that the screen images are not as sharp or crisp as their photographic-print counterparts; sharpness can be improved by higher-resolution scanning, but the higher dpi will result in larger sizes of the digital files. The main uses of epipolar images would generally be in landslide mapping and for determination of contacts between bedrock and unconsolidated Quaternary deposits. They may also aid discussion between geologists in different offices as discussed later in this report.

## **Classification**

### **Unsupervised Classification (Figure 24):**

Evaluation of this process was limited to only a few derivative images, therefore, results and conclusions are guarded. As seen in Figure 24, the results of classification are generally similar in both images for the south half of Valyermo Quadrangle. Several local differences between the two images are apparent, however, in the north half. The K-means image, for example, shows more discrimination of alluvial fans and their component deposits. Both procedures had problems in that they classified parts of different fans into the same class, which is incorrect and thus misleading to the geologist. For certain geologic units, neither sufficiently classified the entirety of the units. In summary, neither was as useful for geologic applications as many of the other images discussed above, but again our evaluation was not rigorous.

In general, classification procedures work best with surface materials and features that have consistent spectral signatures (e.g., lawns, cultivated fields, artificial surfaces, water bodies). Natural landscapes, which typically consist of mixtures of rock/soil and vegetation, are more difficult to classify because of their inherent variability (weathering of rock, variety of species of vegetation, etc.).

## **Combination Images**

### **ASTER VNIR Combined With ASTER SWIR As Band Ratios (Figure 25):**

Because of delays in discovering how to combine bands of different spatial resolutions in ENVI, our evaluation of this type of combination image was very limited. We found that one rendition highlighted much detail on variations in the alluvium of Big Rock fan. Otherwise, this combination did not provide noteworthy information compared to other imagery.

### **Landsat TM 432 Fused With Intermap Radar (Figure 26):**

This combination demonstrates striking sharpness of detail in the overall image. Differences in the appearances of the Devils Punchbowl Formation and the young alluvium west of it are well-defined. Some spectral information from the Landsat 7 image is enhanced, while other information is degraded so that it is not as clear as on the original Landsat image. Another positive is that the brightness of the radar enhances the 3-dimensional appearance of the image and highlights some structural features better than the original Landsat image. There is a problem with pixel colorations at the south edge of the image because of shadowing, and there is loss of some local textural detail in the landscape.

### **ASTER TIR (Band 13) Fused With Intermap Radar (Figure 27):**

The spectral information from ASTER Band 13 that is part of this image appears to be overwhelmed by that of the radar image with which it is merged; therefore, it is not a particularly useful combination image. One problem is that the sharpening ratio of 90:2.5 is probably far too large.

## **Field Observations**

Although we had abundant remote-sensing imagery to cover the study area, field observations were still required to check the validity of our interpretations of the imagery and to identify features that were ambiguous on the imagery.

## **ANCILLARY PRODUCTS FROM THIS STUDY**

Three main ancillary products were derived from this project, two of which were not originally planned. They are functional in nature, designed to aid project

management and improve both communication and use of remote-sensing data among SHMP technical staff:

**1) Raster Library/Directory (R:Drive):** To aid housekeeping for our project, we designed a repository on the SHMP server to store our remote-sensing raster files. After discussion with other staff, it was apparent that this approach could be broadened to include other raster files in SHMP, with selected availability to all technical staff. This all-encompassing repository for raster files is designated the “R:Drive.” A sample view of the hierarchical design of this drive is shown in Figure 35.

**2) Derivative Images for Staff Use (Color-infrared composite, shaded relief, principal components, etc.):** For each quadrangle in the study area, we prepared a set of standard images to aid staff directly in their mapping/zoning work and stored them in the R:Drive so that staff could directly access them. We also generated customized images upon request by SHMP staff to satisfy their specific needs.

**3) Status Table of Remote-Sensing Products (NOLARSstatus.xls):** We developed an Excel table that lists the technical specifications and status of each of the remote-sensing products we obtained or generated for the study area (Table 4). We initially developed this product to aid our own internal housekeeping in the NOLARS project, but realized later that all SHMP staff could benefit from access to it. Correspondingly, it evolved into a dynamic document accessible for viewing by all staff to track availability and specifications of products pertinent to each USGS 7.5-minute quadrangle in the study area. The table resides in the R:Drive repository.

In addition to the above, we prepared a set of color posters and a PowerPoint presentation about this project, which were used for technical outreach to SHMP staff and other interested parties.

## CONCLUSIONS

The following conclusions pertain to which evaluated imagery and algorithms worked best for the six specific geologic applications in SHMP mapping and zoning for this study area:

### **1) Delineation of contacts between bedrock and unconsolidated Quaternary deposits:**

For this application, remote-sensing imagery ranged from highly useful in some parts of the study area to minimally useful in other parts. Its best use was for juxtaposed alluvial and bedrock areas that have both different spectral signals and conspicuously different topographic signatures (for example, a flat modern

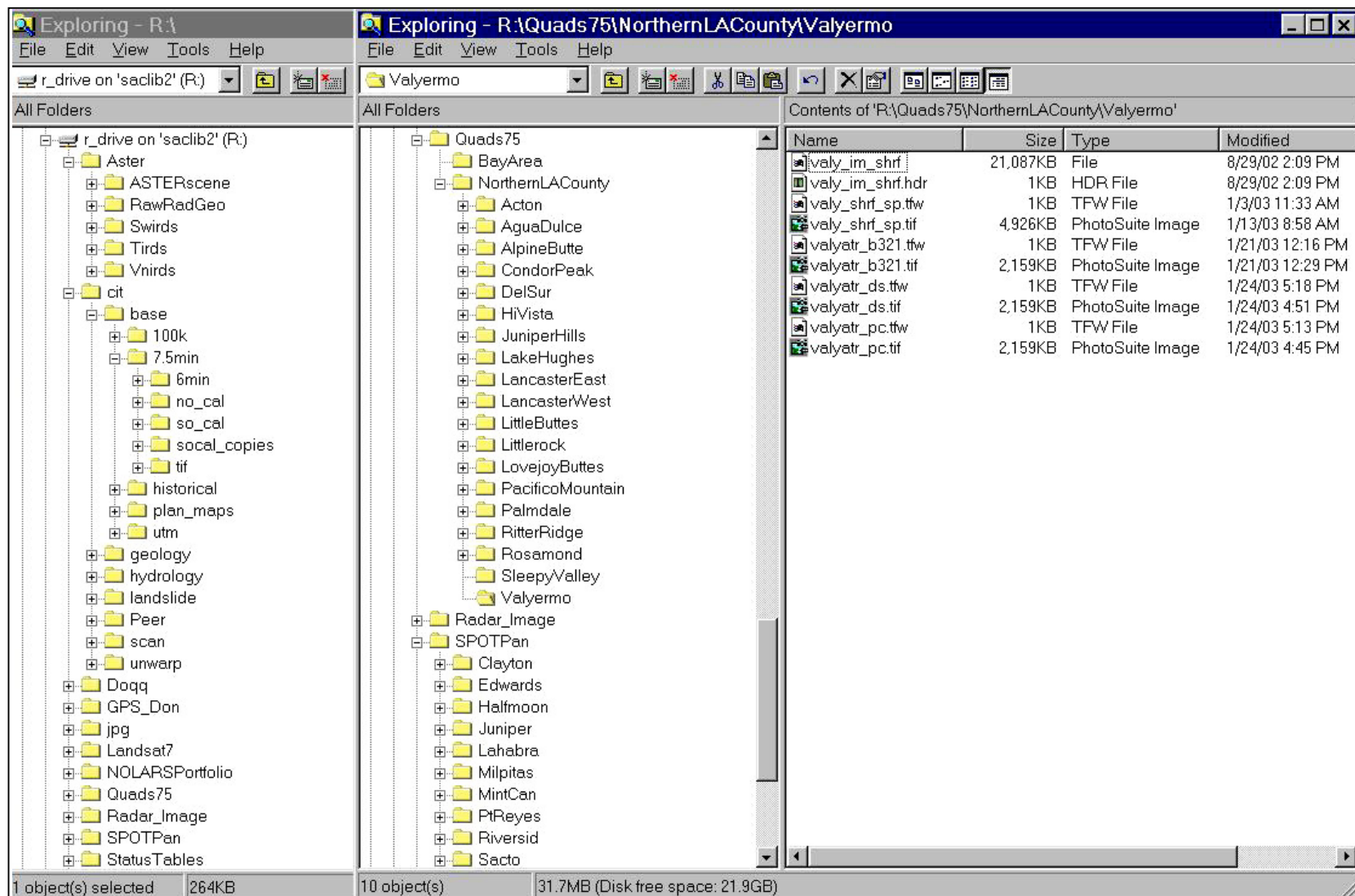


**FIGURE 35** – Sample of directory of the R:Drive raster library developed for the NOLARS project. Imagery for Valyermo Quadrangle is highlighted. This library will be used for future SHMP study areas

Directory Key:

	r_drive on 'saclib2' (R\.....)		P:\projects\tri4\dgn\geol_orig
	P:\projects\tri4\dgn\areatozone		G:\7.5_RAW\FEMA3

**TABLE 4** – Example of the status table for the NOLARS project. The format of this dynamic table can be used as a housekeeping tool for future SHMP projects.

stream channel between steep hills of bedrock). Shaded relief (generated from Intermap and USGS DEMs) and principal components-based algorithms were most applicable in these areas.

Areas that constituted intermediate usefulness of the imagery are exemplified by the low-relief bedrock/alluvial terrain in the Juniper Hills and Valyermo quadrangles along the transition from Antelope Valley across the San Andreas Fault Zone. One major challenge in delineation of contacts of bedrock with unconsolidated Quaternary deposits in this low-relief geomorphic environment is that the contacts commonly are not sharply defined by differences in spectral signal; slope wash of similar lithologic (and thus spectral) composition forms a transitional zone between the actual outcrop and alluvial sediment in the adjacent bottom lands. A possible solution to this problem of delineation is to prepare hill-shade images with high-resolution DEMs that can portray subtle changes in topography.

Imagery was least useful in the vegetation-covered contact zone along the range-front in Lake Hughes and Del Sur quadrangles; although shaded relief provided some indication of the contact, the dominance of spectral signals by vegetation, which did not differentiate itself according to the underlying lithology, prevented conclusive segregation of bedrock from unconsolidated alluvium (Figure 36). Overall, remote-sensing imagery worked best in the eastern part of the study area compared to the western part, largely because of interference by vegetation in the latter.

## **2) Discrimination of alluvial deposits (fans, modern stream channels, etc.) from one another:**

Of the four “field” applications described here among the six SHMP geologic applications, this one derived the most benefit from the remote-sensing imagery. Where pristine (undeveloped), individual alluvial fans in the eastern half of the study are dramatically apparent on most imagery, particularly the enhanced versions of principal components algorithms (MNF, PCA, Decorrelation Stretch of ASTER). The best examples are the currently active Big Rock and Little Rock fans in the eastern part of the study area. Older fans are also easily recognizable particularly because of their surface textures related to degree of dissection, which can be well-displayed on shaded-relief and hill-shade imagery. In culturally disturbed areas (urbanization, agriculture), fans are less distinct on the imagery, but experimentation with color combinations can make remnant evidence of the fans more visible. Within individual fans, active channels are spectrally distinct; again, Big Rock and Little Rock fans contain the best examples.

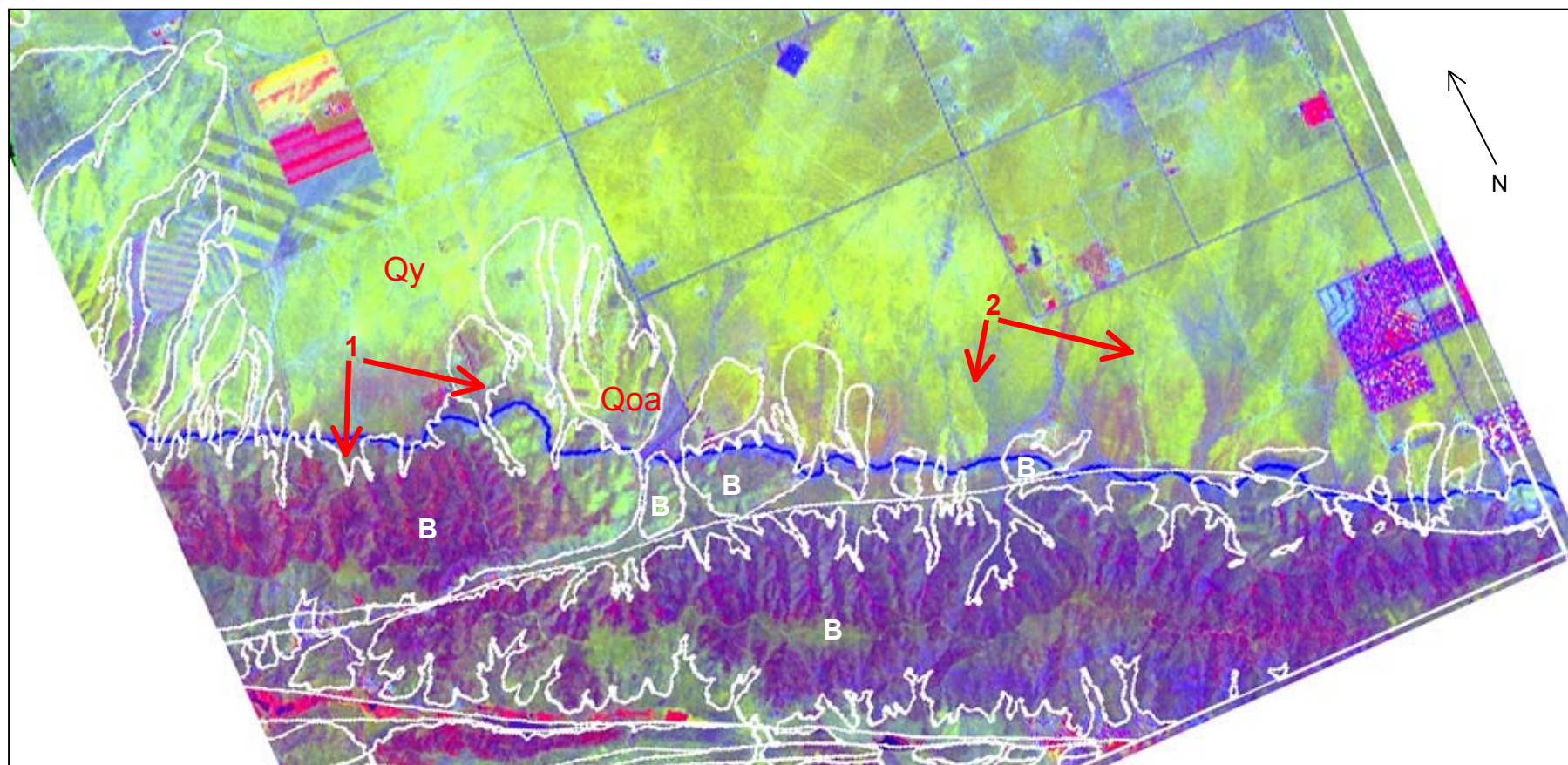


**FIGURE 36**— Example along the California Aqueduct in Del Sur Quadrangle where remote-sensing imagery is ambiguous for delineation of the contact between bedrock and unconsolidated Quaternary deposits (1). Contacts of Dibblee (2002b) are superimposed on a subset of the ASTER image. “B” indicates bedrock, “Qoa” indicates older alluvium of dissected fans, and “Qya” indicates younger alluvium of the main floor of Antelope Valley. Use of other algorithms plus shaded relief may enable some delineation of the contact. The image also has potential to differentiate alluvial subunits within the Qya unit at (2).

**Sensor:** ASTER

**Algorithm:** Decorrelation Stretch

**Band Order:**

### **3) Discrimination of bedrock units from one another:**

Within the bedrock terrains of the study area, successful discrimination of bedrock units from one another by remote-sensing imagery ranged from high to low. The most important influence on success was the percentage of vegetative cover. No amount of image-processing will significantly help discriminate lithology in areas obscured by vegetation that dominates the spectral signal unless there is a direct unique correlation between the vegetation community and the underlying rock or there is a preference of vegetation to concentrate along structural features of the rock (e.g., stratification). Because vegetation is generally sparse in much of the eastern part of the study area and relatively abundant in the western part, successful discrimination was much more common in the eastern part. Even within this eastern region, some lithologic units were more easily discriminated than others; examples include Tertiary volcanic and sedimentary rock, carbonate lenses in plutonic and metamorphic complexes, and individual subunits within plutonic complexes. Of the imagery evaluated, those in the principal-components family (PCA, MNF, Decorrelation Stretch) applied to ASTER and Landsat 7 were the most helpful in discrimination.

### **4) Recognition and delineation of landslides:**

For this study area, remote-sensing imagery in general was not found to be especially useful for recognition and mapping of landslides. One problem with evaluating landslides here is that the climate is semi-arid to arid and most of the landslides are very old and thus not conspicuous, especially in the Pelona Schist terrane. Of the imagery evaluated, we found those of the topographic-modeling group, particularly shaded relief (generated from Intermap and USGS DEMs), to be most useful for this application. For future study areas, remote-sensing imagery may be more useful in temperate regions with moderate to abundant rainfall, where landslides may reveal themselves more easily through moisture, vegetation, and topographic-geomorphic anomalies.

### **5) Verification of cartographic registration of digital geologic maps:**

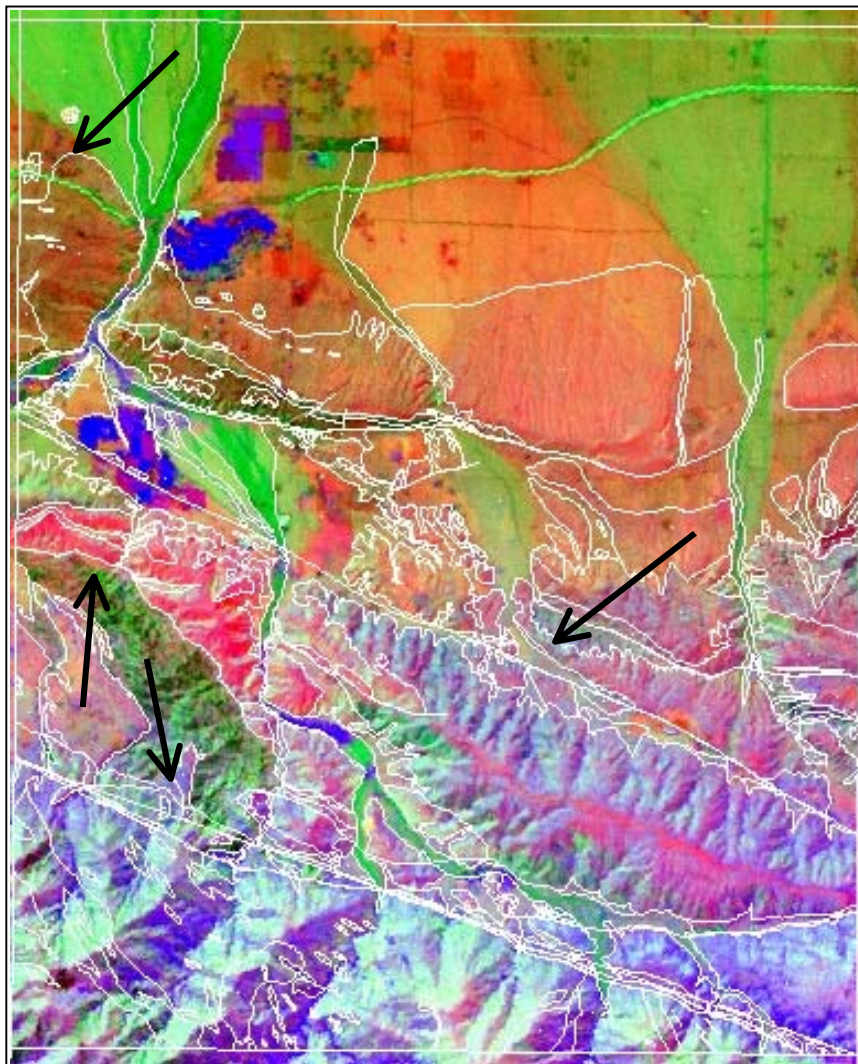
Assuming it is accurately georeferenced and orthorectified, certain remote-sensing imagery was excellent for checking the accuracy of cartographic geo-registration of digital vector layers of the geologic maps with SHMP digital base maps. For example, the two vector layers for the maps by Ponti and Burke (1980) and Ponti and others (1981) were quickly found to have serious geo-registration errors by visual analysis of remote-sensing imagery. We found shaded-relief imagery generated from the USGS and Intermap DEMs to be among the best for this application; the most effective means of analysis of geo-registration was by visual observation of the digitized contacts between recent alluvial deposits and bedrock.

## **6) Representation of previously mapped geologic contacts:**

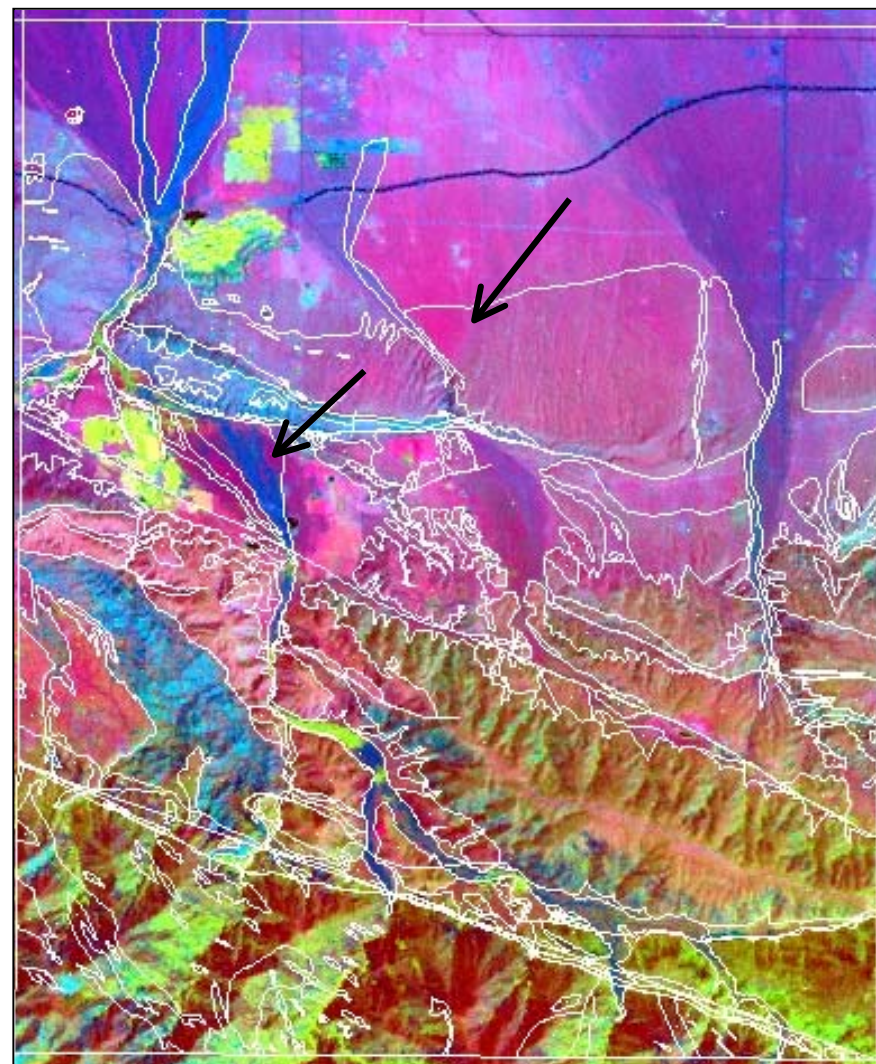
All published and unpublished geologic maps have inherent errors and levels of detail in how they portray contacts between lithologic units. These conditions result from many factors such as scale and purpose of the map, ease of recognizing the contacts on the ground, ease of transferring the locations of the contacts to the base map, etc. Remote-sensing imagery ranged widely, from excellent to poor, in its ability to offer visible evidence of the actual contacts, which could be compared to the geologists' portrayal of these contacts on geologic maps. We found that many contacts in the arid parts of the study area, particularly in the alluviated areas of Antelope Valley and along the eastern part of the San Andreas Fault Zone, were conspicuous upon visual analysis of some of the imagery; this imagery thus served as a legitimate "base map," or control, for the true location of the contacts when attempting to determine the quality of the contacts shown on the geologic maps of the study area. Images generated from the principal components family of algorithms (PCA, MNF, Decorrelation Stretch) were especially useful for this purpose (Figure 37). In the vegetation-dominated parts of the study area (high-elevation mountain areas and the westernmost part of Antelope Valley), however, the imagery was of marginal or no use for determining the accuracy and detail of previously mapped contacts; in some cases shaded relief was somewhat useful in checking where contacts are defined by abrupt topographic changes (e.g., low-relief unconsolidated alluvium juxtaposed with high-relief bedrock areas).

**The following additional conclusions represent what we believe are the most pertinent to the needs of SHMP in the future:**

- Remote-sensing imagery can provide a low-cost, rapid way to check previous geologic mapping by other geologists and resolve conflicts in geologic interpretation for certain areas.
- Remote-sensing imagery allow staff to see the context of their individual quadrangles relative to the entire study area. It helps reduce the potential for individuals to "not see the forest for the trees."
- Remote-sensing imagery is a valuable field tool that aids both location of oneself in the field and geologic interpretation and mapping. Several staff used plots of shaded relief and DOQQ imagery when in the field. We anticipate that CGS staff will eventually be using field computers routinely and that imagery files will be loaded on them as back-layers to aid mapping.



(a)



(b)

**Figure 37** - Demonstration of use of imagery as a back-layer to check and modify the previously mapped geologic contacts of Dibblee (2002c), shown in white, for Valyermo Quadrangle. Contacts that could definitely or possibly be modified based on comparison with the image are marked with arrows.

**Sensor:** Landsat 7 ETM VNIR

**Algorithm:** a) Minimum Noise Fraction, b) Principal Components Analysis

**Band Order:** a) MNF3, MNF2, MNF1 b) PC3, PC2, PC1

- Georeferencing, including conversion of imagery from native to different projections, although occasionally time-consuming, is an essential step for SHMP staff to use the imagery in their GIS applications. To make interpretations of geology and to modify geologic contacts, imagery must be closely registered with SHMP base maps. We found that the ASTER imagery received from the vendor was about 3-4 pixels in locational error, but these can be substantially reduced through warping (image-to-map or image-to-image) or by selection of additional ground control points.
- The specific remote-sensing imagery and techniques used in this project in Los Angeles County may or may not prove especially useful for future SHMP projects. Each study area is unique in its physical setting (topography, geology, vegetation, cultural modifications), thus remote-sensing tools have to be customized or modified accordingly. For example, because of masking by vegetation, refinement of lithologic units in temperate areas (moderate to high rainfall) by remote-sensing imagery may be more difficult.
- To extract the most information from a given multispectral dataset, one needs to process it in different ways to bring out the different information. In other words, no single remote-sensing image will be adequate by itself in providing all possible information on geologic features. For example, we observed that a decorrelation stretch image may highlight certain features of a particular area better than does a principal components image, but it may be vice versa in a different area. The ideal basic procedure should be: 1) apply algorithm/transformation of the raw data, 2) georeference the derived image, 3) overlay the vector layers of geology to analyze and modify the geology as warranted, and 4) field-check if necessary. The goal here is both to maintain the integrity of the original remote-sensing data and to achieve the closest possible georeferencing between the imagery and SHMP base maps and vector data layers.
- Fieldwork and traditional stereographic pairs of aerial photographs are still, and will continue to be, required tools in the geologic compilations and landslide inventories conducted for SHMP. Remote-sensing imagery is a complement to traditional photography and must be checked in the field.
- Because of its relatively coarse spatial resolution (15-m, 30-m, 90-m), the multispectral data evaluated in this study are best suited in many cases to “blocking out” areas of lithologic units rather than for drawing accurate boundaries around these units when mapping at scales of 1:24,000 or larger.
- Although less-experienced staff may at first be daunted by the seemingly endless ways to process and display remote-sensing imagery, many of

the steps to produce these images are simple or transparent when using image-processing software like ENVI. These steps can be learned quickly by staff geologists to integrate the imagery with other datasets pertinent to their specific quadrangles of interest.

- Staff who use remote-sensing imagery must be aware that there is a difference between situations where groups of pixels are ambiguous (i.e., uncertainty about what the group of pixels represent on the ground) versus situations where groups of pixels are misleading (e.g., unsupervised classification groups pixels incorrectly).
- Color combinations, whether in RGB or other color space, assigned to any display of an image must be chosen through experimentation to assure that ground features shown on the image are displayed in a conspicuous manner for recognition and interpretation. For example, an MNF-derived image with three bands should be displayed in color combinations of 123, 321, 132, etc., if it is found that the algorithm has strong potential for geologic interpretation.
- Viewing of imagery on both computer monitors and paper plots is necessary because both have their advantages and disadvantages. Monitors tend to display the imagery in sharper detail and more vivid colors than paper plots. On the other hand, paper plots allow the geologist to observe and analyze at a single glance the entire image at a more useful scale; when using a monitor, only one part of an image can be viewed at larger scales at any one time.
- Integration of diverse remote-sensing datasets during analysis is a key to enhancing their usefulness. For example, when observing and analyzing satellite imagery, it is advisable to also observe companion DOQQ images so that one can assess the “real” surface conditions, such as vegetation cover, that contribute to the spectral display of the imagery.
- Basic displays (true-color, color infrared composite), 3-D surface view, and combination images (seismic-hazard zones draped over shaded relief) are generally the most useful imagery for public presentations. Basic displays are notable for highlighting topography if that is a feature of interest.
- Anaglyph and epipolar stereo images have the potential for what we term “stereo-conferencing.” This concept involves creation of stereo images as data files that can be shared by staff in different locations. For example, such files can be viewed “on-screen” simultaneously by two staff in different offices with either anaglyph glasses or a ScreenScope to allow discussion of landslide features of mutual interest in adjacent quadrangles. This situation arose when Ante in Sacramento and Pam in Los Angeles were responsible for two adjacent quadrangles (Ritter Ridge

and Sleepy Valley) that had difficult-to-interpret landslide conditions. Both could have used this method to discuss, over the telephone, their resolution of landslide properties at the boundary between the quadrangles while viewing the areas of interest in stereo on their computer monitors.

- It may be useful to classify (perhaps 3-5 classes) the vegetation-index images (NDVI, tasseled cap) and then vectorize those classes to segregate vegetated areas from rock/soil areas to benefit fieldwork as well as provide an overlay to assist interpretation of other imagery. Color-infrared, NDVI, and tasseled cap would also be the most useful displays for highlighting cultivated areas.
- The remote-sensing community is broadening its research and application of sophisticated “complex” algorithms as a complement to the traditional “basic” algorithms. Specific geologic information can be extracted by using carefully selected transformations to represent each of the three color components of an image. One example for geologic mapping using ASTER data as cited by Larry Rowan at the 2003 ASTER Workshop is:

Red = Band 14/ Band 12

Green = (Band 1/ Band 2) + (Band 5/ Band 3)

Blue = Minimum Noise Fraction Band 1

## **RECOMMENDATIONS ON REMOTE SENSING FOR FUTURE SHMP PROJECTS**

Aside from the specific evaluations and conclusions described above, which constituted the main purpose for this study, we offer several recommendations on use of remote-sensing products in future SHMP projects including those now starting in the San Francisco Bay Area and the San Bernardino region.

- At the beginning of each new project, assemble a small technical team to evaluate what remote-sensing data and tools might be useful to the project.
- Provide each staff geologist with remote-sensing products to aid their mapping (geologic, liquefaction zoning, landslide inventory, landslide zoning). All technical staff should have the freedom to use whatever remote-sensing products are available and useful to them.
- Make clear to SHMP staff that ENVI is available for all of them to use on a “community” machine (Sac, SF, LA). It can be used by anyone at any time as long as our number of licenses isn’t exceeded at any one moment.

- Ante should continue providing derivative remote-sensing products to technical staff as needed and also advance his knowledge of remote sensing and associated image-processing software, particularly ENVI and ILWIS. He can serve as an advisor to SHMP staff on the best ways to use remote sensing to enhance their work.
- Prepare a protocol for research, acquisition, and incorporation of remote-sensing data into each new SHMP project. The protocol would include a list of standard imagery that would be posted in the R:Drive for use by all staff during mapping and zoning of their quadrangles. The imagery that qualifies for this list would be either already in the DOC/CGS archives (e.g., SPOT), free, or of nominal cost. Additional imagery would be obtained according to its cost versus potential benefit.
- For public viewing, incorporate remote-sensing imagery into Geomedia Web summaries of project areas being studied by SHMP.
- Provide training in remote-sensing principles for interested technical staff, preferably through free or low-cost on-line modules or in-Department workshops. At minimum, encourage staff to review standard textbooks on remote sensing and image interpretation (e.g., Sabins, 1997; Lillesand and Kiefer, 2000, both of which are in the CGS library) to familiarize themselves with or refresh their knowledge on those topics. One option for training is to have Ante give instruction on specific applications of remote sensing to tasks in SHMP. Another option is to have colleagues like Robert Yoha in OTS or Pete Roffers in SMIP give training sessions as part of their groups' services of outreach to staff.
- Establish digital housekeeping for remote-sensing data and customized imagery generated from those data.
- Determine in a general way how remote-sensing imagery can be use in the following regions:
  - Arid (sparsely vegetated)
  - Temperate (moderately to heavily vegetated)
  - Densely urbanized
- Consider sharpening of 15-meter ASTER images with higher-resolution images like the 5-meter IRS panchromatic, which can be purchased for about \$200-250/quadrangle.
- Within Intergraph, automate the process of attribution for direction (azimuth) of landslide movement by combining the vector layer of landslide inventory with a back-layer image of shaded relief so that staff

can visually determine/confirm the “downslope” direction of landslide movement (Figure 34). An automated tool is available for determining azimuth on-screen; there should be a way to link the corresponding derived azimuth value to the inventory database so that manual entry of the value is eliminated.

- Encourage staff working on inventories of landslides to try “heads-up” analysis and digitizing of landslides from aerial photographs and shaded-relief imagery to eliminate the steps of manual drawing and scanning used to transfer landslide boundaries from conventional stereo photographic prints to digital layers.
- The “open-ended” nature of image processing can lead to dead-ends and large expenditures of time to find useful algorithms in a specific study area. Because of the production-oriented nature of SHMP projects, algorithms must be established early in each project for staff to apply to evaluation and mapping of their individual quadrangles. We recommend that SHMP develop a scheme of standard algorithms, to be used in all study areas, plus determine additional algorithms unique to each study area. One or two staff could research the latter during initiation of each new project. At this point, we recommend that the principal components-based transformations (PCA, MNF, DS) and topographic modeling of imagery should be used in each study area.
- Encourage staff to view imagery of their quadrangles via “index sheets,” which is the display of different images of a quadrangle together as a mosaic so that the properties developed by each processing algorithm can be quickly compared from one image to another.

## REFERENCES

- Barrows, A.G., 1979, Geology and fault activity of the Valyermo segment of the San Andreas Fault Zone, Los Angeles County, California: California Division of Mines and Geology Open-File Report 79-01, scale 1:12,000.
- Barrows, A.G., 1980, Geologic map of the San Andreas Fault Zone and adjoining terrane, Juniper Hills and vicinity, Los Angeles County, California: California Division of Mines and Geology Open-File Report 80-02, scale 1:9,600.
- Barrows, A.G., Kahle, J.E., and Beeby, D.J., 1976, Geology and fault activity of the Palmdale segment of the San Andreas Fault Zone, Los Angeles County, California: California Division of Mines and Geology Open-File Report 76-6 LA, scale 1:12,000.

- Carpenter, E.J. and Cosby, S.W., 1926, Soil survey of the Lancaster area, California: U.S. Department of Agriculture, Bureau of Soils, scale 1:63,360.
- Dibblee, T.W., Jr., 1959, Geologic map of the Alpine Butte quadrangle, Los Angeles County, California: U.S. Geological Survey Map MF-222, scale 1:62,500.
- Dibblee, T.W., Jr., 1960, Geologic map of the Lancaster quadrangle, Los Angeles County, California: U.S. Geological Survey Map MF-76, scale 1:62,500.
- Dibblee, T.W., Jr., 1961, Geologic map of the Bouquet Reservoir quadrangle, Los Angeles County, California: U.S. Geological Survey Map MF-79, scale 1:62,500.
- Dibblee, T.W., Jr., 1996a, Geologic map of the Acton quadrangle, California: Dibblee Foundation Map DF-59, scale 1:24,000.
- Dibblee, T.W., Jr., 1996b, Geologic map of the Agua Dulce quadrangle, California: Dibblee Foundation Map DF-58, scale 1:24,000.
- Dibblee, T.W., Jr., 1997, Geologic map of the Sleepy Valley and Ritter Ridge quadrangles, California: Dibblee Foundation Map DF-66, scale 1:24,000.
- Dibblee, T.W., Jr., 2001, Geologic map of the Pacifico Mountain and Palmdale (south half) quadrangles, California: Dibblee Foundation Map DF-76, scale 1:24,000.
- Dibblee, T.W., Jr., 2002a, Geologic map of the Juniper Hills quadrangle, California: Dibblee Foundation Map DF-79, scale 1:24,000.
- Dibblee, T.W., Jr., 2002b, Geologic map of the Lake Hughes and Del Sur quadrangles, California: Dibblee Foundation Map DF-82, scale 1:24,000.
- Dibblee, T.W., Jr., 2002c, Geologic map of the Valyermo quadrangle, California: Dibblee Foundation Map DF-80, scale 1:24,000.
- Jensen, J.R., 1996, Introductory digital image processing – A remote sensing perspective: Prentice Hall, Upper Saddle River, New Jersey, Second Edition, 316 p.
- Lillesand, T.M. and Kiefer, R.W., 2000, Remote sensing and image interpretation: John Wiley and Sons, New York, New York, Fourth Edition, 724 p.

- Noble, L.F., 1954, Geology of the Valyermo Quadrangle and vicinity, California: U.S. Geological Survey Map GQ 50, scale 1:24,000.
- Ponti, D.J. and Burke, D.B., 1980, Map showing Quaternary geology of the eastern Antelope Valley and vicinity, California: U.S. Geological Survey Open-File Report 80-1064, scale 1:62,500.
- Ponti, D.J., Burke, D.B., and Hedel, C.W., 1981, Map showing Quaternary geology of the central Antelope Valley and vicinity, California: U.S. Geological Survey Open-File Report 81-737, scale 1:62,500.
- Sabins, F.F., 1997, Remote sensing – Principles and interpretation: W.H. Freeman and Company, New York, New York, Third Edition, 494 p.
- Woodruff, G.A., McCoy, W.J. and Sheldon, W.B., 1970, Soil survey of the Antelope Valley area, California: U.S. Department of Agriculture, Soil Conservation Service, 187 p.

## APPENDIX A

### Abbreviated Glossary of Remote Sensing

**Color Space:** A three-dimensional means of mathematically portraying color. For example, the standard RGB color space is represented by a cube with each of the three axes (x, y, and z) representing one of the three primary additive colors, red, green, or blue. Other ways of portraying color use spheres and cones. See Lillesand and Kiefer (2000, p. 525) and Sabins (1997, p. 275).

**Decorrelation:** A process of producing uncorrelated bands of data, which can then be displayed for improved visual interpretation (see “uncorrelated” below). Principal components analysis (PCA) is one way of decorrelating bands of remote-sensing data; “decorrelation stretch” is a specific subtype of PCA.

**Dimensionality:** The number of bands in a dataset that must be analyzed to produce useful results. In processing multispectral and hyperspectral datasets, a major goal is to reduce their dimensionality.

**Hyperspectral:** Data that are collected by a sensor in many wavelength bands. The airborne instrument AVIRIS collects data for 224 bands, thus it is a hyperspectral sensor.

**Multispectral:** Data that are collected by a sensor in several wavelength “bands,” or channels. For example, ASTER collects multispectral data in 14 individual bands.

**Panchromatic:** A single wavelength band that is displayed as a grayscale (black and white) image.

**RGB:** Acronym for red, green, and blue. All color images generated from a particular sensor are designated in this report by band numbers using this order of colors. For example, “432” for a color ASTER image means that Band 4 was assigned red, Band 3 was assigned green, and Band 2 was assigned blue.

**SWIR:** Acronym for the short-wave-infrared portion of the electromagnetic spectrum.

**TIR:** Acronym for the thermal-infrared portion of the electromagnetic spectrum.

**Uncorrelated:** Lacking redundancy or similarity when referring to the information contained in bands of data. Typically, the data in the various wavelength bands collected by a multispectral remote-sensing instrument are commonly similar from one band to the next, which means that each band conveys basically the same information. Remote-sensing practitioners attempt to “reduce” this

correlation, or redundancy, between bands by mathematically transforming the data in ways (e.g., principal components analysis) that attempt to produce new “bands” that are uncorrelated.

**Variance:** For a single band of data from a sensor, its “variance” is defined statistically as the average squared deviation of all possible observations from the sample mean. Qualitatively, one can loosely think of it as the degree of variation in the data.

**VNIR:** Acronym for the visible and near-infrared portions of the electromagnetic spectrum.

## **APPENDIX B**

### **REPRESENTATIVE ON-GROUND PHOTOGRAPHS SHOWING SURFACE CHARACTERISTICS OF THE STUDY AREA**

The following photographs were taken in the field during the NOLARS project. They were selected as representative examples of the different types of terrain and surface cover in the study area, which directly influence the spectral responses that appear on associated remote-sensing imagery. Figure B1 is a saturated-stretch transformation of the 2000 Landsat 7 ETM image of the study area that shows the locations of the photographs and their directions of view. The remaining figures are placed in an order that approximately takes the viewer from the mountainous areas of the southern part of the study area, through the transition zone between the mountains and Antelope Valley, and finishes with landscapes in the valley where it comprises the northern part of the study area.



**Figure B1-** Saturated stretch of a Landsat 7 ETM 321 image showing the locations and directions of views of photographs displayed in the following figures.



**FIGURE B2** -View south-southeast along the summit ridge of Sierra Pelona from the western edge of Ritter Ridge Quadrangle. Sierra Pelona, which is underlain by Pelona Schist, has notable contrasts in vegetation types ranging from low-growth grassy mats (foreground) to dense chaparral (distance). Outcrop not shielded by vegetation is uncommon. Although difficult to recognize, a number of landslides were mapped on the chaparral slopes of Sierra Pelona visible here.



**FIGURE B3** - View south to Pinyon Ridge from Big Pines Highway at Mile High in Valyermo Quadrangle. The part of the ridge shown here is underlain by quartz dioritic and gneissic rocks with a high-percentage cover of juniper and pinyon trees. It is one example of how widely varied the type and amount of vegetative cover is within the study area.



**FIGURE B4** - View west from Shoemaker Canyon along Big Pines Highway to ridges above Big Rock Springs in Valyermo Quadrangle. On the left is the western terminus of Pinyon Ridge; the mottled area on the lower slopes is composed of quartz diorite and gneissic quartz diorite with lighter areas possibly comprising more-silicic intrusions. The ridge in the central distance is composed of marine sedimentary rock of the San Francisquito Formation. Also apparent are several landslide scars that head along the summit of the ridge. This geologic unit is conspicuously displayed on several images derived from the ASTER and Landsat 7 ETM scenes.



**FIGURE B5** - View west-northwest along the San Andreas Fault Zone and the California Aqueduct to Palmdale. Taken from the east edge of Juniper Hills Quadrangle, this view shows the more gradual transition between Antelope Valley and the San Gabriel Mountains compared to the more abrupt transition characteristic of the western part of the study area in the Lake Hughes and Del Sur Quadrangles. Vegetation here is more desert-like, characterized by scattered juniper and sagebrush set among bare soil and rock. Contacts between bedrock and unconsolidated sediment are not especially distinct because of the low, rolling topographic relief.



**FIGURE B6** - View easterly toward Holcomb Ridge in Valyermo Quadrangle from a spur between Pallett and Holmes creeks in Juniper Hills Quadrangle. As in Figure B5, sparse desert-type vegetation is present on a rolling, low-relief terrain underlain by granitic bedrock covered in places by slope wash and channel alluvium.



**FIGURE B7** - Telephoto view to the east-southeast from the vicinity of Willow Springs Road near the west edge of Del Sur Quadrangle showing the transition zone from Antelope Valley to the San Gabriel Mountains. This photo displays several characteristic features of the study area including: 1) Gently sloping, dissected older alluvial fan in the foreground covered by grass and sagebrush; this cover is typical of the western part of the study area, which receives more moisture than the eastern part, 2) undissected younger alluvial fan in the middle distance, covered dominantly by grass, 3) urbanization of the Palmdale-Lancaster area in the middle distance encroaching on the flanks of Portal Ridge to the right, and 4) main crystalline massifs of the San Gabriel Mountains rising abruptly in the far distance.



**FIGURE B8** - View west-northwest along the transition zone between gently sloping alluvial fans of Antelope Valley (right) and granitic bedrock ridges (left) in Del Sur and Lake Hughes quadrangles. This zone demonstrates the need to use vegetation type and distribution as guides to the contact between bedrock and unconsolidated sediment because change in topography in this area is not always sufficient by itself to identify this contact. Here the granitic rock in places supports small clumps of sagebrush, whereas the fans support grass.



**FIGURE B9** - View south from Mount Emma Road in the northwest corner of Juniper Hills Quadrangle. Shown here is the surface of unconsolidated alluvial-fan material mapped as part of the Q6 series of geologic units by Ponti and others (1981), which is older than the deposits shown in Figures B11 and B12. The low ridge in the middle distance is mapped by Dibblee (2002a) as Tertiary sedimentary rock of the Anaverde Formation.



**FIGURE B10** - Roadcut along Mount Emma Road in the northwest corner of Juniper Hills Quadrangle. This unconsolidated material comprises the alluvial fan shown in Figure B9.



**FIGURE B11** - View northwest across older unconsolidated alluvial deposits of Little Rock fan, south of Palmdale Boulevard and just west of the active channel displayed in Figure B12. This type of deposit differs from the active channels by 1) hummocky surface caused by windblown material collecting around the base of shrubs, 2) dominance of fine rather than coarse fraction of sediment at the ground surface, 3) darker color of sediment and its “soil-like” appearance at the surface, 4) presence of Joshua trees, and 5) otherwise much greater variety of vegetation types. It is mapped as part of the Q7 series of geologic units by Ponti and others (1981).



**FIGURE B12** - View northeast across the flat (non-hummocky), clean gravel of an active channel on the Little Rock fan south of Palmdale Boulevard (east of Figure B11). Mapped either as geologic unit Qsc or Qsvc by Ponti and others (1981), modern channels such as these are conspicuous on remote-sensing images that are processed to bring out strong contrasts in color (Minimum Noise Fraction, Principal Components).



**FIGURE B13** - Comparison of sediment exposed at the surface of the deposits shown in Figures B11 and B12. On the left is characteristic gravel of the active channel (B12), while on the right is the finer-grained sediment of the older deposit (B11).



**FIGURE B14** - View southeast to Saddleback Butte in Hi Vista Quadrangle. Situated in the northeast part of the study area, this location demonstrates the sparsely vegetated “desert” extreme of the study area, which contrasts with the more-moist conditions of the Lake Hughes area in the southwest part of the study area. Seen here are the sheetwashed pediment in the foreground, the gradually inclined zone of slope wash and colluvium in the middle distance, and the steep-sloped granitic inselberg in the far distance.



**FIGURE B15** - View northeast toward Rosamond Lake from East Avenue E at the northern edge of the study area. Seen here is a low hummocky terrain dominated by fine wind-blown sand, which is widespread north of Lancaster and includes the lowest elevations of the study area. This region represents the distal-most parts of the alluvial deposits shed off the surrounding mountains above Antelope Valley.